NTNU
Norwegian University of
Science and Technology

An experimental study of unfrozen water content in fine grained permafrost soils

Marte Sundby Nybo

Civil and Environmental Engineering
Submission date: July 2017
Supervisor: Gustav Grimstad, IBM
Co-supervisor: Arne Instanes, UNIS

Norwegian University of Science and Technology
Department of Civil and Environmental Engineering

NORWEGIAN UNIVERSITY OF SCIENCE AND TECHNOLOGY
DEPARTMENT OF CIVIL AND ENVIRONMENTAL ENGINEERING

Report Title: **An Experimental Study of Unfrozen Water Content in Fine Grained Permafrost Soils**	Date: 07.29.2017 Number of pages (incl. appendices): 111			
	Master Thesis	X	Project Work	
Name: Marte Sundby Nybo				
Professor in charge/supervisor: Professor Gustav Grimstad				
Other external professional contacts/supervisors: Professor II Arne Instanes (UNIS)				

Abstract:

The strength of a soil increases when the ground freezes, but some of the water will remain unfrozen. Unfrozen water content is an important thermal property of a soil as flowing water may supply heat, reduce the strength, and thawing ground will experience reduced soil strength and increased settlements. Thus, estimating the unfrozen water content is important for geotechnical design considerations in permafrost areas. Additionally, hydraulic and thermal responses of climate changes can be simulated.

Reliable methods for determining unfrozen water content in frozen soil exist, but requires sophisticated instruments and is time consuming. For engineering purposes, more simple and efficient methods are desired. In this thesis, more recently developed methods for determining unfrozen water content in fine grained soils have been examined, liquid limit determination and water potential testing in particular.

Soil samples from Longyearbyen and Trondheim have been examined and tested in the laboratories of UNIS and NTNU, using liquid limit determination and water potential testing. The test methods have been evaluated and compared against each other. New parameters adapted to Norwegian clays are proposed for the liquid limit determination.

A geothermal Plaxis model for finding thermal properties of fine grained soils are tested on the soils. The model estimates the frost penetration depth, and the result is compared to results obtained by hand calculations. With improvements, the model has potential to become a useful tool in geotechnical designs in permafrost areas.

Keywords:

1. Frozen ground engineering
2. Unfrozen water content
3. Water potential
4. Liquid limit

NTNU
Faculty of Engineering Science and Technology
Institute of Civil and Environmental Engineering

MASTER DEGREE THESIS

Spring 2017
for

Student: Marte Sundby Nybo

An Experimental Study of Unfrozen Water Content in Fine Grained Permafrost Soils

BACKGROUND

When the temperature in soil falls below the nucleation temperature of ice crystals, ice will form in the pores of the soil. Part of the pore water in the soil will remain unfrozen as liquid layers on particle surfaces. The presence of unfrozen water affects the heat flow in the ground and the mechanical properties of the soil. In permafrost engineering design, the unfrozen water vs. temperature curve is an important factor in the evaluation of bearing capacity, settlement and stability analysis of structures and foundations.

TASK

Task description
The master project includes investigating methods for determining unfrozen water contents in soils, and compare two different methods for finding unfrozen water content depending on temperature in fine grained soils. To investigate the effect of unfrozen water content on thermal flow in the soil, a model is tested on the investigated soils.

Objective and purpose
The master project contains the following main points:

1. Literature study. Presentation and discussion of different methods for determining unfrozen water content in frozen soils (i.e. calorimetry, differential scanning calorimetry, nuclear magnetic resonance, time-domain reflectometry, water potential, liquid-limit test etc.).

2. Experimental study of unfrozen water content vs. temperature of selected fine-grained soils
   - Water potential and liquid limit tests are performed in the geotechnical laboratories at UNIS and NTNU.
   - Soil samples from Longyearbyen are used in the analysis at UNIS' geotechnical laboratory in Longyearbyen.
   - It is an option to test reference fine grained soils from the Trondheim area (i.e Eberg leire, quick-clay etc.) at NTNU.

3. Modelling: One-dimensional geothermal modelling to investigate the effect of the unfrozen water content on heat flow in the tested soils.

Professor in charge: Gustav Grimstad

Other supervisors: Arne Instanes

Department of Civil and Transport Engineering, NTNU
Date: 06.03.2017

Professor in charge (signature)

Preface

This paper is the master thesis in Geotechnical Engineering at the Norwegian University of Science and Technology (NTNU) as part of the MSc in Civil and Environmental Engineering. The work is performed within the Department of Civil and Transport Engineering, in cooperation with the University Center in Svalbard (UNIS) and Norwegian Geo-Test Sites (NGTS).

Professor Gustav Grimstad at NTNU and Professor II Arne Instanes at UNIS have been the supervisors, and laboratory work has been performed at NTNU and UNIS. The thesis was carried out during the spring semester of 2017.

Trondheim, 07.29.2017

Marte Sundby Nybo

Acknowledgements

I would like to thank the following persons for their great help during the master thesis.

Arne Instanes - For giving me the opportunity to work with this interesting topic and for providing help and guidance during this work.

Gustav Grimstad - For providing help and guidance during the work of the thesis.

Seyed Ali Ghoreishian Amiri and Hooman Rostami - For assistance and discussions of the thermal analysis in Plaxis.

UNIS/NGTS - For accepting me as a guest master student and providing me with economical support, laboratory equipment, and work space during my stay at UNIS.

My fellow NTNU students - For motivation, help, and relevant discussions.

M. S. N.

Summary and Conclusions

The soil strength increases when the ground freezes, but some of the water will remain unfrozen. Unfrozen water content is an important thermal property of a soil as flowing water may supply heat, reduce the strength, and thawing ground will experience reduced soil strength and increased settlements. Thus, estimating the unfrozen water content is important for geotechnical design considerations in permafrost areas. Additionally, hydraulic and thermal responses of climate changes can be simulated.

Reliable methods for determining unfrozen water content in frozen soil exist, but requires sophisticated instruments and is time consuming. For engineering purposes, more simple and efficient methods are desired. In this thesis, more recently developed methods for determining unfrozen water content in in fine grained soils have been investigated, liquid limit determination and water potential testing in particular. Soil samples from Longyearbyen and Trondheim have been investigated in the laboratories of UNIS and NTNU, using liquid limit determination and water potential testing. Tests show that liquid limit determination underestimates the unfrozen water content in frozen soils, and the method is cumbersome and time-consuming. New parameters adapted Norwegian clays are proposed. The water potential testing, based on thermodynamic calculations, is more accurate and straightforward.

A geothermal Plaxis model for finding thermal properties of fine grained soils are tested on the soils, but gave unexpected results regarding frost penetration depth. The model should be investigated more thorough and improved, and can be a useful tool in geotechnical designs in permafrost areas. Frost depth penetration has also been estimated by hand calculations, giving more reliable results. It was found that underestimating the unfrozen water content will provide a smaller calculated frost penetration depth.

Sammendrag

Når grunnen fryser vil fastheten i jordmaterialet øke, men noe av jordens vanninnhold forblir ufrosset. Ufrosset vanninnhold er en viktig termisk egenskap innenfor geoteknikk ettersom strømmende vann kan tilføre varme og redusere jordens fasthet. Tinende grunn vil oppnå redusert fasthet, noe som fører til økte setninger. For geotekniske beregninger i områder med permafrost er det derfor viktig å kunne estimere mengden ufrosset vann. I tillegg kan mengden ufrosset vann gi informasjon om de hydrauliske og termiske virkningene av klimaendringer.

Det eksisterer flere pålitelige metoder for å estimere ufrosset vanninnhold i fros-sen jord, men for mange av metodene er det nødvendig med avansert utstyr, og de er til dels tidkrevende. For ingeniørtekniske formål er det ønskelig med enklere og mer effektive metoder. I denne oppgaven undersøkes nyere metoder for å estimere ufrosset vanninnhold i finkornede jordarter, med spesielt fokus på støtflytgrense-metoden og vannpotensial-metoden. Det er utført laboratorieundersøkelser med disse to metodene på jordprøver fra Longyearbyen og Trondheim. Resultater fra testene viser at støtflytgrense-metoden underestimerer det ufrossede vanninnholdet, og metoden er tungvint og tidkrevende. For denne modellen er parametre tilpasset norske leirtyper foreslått. Vannpotensial-metoden, som er basert på termodynamiske beregninger, er mer nøyaktig og enklere å gjennomføre.

En geotermisk Plaxis-modell for å finne termiske egenskaper for finkornede jordarter er testet på de ulike jordtypene. Den beregnede frostdybden i modellen er ikke som forventet, og modellen bør undersøkes videre og forbedres. En forbedret versjon av modellen vil være et nyttig verktøy for geotekniske vurderinger i områder med permafrost. Frostdybden er også anslått ved bruk av håndberegninger, noe som gir mer pålitelige og tilfredsstillende resultater. Resultater fra håndberegningene viser at ved å bruke underestimerte verdier for ufrosset vanninnhold vil beregnet frostdybde være mindre enn den reelle.

Contents

Preface ii

Acknowledgements iii

Summary and Conclusions iv

Sammendrag v

1 Introduction **1**

1.1 Background 1

1.2 Objectives 3

1.3 Limitations 3

1.4 Approach 4

1.5 Structure of the Report 4

2 Literature Review **5**

2.1 Ground Temperatures 5

2.2 Permafrost Features 7

2.3 Physical Properties of Frozen Ground 8

2.4 Unfrozen Water Content in Frozen Soil 9

3 Methods for Determining Unfrozen Water Content **13**

3.1 Selection of Methods 14

3.1.1 Dilatometry 14

3.1.2 Differential Thermal Analysis and Differential Scanning Calorimetry 14
3.1.3 Adiabatic and Isothermal Calorimetry 15
3.1.4 Nuclear Magnetic Resonance 15
3.1.5 Time-Domain Reflectometry 16
3.1.6 Contact Method 17
3.2 Liquid Limit Determination 18
3.3 Water Potential Determination 19
3.3.1 Theory 19
3.3.2 Procedure of Measuring Water Potential 21
3.3.3 Thermodynamic Calculations for Finding Unfrozen Water Content 22
3.3.4 Thermodynamic Calculations for Finding Nonclathrate Water Content . . . 24
3.3.5 Previous Tests and Results 25

4 Experiments **27**

4.1 Liquid Limit Determination 27
4.1.1 Purpose and Theory 27
4.1.2 Hypothesis 27
4.1.3 Equipment 27
4.1.4 Test Procedure 28
4.2 Water Potential Determination 29
4.2.1 Purpose and Theory 29
4.2.2 Hypothesis 29
4.2.3 Equipment 29
4.2.4 Test Procedure 30

5 Analysis and Results **31**

5.1 Liquid Limit Determination 31
5.1.1 Lilleby 32
5.1.2 UNIS East 33
5.1.3 NGTS: AD-d-4-4 33
5.1.4 NGTS: AD-d-2-4 34
5.2 Water Potential Determination 35
5.3 Comparisons of the Results 37
5.3.1 Lilleby 37
5.3.2 UNIS East 38
5.3.3 NGTS: AD-d-4-4 and AD-d-2-4 38
5.4 Discussion 39

6 Geothermal Model Proposition 44

6.1 Heat Flow in Soils 44
6.1.1 Frost Depth 45
6.1.2 Thawing of Frozen Soil 47
6.2 Plaxis Model 47
6.2.1 Choice of Parameters 48
6.2.2 Results 49
6.3 Hand Calculations 51
6.3.1 Thermal Parameters 51
6.3.2 Calculations and Results 52
6.4 Discussion and Conclusions 53

7 Summary and Recommendations for Further Work 55

7.1 Summary and Conclusions 55

7.2 Discussion 56
7.3 Recommendations for Further Work 57

Bibliography **58**

A Acronyms **62**

B Nomenclature **63**

C Soil Samples **68**

C.1 Lilleby 68
C.2 UNIS East 70
C.3 NGTS site: AD-d-2-4 and AD-d-4-4 72

D Liquid Limit Linear Regression **75**

D.1 Linear Regression for Finding Water Content at 25 drops 75
D.2 Linear Regression for Finding Water Content at 100 drops 77

E Adapted Parameters for Liquid Limit Determination **79**

F Results From the Plaxis Geothermal Model **84**

F.1 Results From Testing With Surface Temperature of -3 °C 84
F.2 Results From Testing With Surface Temperature of -10 °C 88

List of Figures

2.1 Trumpet curve, surface and ground temperatures 6

2.2 Temperature profile in permanent frozen soil 7

2.3 Mass-volume relationships for frozen and unfrozen soil 10

2.4 Cooling curve for soil water and ice 12

4.1 Casagrande's liquid limit device 28

5.1 Unfrozen water content - temperature curve from liquid limit determination . . . 32

5.2 Unfrozen water content - temperature curve from liquid limit determination, Lilleby 32

5.3 Unfrozen water content - temperature curve from liquid limit determination, UNIS East 33

5.4 Unfrozen water content - temperature curve from liquid limit determination, NGTS: AD-d-4-4 34

5.5 Unfrozen water content - temperature curve from liquid limit determination, NGTS: AD-d-2-4 34

5.6 Results of water potential testing at 15 and 25 °C, Lilleby clay 35

5.7 Results of water potential testing at 15 and 25 °C, UNIS East clay 36

5.8 Results of water potential testing at 15 and 25 °C, soil from NGTS site 36

5.9 Unfrozen water content vs. temperature found by liquid limit determination and water potential determination, Lilleby 37

5.10 Unfrozen water content vs. temperature found by liquid limit determination and water potential determination, UNIS East 38

5.11 Unfrozen water content vs. temperature found by liquid limit determination and water potential determination, NGTS site 38

5.12 Unfrozen water content vs. temperature found by water potential determination and adapted liquid limit determination, AD-d-2-4 40

5.13 Unfrozen water content vs. temperature found by water potential determination and adapted liquid limit determination, AD-d-4-4 41

5.14 Unfrozen water content vs. temperature found by water potential determination and adapted liquid limit determination, UNIS East 42

5.15 Unfrozen water content vs. temperature found by water potential determination and adapted liquid limit determination, Lilleby 43

6.1 Correction coefficient λ in the modified Berggren equation 46

6.2 Relationship between undrained shear strength $s_u(c_u)$ and undrained Young's modulus E_u 48

6.3 Saturation of ice with frost depths Plaxis model, −3 °C 50

6.4 Saturation of ice with frost depths Plaxis model, −10 °C 51

C.1 Grain Size Distribution Lilleby Clay 69

C.2 Grain Size Distribution Unis East Clay 71

C.3 The Adventdalen area with drill site marked for investigations performed by Graham L. Gilbert 72

C.4 Simplified sedimentary log with facies and facies association distributions 73

C.5 Distribution of grain size parameters 74

D.1 Linear regression Lilleby, $w_{N=25}$ 75

D.2 Linear regression UNIS East, $w_{N=25}$ 76

D.3 Linear regression NGTS: AD-d-4-4, $w_{N=25}$ 76

D.4 Linear regression NGTS: AD-d-2-4, $w_{N=25}$ 76

D.5 Linear regression Lilleby, $w_{N=100}$ 77

D.6 Linear regression UNIS East, $w_{N=100}$ 77

D.7 Linear regression NGTS: AD-d-4-4, $w_{N=100}$ 78

D.8 Linear regression NGTS: AD-d-2-4, $w_{N=100}$ 78

E.1 Unfrozen water content vs. temperature found by water potential determination and adapted liquid limit determination, AD-d-2-4 80

E.2 Unfrozen water content vs. temperature found by water potential determination and the adapted liquid limit graph, AD-d-4-4 81

E.3 Unfrozen water content vs. temperature found by water potential determination and the adapted liquid limit graph, Lilleby 82

E.4 Unfrozen water content vs. temperature found by water potential determination and the adapted liquid limit graph, UNIS East 83

F.1 Deformed mesh PLAXIS model, −3 °C 85

F.2 Temperature distribution Plaxis model, −3 °C 86

F.3 Saturation of ice Plaxis model, −3 °C 87

F.4 Deformed mesh Plaxis model, −10 °C 88

F.5 Temperature distribution Plaxis model, −10 °C 89

F.6 Saturation of ice Plaxis model, −10 °C 90

List of Tables

5.1 Results from liquid limit determination 31

5.2 Adapted parameters for liquid limit determination formulas 39

6.1 General and mechanical parameters in Plaxis model 49

6.2 Thermal parameters in Plaxis model 49

6.3 Parameter used in the model for heat flow 52

6.4 Calculated values in heat flow model 53

C.1 Design Parameters Lilleby 70

C.2 Design Parameters UNIS East 71

Chapter 1

Introduction

1.1 Background

The definition of frozen ground is soil or rock with a temperature below 0 °C. Permafrost is defined as soil or rock with temperatures below 0 °C over at least two consecutive winters and the intervening summer (Andersland and Ladanyi, 1994). When the ground freezes the strength increase is considerably high as the ice functions as a bonding agent and prevents water seepage. Seasonal frozen ground is frozen during colder periods of the year, and is associated with certain terrain features, such as ice wedges, ice-wedge polygons, pingos, and thermokarst topography reflecting the geomorphic processes (Andersland and Ladanyi, 1994). Seasonal frozen ground above permafrost is known as the active layer. Complex geology and layering below these features may cause construction problems. Thus, it is important for engineers to understand the processes and effects of freezing and thawing in permafrost areas, the mechanical properties of frozen soils, and thus be able to utilize the advantages of the frozen soil.

Frozen soil has high compressive strength and low tensile strength, and ground freezing is used in stabilizing the ground during excavations, structural underpinning for foundations, and for temporary control of groundwater flow. Boring and sampling provides information about strata, soil classification, and strength of frozen and unfrozen soil. The thermal properties of the soil depend on soil type, density, and water content. Freezing ground will expand and cause frost heave and increased lateral passive earth pressure. Furthermore, information about groundwater and temperature conditions in the ground is important for controlling the stability. Flowing water may supply heat to the soil, reducing the strength, and thawing ground will experience reduced soil strength, and thus increased settlements.

Seasonally frozen ground and permafrost is found in cold regions, defined in terms of air temperatures, snow depth, ice cover on lakes, and frost penetration depth. The isotherm for 0 °C mean temperature during the coldest month of the year, or a seasonal frost penetration of 300 mm once in 10 years, are generally accepted southern limits of the cold region on the northern hemisphere (Bates and Bilello, 1966). The freezing temperature of a soil type depends on the

content of minerals, organic material, and water. It is usually assumed that the mean annual ground surface temperature must be at least −3 °C for permafrost to exist.

Even though ground is frozen, it will contain a certain amount of unfrozen water, depending on soil type and temperature. Climate changes cause increased temperatures in the arctic resulting in thawing of permafrost, decreased sea ice and glacier ice mass, and shifted biological indicators (Kurylyk and Watanabe, 2013). The hydrological regime changes, as the interaction between ground water and surface water increases. By estimating the unfrozen water contents in arctic areas, it is possible to simulate hydraulic and thermal responses of climate changes.

Furthermore, the importance of knowing the unfrozen water content w_u in fro-zen soils has increased due to exploitation in arctic and subarctic regions, and developments within road and airfield construction techniques. Construction in permafrost areas will change the thermal regime and thus degrade the permafrost table (Tice et al., 1976). For assessing the impact of local disturbance of the soil, it is essential to be able to calculate the unfrozen water content of the soil based on temperature changes. When constructing in permafrost areas, it may be necessary to refrigerate members of the structure, and the amount of water to be frozen is thus significant information. Reliable methods for determining unfrozen water content in frozen soil exist, but requires sophisticated instruments and is usually time consuming. The increased interest in determining the unfrozen water content for engineering purposes, creates a desire for more simple and efficient methods.

Previously, the most familiar method for obtaining phase composition data has been the adiabatic calorimeter. The method has shown good results. Other methods used for this purpose are described thoroughly by Anderson and Morgenstern (1973). Specific surface area of fine-grained materials is a fundamental property, and is used for describing physical and chemical characteristics of soil. The equilibrium ethylene glycol retention method is widely accepted for finding this property. A method should include both internal and external specific surface area. The Atterberg limit tests were intended for agricultural soils, but ensuing studies showed relationships between Atterberg limits and critical bearing points of soils (Terzaghi, 1926). Casagrande (1932) showed relationships between Atterberg limits and shear strength of soils, that was later used for classifying soils. Later, other correlations between Atterberg limits and soil properties has been showed, e.g. between liquid limit and surface area of soils.

Tice et al. (1976) found that a useful correlation exists between unfrozen water content of frozen soils and liquid limit flow curves. Liquid limit is found in accordance with the A.S.T.M. (American Society for Testing and Materials 1950) procedure (ASTM D4318 - 05, 2005) and the unfrozen water content is measured by the isothermal calorimetric method of Anderson and Tice (1973) and Anderson and Banin (1973).

Istomin et al. (2015, 2017) proposes a new method for estimating unfrozen and nonclathrate water contents in frozen soils. The method includes measuring the water potential and activity of water in soils, depending on temperature and water content, and use the results in thermodynamic calculations to determine the temperature associated with the unfrozen water content. The method has not yet been established, and testing remains for the method to be generally accepted.

The Norwegian Geo-Test Sites (NGTS) program is a Research and Development (R&D) program led by NGI (Norwegian Geotechnical Institute), including NTNU, UNIS, SINTEF (The Foundation for Scientific and Industrial Research) and the Norwegian Public Roads Administration. The program establishes five national test sites used as field laboratories for development, testing and verification of new innovative methods for site investigations and testing procedures (NGI, 2016). The purpose is to develop more cost effective and sustainable geotechnical solutions, and to reduce risks caused by climate changes, floods, and landslides. One of the test sites is located at Svalbard, and is representative for permafrost. Laboratory investigations will be performed to identify geotechnical parameters for permafrost sites. UNIS/SINTEF are coordinators for the site at Svalbard, and Arne Instanes is the project coordinator for the work performed there. Soil from the site will be investigated in this thesis.

1.2 Objectives

In this master thesis, soil from Svalbard, extruded in conjunction with the NGTS program, and soil from a construction site in Trondheim will be investigated. The main objectives of the master thesis are

1. To investigate methods for determining unfrozen water content in soils and discuss the efficiency of different methods.
2. To study the unfrozen water content vs. temperature in fine grained soils using the liquid limit determination and water potential measurements.
3. To present a one dimension geothermal model for investigating the effect of the unfrozen water content on heat flow in fine-grained soils.

1.3 Limitations

The results and conclusions obtained in this thesis is based on soil from only three different sites, two in Longyearbyen and one in the Trondheim area. For more reliable results, additional soils should be investigated. Due to lack of other accessible soils and the time limitation, that was not done in this thesis.

The water potential testing on the soils from the NGTS site was performed only on one temperature. AD-d-2-4 was tested only on 25 °C, and AD-d-4-4 only on 15 °C, due to the limited amount of soil available. Additionally, no previous testing is performed on these soils, which exclude the possibility of using them in the geothermal model.

Results for both liquid limit determination and water potential testing are dependent on human accuracy. The error is more prominent in liquid limit testing. To minimize human source of

error, more testing on the same soil should be performed. The time limit prevents the possibility of more extensive testing on the soils.

The Plaxis model only considers the effects of unfrozen water content on heat flow in soils. To obtain a more realistic model, other factors should be included, such as water flow, creep, and mechanical loads and deformations.

1.4 Approach

The first part of the master thesis is a literature study presenting and discussing different methods for determining unfrozen water content in frozen soils. Then an experimental study of selected fine grained soils is performed in the geotechnical laboratories at UNIS and NTNU. The study includes water potential and liquid limit tests on soil samples from Longyearbyen and fine grained soils from the Trondheim area. Lastly, a one-dimensional geothermal model to investigate the effect of the unfrozen water content on heat flow in the tested soils is applied, including the results from the laboratory work.

1.5 Structure of the Report

The rest of the report is structured as follows. Chapter 2 gives complementary information about permafrost and physical properties of frozen soil. Chapter 3 presents a selection of methods for determining unfrozen water content in frozen soils. Chapter 4 describes the experiments performed in laboratories at UNIS and NTNU, and the results are presented, interpreted and commented in chapter 5. The results for the unfrozen water content in frozen soils are used in a simple one dimensional model investigating the effect of unfrozen water content on heat flow in the tested soils. The model is presented in chapter 6. Chapter 7 summarizes the findings and gives recommendations for further work on the topic. Appendices include acronyms, nomenclature, information about the soil samples tested in the laboratory, detailed descriptions of calculations performed within chapter 5, and additional results from the geothermal model.

Chapter 2

Literature Review

2.1 Ground Temperatures

Ground temperatures are dependent on air and ground surface temperatures, heat flow from the interior of the earth, and soil thermal properties. The thermal properties are different for frozen and thawed soil. Additionally, the temperature is affected by snow cover, vegetation, and other climatic factors. The ground surface temperature fluctuates daily and annually, and can be estimated by

$$T_{s,t} = T_m + A_s \cdot \sin\left(\frac{2\pi t}{p}\right) \tag{2.1}$$

where T_m is the mean annual temperature, A_s is the surface temperature amplitude, t is the time, and p is the period, either 24 hours or 365 days. The surface temperature curve may be fitted to the measured temperatures, resulting in a shifted curve described by equation 2.2.

$$T_{s,t} = T_m - A_s \cdot \cos\left(\frac{2\pi t}{p} - \frac{2\pi\phi}{p}\right) \tag{2.2}$$

where ϕ is the phase lag in the same unit as the period p. When the heat flow from the interior of the earth is assumed negligible, the ground temperature can be calculated by the following simplified formula

$$T_{z,t} = T_m + A_s \cdot \exp\left(-z \cdot \sqrt{\frac{\pi}{\alpha_u p}}\right) \cdot \sin\left(\frac{2\pi t}{p} - z \cdot \sqrt{\frac{\pi}{\alpha_u p}}\right) \tag{2.3}$$

where α_u is the soil thermal diffusivity. Other parameters are as previously described. The am-

plitude of the maximum or minimum temperature at a certain depth decreases exponential, represented by formula 2.4 and figure 2.1.

$$T_z = T_m \pm A_s \cdot \exp\left(-z \cdot \sqrt{\frac{\pi}{\alpha_u p}}\right) \tag{2.4}$$

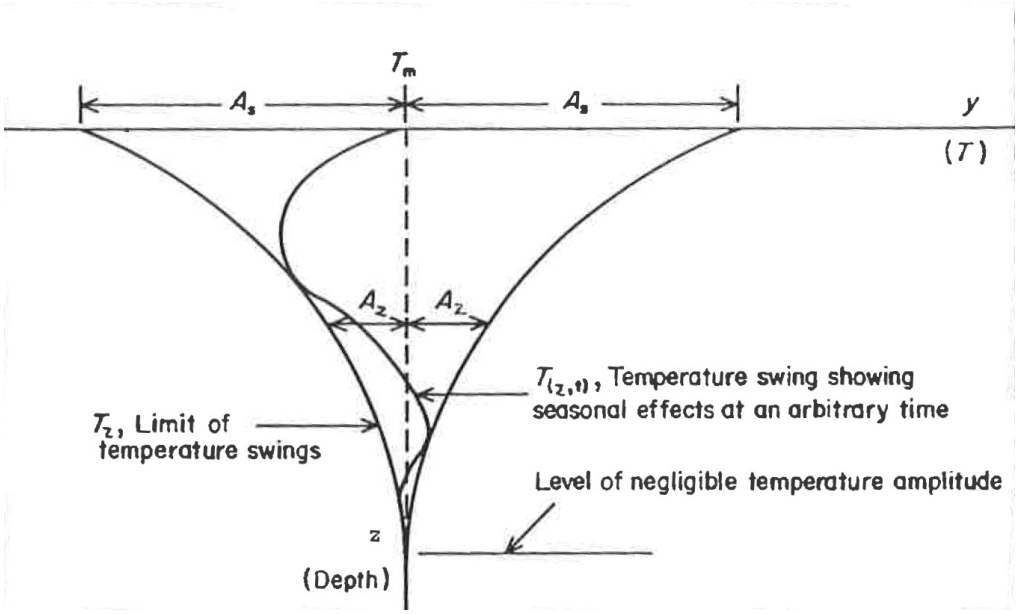

Figure 2.1: Trumpet curve, surface and ground temperatures (Andersland and Ladanyi, 1994).

The active layer of the ground is the upper layer with temperatures fluctuating between positive and negative degrees Celsius. A layer of constantly unfrozen soil may separate the active layer and the underlaying permafrost, but this layer is not always present. The thickness of the active layer depends on several factors, such as temperatures, soil type and moisture content, surface conditions, and topography. Figure 2.2 explains the layers of the ground and the temperature profile the ground experiences through the year. Below the point of zero annual temperature changes, the geothermal gradient describes the increasing of temperature with depth.

The annual freezing of the active layer causes a frost heave as the freezing surface is moving downward. The heave is a result of the volume of water increasing ~ 9% during freezing, and the formation of ice lenses due to water migration by capillary action through soil pores toward the freezing surface (Andersland and Ladanyi, 1994). Areas with inhomogeneous soil will experience uneven heave of the surface. During periods of warmer temperatures, the soil in the active layer thaws. The ground experiences settlements due to the phase change and drainage of excess water. As the upper layer starts thawing, there is a period where the downward drainage path is blocked by still frozen soil and the pore-water pressure in this layer will be temporary high, which my cause damage to infrastructure located above this zone.

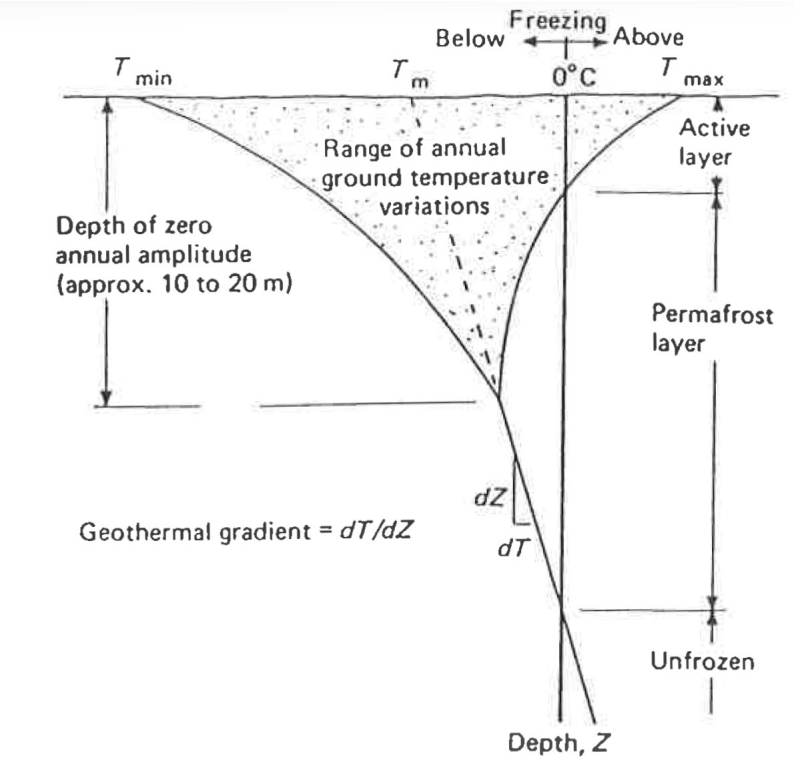

Figure 2.2: Temperature profile in permanent frozen soil (Andersland and Ladanyi, 1994).

2.2 Permafrost Features

The definition of permafrost is rock or soil below 0 °C over at least two consecutive winters and the intervening summer (Brown and Kupsch, 1974). The condition is controlled by climate and terrain factors, and the thickness of frozen soil is controlled by mean annual surface temperature T_m and the heat flow from the interior of the earth. The geothermal gradient (shown in figure 2.2) has been measured to range between 1 °C per. 22 m and 1 °C per. 160 m (Brown et al., 1981). The frozen soil may contain moisture as unfrozen water or ice.

Geographically, permafrost can be divided into discontinuous and continuous permafrost, limited by the -5 °C isotherm of mean annual ground temperature, measured just below the level of annual variation. Lakes and rivers of different sizes have various impact on the permafrost thickness due to freezing and thawing, and water circulation. An unfrozen zone will appear under unfrozen lakes, reducing the thickness of the permafrost layer.

Ground surface features indicates underlying frozen ground conditions. Examples of features are ice wedges, pingos, thermakarst terrain and patterned ground including polygons, circles, and stripes. Ice wedges are vertically masses of pure ice caused by cracks filled with water that freezes in low temperature. Ice wedges can create ridges on the surface making an ice polygon pattern. The polygon diameter varies because of variations in frozen soil strength and width of the stress release zone. Ice wedges are most common in continuous permafrost zones. Pin-

gos are conical asymmetric hills with a core of massive ground ice covered by vegetation and soil. They are caused by the uplift pressure from water freezing, and are by definition 10 m or higher and 100 m or wider. Thermokarst are different surface features caused by differential melting of ground ice because of changes in the thermal regime. Lateral permafrost degration (backwearing) is caused by erosion exposing ground ice. When ground ice melts, the ground experiences collapsing. Permafrost degration from above (downwearing) happens in level areas and are caused by an increased active layer resulting in settlements creating toughs and ponds. Patterned ground is a collective term for characteristic geometrical ground surface patterns, that may be sorted. Sorting means separating stones and fines, and is caused by cycles of frost heaving, thawing, and thrusting in grains with different water-holding capacity. Polygons associated with ice wedges is an example of non-sorted patterned ground in flat areas. In slopes, elongation creates stripes.

2.3 Physical Properties of Frozen Ground

The physical properties of frozen ground depends on freezing and thawing processes, and the seasonal and long term temperature changes. In general, frozen ground has increased strength and decreased permeability. During freezing, frost heave occurs because of the expansion of water freezing to ice. The effect of the freezing depends on expelled water and the rate of temperature lowering. When testing silt or silty sand in laboratories, the water freezes in-situ when the temperature change is rapid. When the temperature is lowered gradually, the water accumulates creating ice layers parallel to the surface expanded to the low temperature. In the field, ice layers in silty soil can be several centimeters thick. Water migration through soil voids result in frost heave, and the water supply from the ground controls the ice growth and thus the frost heave. Coarse layers and clay prevents the capillary action, and the system is considered closed. Open systems have a vertical distance between water table and freezing depth smaller than the height of capillary rise of the soil (Holtz and Kovacs, 1981). The maximum capillary rise, h_c, can be found from:

$$h_c[\text{m}] = \frac{0.03}{d[\text{mm}]} \tag{2.5}$$

where the effective pore diameter $d \approx 20$ % of the effective grain size D_{10}. In grain size distribution testing, D_{10} is known as the sieve size where only 10 % of the soil grains passes. Continually water supply from the water table results in continually ice lens growth in the freezing periods. The ice growth is controlled by the soil permeability. Hence, variable soil permeability causes nonhomogeneous frost heave. During thawing periods, the soil surrounding the ice lenses becomes highly saturated, and experiences significant loss of bearing capacity.

When soil is thawed, ice melts and the soil has to develop a new equilibrium void ratio ($e = V_v/V_s$). As the amount of melt water may exceed the absorbing capacity of the soil, excess pore pressure may temporary arise in the fine-grained soil with low permeability, until the drainage

is completed. During fast thawing, the soil and water may become a slurry with very low bearing capacity. Thaw settlement occurs from phase change, weight of the soil, and applied load. Under constructions, railways and highways in particular, it is important to control the drainage and know the consolidation behaviour of the soil.

Frost actions describes the detrimental processes of frost heave, thawing settlements, and thaw weakening of the foundation. Basic conditions for frost actions are frost-susceptible soils, water supply, and low temperatures allowing the water to freeze. If the active layer has underlying frozen soil, only lateral drainage will be possible, giving a closed system.

For engineers, it is possible to utilize the properties of frozen ground, such as high compressive strength, great bearing capacity and the impermeability considering water seepage, in different frozen earth structures. The strength of frozen ground is a combination of frictional resistance and interface between soil particles, dilatancy component, and interaction between ice and grains. Frozen Ottawa sand and frozen Sault Ste. Marie clay was tested at -12 °C (Andersland and Ladanyi, 1994). The clay had a larger unfrozen water component and showed more plastic behavior than the sand, while the sand had a compressive strength almost twice the compressive strength of the clay. The sand was tested frozen and unfrozen, with the same confinement and temperature, and showed compressive strength 8.5 times higher when frozen compared to unfrozen state. Tests on freezing clay gave the same effect, but the increased strength when frozen was smaller than for the sand.

Unfrozen clean sand and gravel has a permeability of 864 m/day $\approx$ 1 cm/s when unfrozen, but the permeability approaches zero when frozen (Andersland and Ladanyi, 1994). This can be utilized in excavations, and in some projects it is advantageous to perform work in the winter to lower the drainage and dewatering costs. In poorly drained areas, work below the water table can be done in the winter, when the bearing capacity is much higher than in the summer, and drainage expenses can be avoided.

In cold regions, ice and snow can substitute soil materials in temporary constructions. Freshwater ice has high resistance to deformations due to short-time loadings. Sea water has various properties, based on the salinity. Sufficient conditions regarding temperatures, terrain, water access, and suitable equipment are required for these conditions. The freezing rate of water depends on both temperature and wind conditions.

2.4 Unfrozen Water Content in Frozen Soil

Frozen soil contains soil particles, ice, unfrozen water, and gas or air. Voids are filled with ice, unfrozen water, and air, and soil grains are coated by a thin film of unfrozen water. Unfrozen water content w_u is defined as the mass of unfrozen water M_u divided by the mass of solids M_s, see formula 2.6.

$$w_u = \frac{M_u}{M_s} \cdot 100 \quad [\%] \tag{2.6}$$

The unfrozen water content in frozen soils affects the mechanical properties, i.e. the strength, varying from brittle to plastic. For engineers, the unfrozen water content is critical to determine to achieve successful solutions in cold areas. For pipelines in particular, the unfrozen water content may be crucial for the support and long-term water migration towards the pipelines (Tice et al., 1988). The amount of unfrozen water depends on the physical and chemical composition, and the mineralogy of the soil. Dominant factors are specific surface area, solute concentration, temperature, confining pressure, and initial water content (Anderson and Tice, 1973).

The ice content is altered by solutes in the pore water. Thermal properties of the soil depends on temperature changes, also causing frost actions. In order to identify and classify soils, information about water content, ice content, and frost susceptibility characteristics are required. Schematically the phases can be represented as in figure 2.3.

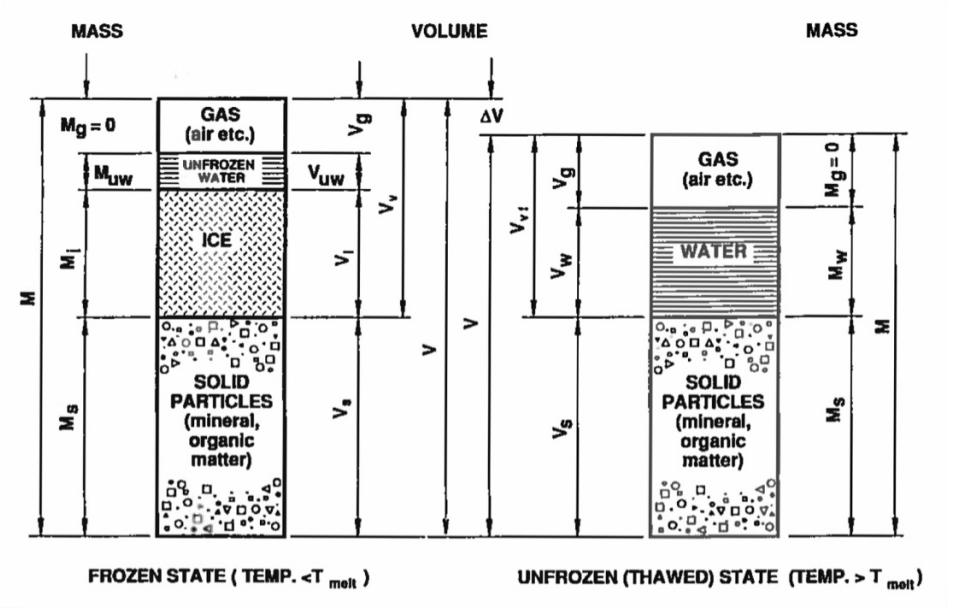

Figure 2.3: Mass-volume relationships for frozen and unfrozen soil (Andersland and Ladanyi, 1994).

Using the mass-volume relationships from the phase diagram and the fact that the mass of water is the sum of mass of ice and and mass of unfrozen water, $M_w = M_i + M_{uw}$, it is possible to find properties of the soil. Void ratio and porosity are given by formula 2.7 and formula 2.8, respectively.

$$e = \frac{V_v}{V_s} = \frac{\rho_s}{\rho_d} - 1 \quad [-] \tag{2.7}$$

$$n = \frac{V_v}{V} \cdot 100 \quad [\%] \tag{2.8}$$

V denotes volume, and $\rho = M/V$ denotes bulk density. The subscripts v, s, and d denotes void, solid, and dry, respectively. V is the total volume, and M is the total mass of the sample. Water content is given by the following formula

$$w = w_u + w_i = \frac{M_w}{M_s} \cdot 100 \quad [\%] \tag{2.9}$$

where w_u is the unfrozen water content, and w_i is the ice content. The vapor phase is usually neglected. As the temperature in the soil drops, water in the soil will freeze and ice will be formed. As seen in figure 2.4, the pore water does not start to freeze until the temperature drops to the supercooled temperature T_{sc}. The formation of ice releases latent heat and the temperature increases to the initial freezing temperature T_f. At T_f, the free water in the soil freezes, and the released latent heat is slowing the cooling process. A significant amount of water exists as unfrozen water film on soil particles, known as bound water. When the temperature has decreased to $T_e \approx -70$ °C, all the free water and most of the bound water is frozen. In frozen soil, ice is found in several forms; from coating on soil particles and small ice lenses to massive ice lenses, layers, wedges, and pingos. The ice growth is controlled by the water supply and the ease of movement, associated with frost heave. The relative ice content is defined by the ice ratio i_r.

$$i_r = \frac{M_i}{M_w} = \frac{w - w_u}{w} \tag{2.10}$$

where M_i is the mass of ice, and M_w is the total mass of water.

The water content in a cohesive soil is of great interest as it changes the properties of the soil. The specific surface is known as the ratio between grain surface area and the volume or weight of the grain, and is large for cohesive soils. Water will modify the attraction between the soil particles, and for soils with large specific surface, the bound water film may be a significant portion of the total water content. Increased water content changes the soil from dry and brittle solid via plastic solid to liquid. Tests performed on soils to define limit values of water content for different soil behaviours, such as Atterberg Limit tests and Casagrande test, are described in standards. Plastic limit w_P distinguish between brittle and plastic behaviour, and liquid limit w_L between plastic and liquid. Atterberg's plasticity index is defined as

$$I_P = w_L - w_P \tag{2.11}$$

The plasticity index describes the range of water content for plastic behaviour of a soil. A clay with water content lower than the plastic limit will crumble when remolded. With higher water content than the liquid limit, it will mobilize no shear strength. The limits increase at lower

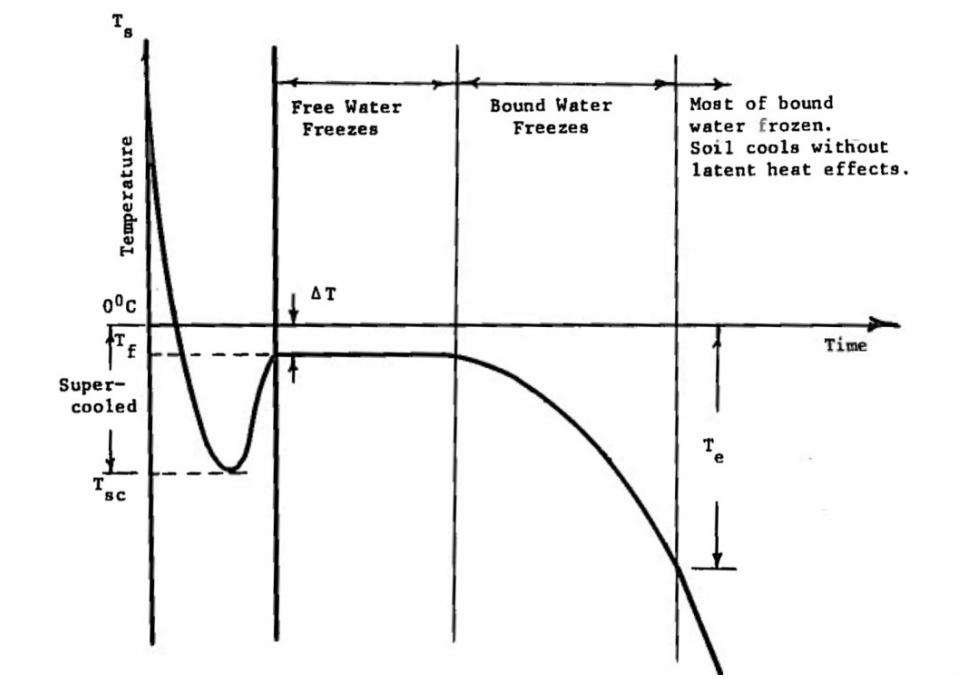

Figure 2.4: Cooling curve for soil water and ice (Andersland and Ladanyi, 1994).

temperatures. The Atterberg tests contribute in classifying soils and clays. To classify frozen soils, characteristics of the soil from frozen state and description of ice strata in the soil are added.

Several methods has been proposed to measure the unfrozen water content in partially frozen and frozen soils. The interest of utilizing clay soils compacted at low water contents as foundations has increased the demand of predicting the unfrozen water content quick and simple. The majority of the tests requires complicated equipment and operators, but also methods for calculating phase composition curves from simpler measurements has been proposed. A selection of the methods is presented in the next chapter.

Chapter 3

Methods for Determining Unfrozen Water Content

Water is found in porous materials, such as rocks and soils, in liquid state as capillary water and film on grains, and in solid state as ice or gas hydrate. Unfrozen water is defined as pore water in equilibrium with ice, and is present within a certain range of negative temperatures. The pore water - pore ice equilibrium is metastable because of crystallization of pore ice to bulk ice, while the pore water - bulk ice equilibrium is stable. The last condition, at different temperatures below 0 °C, is considered in this chapter.

Unfrozen water affects the strength and the hydraulic and thermal conductivity in soils, and influences the freezing and thawing processes in frozen soils. Unfrozen water exists in frozen soils because of the depressed melting point of water induced by absorption forces and the particle surface curvature (Watanabe and Mizoguchi, 2002). The concentration of solutes will also affect the melting point temperature of ice in soils. Unfrozen water affects the physicochemical and mechanic properties of soils and sediments, and the amount of unfrozen water depends on the porous media and temperature below 0 °C. Nonclathrated water can exist in hydrate-containing sediments and is defined as pore water in equilibrium with gas hydrate phase (Istomin et al., 2015). The amount of nonclathrated water depends on the gas pressure and the chemical nature of hydrate forming gas (e.g. methane, carbon dioxide, and nitrogen) in addition to type of material and temperature.

Several methods has been developed to determine unfrozen water content in frozen soil in relation with temperature, salinity, and type of soil. The methods vary in accuracy and complexity. Researchers have tried to find empirical formulas based on simple measurements for predicting the amount of unfrozen water at different temperatures. In this chapter a brief summary is given on a selection of different methods, and a more thorough description will be given on two methods that are further investigated later in this master thesis; the liquid limit determination (Tice et al., 1976) and a method for determination of unfrozen and nonclathrated water content in real and model porous media based on water potential (Istomin et al., 2015). In addition to the methods listed below, unfrozen water content can be estimated by x-ray diffraction, heat

capacity measurements, cryosopic, and adsoption.

3.1 Selection of Methods

3.1.1 Dilatometry

Dilatometry measures the expansion of the liquid water - ice phase change (Carter, 1993). A fully saturated soil sample is sealed in impermeable latex membrane and placed in a liquid filled chamber. The freezing temperature of the liquid must be below the temperatures tested. The chamber is placed in a bath holding a constant temperature. During testing, the temperature in the bath is stepwise changed. When nucleation occurs, the changing proportions of ice and unfrozen water is calculated from the volume of the liquid displaced from the chamber. This is done at each temperature step, giving an unfrozen water content curve. The method can only be performed at temperatures 1 - 2 degrees below 0 °C. The water is assumed to be incompressible and soil water is assumed to have a density change of 9 %, like pure water.

3.1.2 Differential Thermal Analysis and Differential Scanning Calorimetry

Differential thermal analysis (DTA) is called differential scanning calorimetry (DSC) when properly calibrated. In DTA, sample temperature is measured by an electrical thermometer and compared to the temperature of an inert reference substance, while both are exposed to a uniform temperature change. During a phase change, the measured temperature will lag behind or precede the reference substance temperature. This depends on whether the heat is being liberated or absorbed. In a frozen soil during DTA in low temperatures, latent heat of freezing is liberated, corresponding to the amount of ice formed and thus the unfrozen water content (Anderson and Morgenstern, 1973). From several analyses, a relationship between temperature θ and total sample water content w can be obtained, see formula 3.1. The relationship is based on the assumption that the sample is thermally uncoupled from the surroundings. At $\theta = 0$ °C, $w = w_u$.

$$\theta = [(w - w_u) \cdot L] / c \tag{3.1}$$

Unfrozen water content is determined from the water content where θ for the freezing exotherm goes to zero. The procedure does not account for all the energy processes involved, but provides good results according to values obtained from dilatometer and adiabatic calorimeter methods.

3.1.3 Adiabatic and Isothermal Calorimetry

In calorimetry, changes in enthalpy is measured in various processes. Additionally, calorimetry can be used to determine heat capacities. Calorimetry can be performed both adiabatic and isothermal. In adiabatic calorimetry, temperature changes in the process is monitored in a calorimeter, as there is no heat exchange with the surroundings. The adiabatic calorimeter is placed in a container with constant temperature during the process.

A soil specimen frozen to a particular temperature below 0 °C is placed in the calorimeter. The calorimeter is filled with water and the equilibrium temperature is measured when achieved. To calculate the unfrozen water content, specific heat of each soil component must be known, and radiation loss may be accounted for. The test is performed for several temperatures below 0 °C, and the corresponding unfrozen water content is computed. The results provide the basis for an unfrozen water content function.

Isothermal calorimeter method is developed to circumvent the limitations of differential thermal analysis (DTA), where only one point is obtained for the phase composition curve. To obtain equilibrium, the temperature is kept constant during the premeasurement equilibration period. The method is limited to temperatures > -10 °C, because of the difficulty of freezing samples without nucleation occurring before thermal equilibrium is achieved at lower temperatures (Anderson and Morgenstern, 1973).

In isothermal calorimetry w_u is obtained after freezing, and for adiabatic calorimetry it is obtained after thawing. During the warming of a sample a measured and regulated heat input is applied by a coil wound around the container of the sample. During cooling, the applied temperature is lower than the soil sample. The calculated specific heat of the soil during freezing and thawing is specific for a given temperature and soil type (Williams, 1964). The results can be used to calculate the ice formation proceeding in the soil, and thus, the unfrozen water content.

3.1.4 Nuclear Magnetic Resonance

Nuclear Magnetic Resonance (NMR) is a simple and rapid method for obtaining phase composition curves, and thus the unfrozen water content in frozen soils. The method utilizes that unfrozen water has a very narrow spectral line compared to that of ice. The technique is based on the assumption that the unfrozen water content at different temperatures is independent of the ice content. NMR measures induced voltage by changes in the magnetic field. The peak of the voltage decay curve is proportional to the amounts of water and ice in the sample (Watanabe and Mizoguchi, 2002). The signal from ice decreases faster than the signal from liquid water, which allows determination of unfrozen water in the sample from the voltage decay curve.

A soil sample at initial given moisture content is sealed and placed in the NMR probe. Specimen temperature and the first pulse NMR signal amplitude is recorded. For warming cycles, the procedure is repeated for several temperatures up to a temperature where all ice in the soil is

thawed. For cooling cycles, the temperatures is decreased from a temperature slightly below the melting point. The ratio of the gravimetric water content to the first amplitude of the ice-free case for the specimen is determined. The measured first pulse amplitude at the different temperatures is multiplied by the determined ice-free ratio to obtain the unfrozen water content (Tice et al., 1988). The technique can be used in a wide range of temperatures, both at and below melting point of ice in frozen soils. After measurements, the original water content is found.

Tice et al. (1978) test four soils and the results are consistent with results from isothermal calorimetry, but the procedure is much faster. Tice et al. (1988) test 16 undisturbed core samples from Alaska and find that there is a slight difference in unfrozen water content for cooling and warming curves. Logarithms of data obtained during the test were linearly regressed to formula 3.2 and values for soil parameters α and β are obtained. θ is the absolute value of the temperature in Celsius below 0 °C. From the tests it seems like freezing and thawing cycles has a very small impact on the unfrozen water content.

$$w_u = \alpha\theta^{\beta} \quad [\%] \tag{3.2}$$

3.1.5 Time-Domain Reflectometry

Time Domian Reflectometry (TDR) measures the liquid water content w_u in frozen soil by utilizing the fact that ice has much lower permittivity than water. The technique determines the apparent dielectric constant K_a by measuring the propagation velocity and reflection voltage of a transverse electromagnetic wave. The dielectric constant for soil and ice is low ($K_a = 3.2$ for ice, $K_a \approx 2-4$ for soils), while it is much higher for free water ($K_a = 80$ at 20 °C). The dielectric constant depends little on soil type, density, temperature, and salinity, but is highly dependent on liquid water content (Hivon and Sego, 1990).

Topp et al. (1980) present a relationship between dielectric constant and unfrozen water content:

$$K_a = 3.03 + 9.30\,w_u + 146.0\,w_u^2 - 76.7\,w_u^3 \tag{3.3}$$

where K_a is the dielectric constant, and w_u is the unfrozen water content. The method is simple and applicable for most soils, except from very fine-grained and organic soils. In materials with high specific area (very fine-grained soils), K_a decreases because a large amount of water with $K_a < 80$ is absorbed (Smith and Tice, 1988), while saline pore fluids increase the signal because of the high electrical conductivity in saline pore fluids (Hivon and Sego, 1990). The method has later been extended to include volumetric unfrozen water content in frozen soils, and unfrozen water content in saline frozen soils. At low water contents, the method tends to overestimate the unfrozen water content (Patterson and Smith, 1983).

Hayhoe et al. (1983) determines the apparent unfrozen water content in frozen soils *in situ* by

determining the dielectric constant K_a with TDR. Smith and Patterson (1984) reports supplementary experimental data to support the empirical relationship between K_a and w_u in frozen and unfrozen soils. An experimental apparatus was presented for combining a dilatometer for measuring w_u and a TDR parallel line probe for measuring K_a. The measurements are performed simultaneously at a wide range of freezing temperatures for several soil types, such as sand, sandy loam, silty loam and clay loam.

Spaans and Baker (1995) designed a gas dilatometer to calibrate TDR for w_u in frozen soil. Calibrations of drying soil where water is replaced by air cannot be implemented for frozen soils, where water is replaced by ice, as the permittivity of ice is greater than that of air (Spaans and Baker, 1995). Thus, the soil sample is hermetically sealed in the gas dilatometer. Freezing of the soil results in reduced volume of air due to the fact that ice has lower density than water, and increased pressure inside the dilatometer. The amount of water freezing is determined from the measurement of change in pressure while incrementally decreasing the temperature. Spaans and Baker (1995) test two samples of the same soil, with different total water contents, resulting in the same slope but with different intercepts.

3.1.6 Contact Method

The contact method estimates unfrozen or nonclathrate water contents in clay samples directly. The equilibrium water content is measured in a dried sediment plate placed in close contact with two ice plates under isothermal conditions (Yershov et al., 1979). The experiments takes approximately two weeks to carry out.

A modified contact method is developed for measuring the nonclathrate water content. Pore water is measured in equilibrium with bulk gas hydrate at temperatures below and above 0 °C. The weight of a dried soil sample is measured and the sample is placed between two ice plates or ice rich sand plates and loaded into a pressure cell at a predetermined temperature below 0 °C. During the experiment, the temperature is kept at this temperature. By injecting a hydrate-forming gas, the pressure increases to exceed the “ice-gas-hydrate” equilibrium. When equilibrium water saturation is achieved, the gas pressure is at the ambient level. The sample is then withdrawn and weighed, and the weight difference represents the equilibrium moisture content of the sample. At temperatures above 0 °C, the pre-dried and weighed sample is placed between to plates of wet sand and loaded into a pressure cell at predetermined temperature below 0 °C. A hydrate-forming gas is injected to the cell and the cell is heated to a specified positive Celsius temperature. At equilibrium water saturation, the gas pressure is decreased to atmospheric level and the sample is withdrawn and the weight is measured. The weight difference between before and after the experiment represents the equilibrium moisture content.

3.2 Liquid Limit Determination

Tice et al. (1976) document experiments on different soils with varying total water contents and different physical properties. A method of estimating the content of unfrozen water contents at various temperatures from liquid limit determinations is proposed, shown in formula 3.4.

$$w_u = \alpha\theta^{\beta} \quad [\%] \tag{3.4}$$

The unfrozen water content w_u is defined by equation 2.6. α and β are characteristic soil parameters, and θ is temperature in Celcius below freezing, expressed as a positive number. α and β are tabulated values found from several tests (Andersland and Ladanyi, 1994).

For soils not tabulated, a simple procedure is developed for calculating α and β based on liquid limit w_L data. The liquid limit is found by the Casagrande test procedure (e.g., see NTNU Geotechnical Division, 2015, Chap. 4).

The water contents $w_{N=25}$ and $w_{N=100}$ are measured or calculated, and used in the empirical relationships in equations 3.5 and 3.6 with a correlation coefficient of 0.98. The formulas are found from the best fit of the unfrozen water content curve calculated from individual liquid limit flow curves for different soils, and fits well with the unfrozen water content measured by the isothermal calorimetric method performed by Tice et al. (1976).

$$w_{u,\theta=1} = 0.346 \cdot w_{N=25} - 3.01 \tag{3.5}$$

$$w_{u,\theta=2} = 0.338 \cdot w_{N=100} - 3.72 \tag{3.6}$$

Using the values of $w_{u,\theta=1}$ and $w_{u,\theta=1}$ in formula 3.4, α and β can be evaluated, and the complete phase-composition curve can be established for a specific soil. The method shows great correlations with measured values obtained by several tests, such as dilatometry, adiabatic and isothermal calorimetry, x-ray diffraction, heat capacity measurements, nuclear magnetic resonance, and differential thermal analysis (Anderson and Morgenstern, 1973).

The method is widely accepted for many engineering applications, for soils considered not to contain excessive amounts of soluble salts. Dissolved solutes in pore water result in a decreased freezing temperature leading to increased unfrozen water content in the soil. High salinity reduces the frost susceptibility due to decreased freezing index and increased thawing index (Andersland and Ladanyi, 1994, Chap. 3). A soil with high salinity has a lower ice content, resulting in reduced frozen strength and increased creep rate. If the soil contains considerable amounts of soluble salts, a correction to the equations above is required (Banin and Anderson, 1974). For soils with liquid limit $w_L > 100$ %, investigations indicate that the unfrozen water content is noticeably lower than predicted from the equations, and the method is not recommended.

3.3 Water Potential Determination

The water potential method estimates the contents of liquid water in equilibrium with bulk ice and bulk gas hydrate. Water content in equilibrium with bulk ice is defined as unfrozen water, and water in equilibrium with gas and gas hydrate as nonclathrate water. The method is proposed by Istomin et al. (2015, 2017), and the main purpose is to determine a rapid and implicit method.

The test is performed using a Dewpoint Potentiameter, such as WP4-T or WP4C, developed by Decagon Devices. The device measures the pore water potential, dependent on temperature and moisture content, and thermodynamic activity of water at atmospheric pressure. Based on experimental determination of water potential and water activity in porous media, the measured data is used in thermodynamic calculations for determining pressure- and temperature-dependent unfrozen and nonclathrate water content. The water contents calculated by this method show good correlation with results from direct contact measurements for equilibrium water in contact with ice or gas hydrate at given temperatures and pressures (Istomin et al., 2015, 2017).

3.3.1 Theory

Water potential, ψ [MPa], is the potential energy of water per unit volume relative to pure water in reference conditions, and describes the ability of water movement, such as capillary action. The concept of water potential is useful in understanding the movement of water in soils, plants, and animals, and is an important factor within agriculture. Without flow restrictions, water will move from an area with high water potential to an area with lower water potential. Factors affecting the water potential act simultaneously in systems. While solutes decrease the water potential, increased pressure will increase the potential.

In soil physics, water potential describes the thermodynamic state of pore water. The determination of water potential is quite simple, and several methods exists. The WP4-T device measures water potential by the condensation method, detecting water vapor dew point of a gas phase in equilibrium with a porous medium, in the temperature range of 5 °C to 43 °C for natural soils with different particle sizes and moisture contents. The dew point is converted to water vapor pressure p_{wpor} over the soil sample with known moisture content at a given temperature. The accuracy is ±0.1 MPa for water potential of 0 to −10 MPa, and ±1 MPa for −10 to −300 MPa. Additionally, the WP4-T device measures activity of water a as a function of moisture content of the soil w. The error of the determined activity a is $1-2\%$ for $0.8 \leq a \leq 1.0$. Experimental data on water potential and water activity are utilized in thermodynamic calculations to estimate unfrozen and nonclathrated water content as a function of pressure and temperature.

The definitions of activity of water and water potential are given by formula 3.7 and formula 3.8, respectively. Originally, temperature is presented in Kelvin, but the formulas are converted to present the temperature in Celsius.

$$a = \frac{p_{wpor}}{p_w} \quad [\text{-}] \tag{3.7}$$

$$\psi = R(T+273.15)\frac{\rho}{M}\ln\frac{p_{wpor}}{p_w} = R(T+273.15)\frac{\rho}{M}\ln a \quad [\text{MPa}] \tag{3.8}$$

where p_{wpor} is the water vapor pressure of the air above the sample (at atmospheric pressure), p_w the saturation vapor pressure of bulk water at sample temperature, $R = 8.314$ J/(mol K) = 8.314 J/(mol °C) is the universal gas constant, T the sample temperature [°C], $M = 18.015$ g/mol is the molecular weight of water, and $\rho = 1.0$ g/cm^3 is the density of water. The relation between water activity and water potential is also shown in equation 3.9.

$$\begin{aligned} a &= \exp\left[\frac{\psi M}{R(T+273.15)\rho}\right] = \exp\left[\frac{\psi \cdot 18.015}{8.314\cdot(T+273.15)\cdot 1.0}\right] \\ &\approx \exp\left[2.167\cdot\frac{\psi}{(T+273.15)}\right] \end{aligned} \tag{3.9}$$

The pore water potential ψ and water activity a, obtained on the WP4-T device, can be converted to the difference between chemical potentials of bulk water, $\mu_w(T)$, and pore water, $\mu_{wpor}(w,T)$. The difference $\Delta\mu_{w,wpor} = \mu_w - \mu_{wpor}$ is dependent of moisture content and temperature of the sample. The relation between $\Delta\mu_{w,wpor}$ and pore water potential ψ is shown in formula 3.10, and the relation between $\Delta\mu_{w,wpor}$ and activity of water a in formula 3.11.

$$\Delta\mu_{w,wpor}(w,T) = -\psi\frac{M}{\rho} \quad [\text{J/mol}] \tag{3.10}$$

$$\Delta\mu_{w,wpor}(w,T) = -R(T+273.15)\ln a \quad [\text{J/mol}] \tag{3.11}$$

From this, Istomin et al. (2015) show that the thermodynamics of pore water can be completely determined by water potential and activity of water, as functions of moisture content w and sample temperature T. For carrying out water potential of saturated dispersed media on the WP4-T device, Istomin et al. (2015) uses the standard method (Campbell et al., 2007). The method measures sample temperature T_s and dew point temperature T_d of the head space above a sample, for air equilibrated with the sample. The vapor pressure is a function depending on temperature only;

$$p_{wpor} = 0.611\exp\left(\frac{17.502\cdot T_d}{240.97+T_d}\right) \tag{3.12}$$

$$p_w = 0.611 \exp\left(\frac{17.502 \cdot T_s}{240.97 + T_s}\right) \tag{3.13}$$

where T_d and T_s is the dew point temperature and sample temperature, respectively, measured in Celsius. This results in the following formula for water potential:

$$\begin{aligned} \psi &= \frac{R(T + 273.15) \cdot 17.502\rho}{M} \ln \frac{p_{wpor}}{p_w} \\ &= \frac{R(T + 273.15) \cdot 17.502\rho}{M} \left(\frac{T_d}{T_d + 240.97} - \frac{T_s}{T_s + 240.97}\right) \quad \text{[MPa]} \end{aligned} \tag{3.14}$$

3.3.2 Procedure of Measuring Water Potential

Preparing the sample correctly is critical for obtaining accurate results. Measurements performed by Campbell et al. (2007), are made on soil that has been air dried and sieved through a 2 mm sieve. The range of water content added to the soil during testing depends on the clay content of the sample. The sample used for testing is being exposed to the air for several days so that the moisture content is in equilibrium with the air. Based on the definition of water content, (equation 2.9), the following equation is obtained for determining the mass of water to add to a given mass of air dry soil to get the desired water content:

$$M_w = M_{ad} \cdot \frac{w - w_{ad}}{1 + w_{ad}} \tag{3.15}$$

where M_{ad} is the mass of air dry soil, w is the desired final water content, and w_{ad} is the water content of the air dry soil. Between five and ten 50 g samples of sieved, air dry soil are placed in containers and sealed with a lid. Amounts of water to add to produce a set of samples with water contents ranging from air dry to a little wetter than water potential of 1.5 MPa is calculated by equation 3.15. The average air dry water content and the 1.5 MPa water content for a soil can be found from experimental data. The added water is mixed with the soil and the containers with the soil water mixtures are sealed and left to equilibrate for 24 hours.

After the equilibration, sub samples are placed in the WP4-T device, and the suction is determined. Samples with suctions wetter than 1 MPa are discarded, and the water content is found for the rest of the samples by standard procedure (e.g., see NTNU Geotechnical Division, 2015, Chap. 4). Additional samples can be prepared with appropriate water contents to fill in where data are sparse. Alternatively, 5 g samples of air dry soil can be placed in the WP4-T device. The cups are suspended over water to take up water through vapor absorption, and removed at intervals to get a range of suctions. The cups has to be sealed and allowed to equilibrate for 24 hours before the readings. This method is useful for high clay samples, where small amounts of

water cannot be mixed thoroughly with the samples to give a uniform water content.

Campbell et al. (2007) test different soils, from sand to clay, and the result is a model of suction as a function of water content, with very good agreement among samples. The relation is shown in formula 3.16.

$$\psi_t = 10^{aw+b} \tag{3.16}$$

where a and b are soil constants, and w is the water content. Plotting water content vs. the logarithm of suction gives a linear relationship. The accuracy is about 1 %.

Istomin et al. (2015, 2017) use samples of ~ 3.8 cm in diameter and $0.5 - 1.0$ cm height, with moisture content ranging from $0 - 1\%$ to complete saturation. The water potential is measured at maximal water content and the sample is dried step-wise in air until completely dry. The drying is controlled by weighing the sample on a scale with an accuracy of 0.001 g. Moisture content and water potential is measured at every step, in a temperature ranging from 15 °C to 40 °C. Moisture content is measured both before and after the water potential measurement, giving water potential dependent of moisture content and temperature. For dry samples of $10 - 15$ g, the error of moisture content determination does not exceed 0.5 % for samples with $w \geq 5$ %. Water potential and temperature are recorded automatically and can be transferred directly to a computer, using the program Hyper Terminal. The result is values for temperature T, moisture content w and water potential ψ, adapted to activity of water a, and the difference between chemical potentials $\Delta\mu_{w,wpor}(w,T)$.

3.3.3 Thermodynamic Calculations for Finding Unfrozen Water Content

Choosing a bulk phase of pure liquid water at atmospheric pressure $p_0 = 0.1013$ MPa as a standard state, the difference between chemical potential of pore water and chemical potential of pure bulk water at p_0 and different temperatures are considered. The standard state at temperatures below 0 °C, is supercooled bulk water, which is metastable, i.e. stable when subjected to no more than small disturbances. This state exists up to ~ −38 °C. Due to extensive experimental data on supercooled water up to ~ −25 °C, choosing supercooled data as the standard state is not limiting the results. In this procedure, standard conditions are defined as $T_0 = 0$ °C and $p_0 = 0.1013$ MPa.

The unfrozen water content at a given temperature is described as pore water - bulk ice equilibrium (Istomin et al., 2017). Based on thermodynamical properties of pore water in porous medium, an approximate formula for the difference between chemical potentials of bulk supercooled water $\mu_w(T)$ and bulk ice $\mu_i(T)$ is derived (Istomin et al., 2015):

$$\begin{aligned}\Delta\mu_{w,i}(T) &= 6008\cdot\left(1-\frac{T+273.15}{T_0+273.15}\right)\\ &\quad -38.2\cdot\left[(T+273.15)\ln\frac{T+273.15}{T_0+273.15}+\left(T_0+273.15-(T+273.15)\right)\right]\\ &= 6008\cdot\left(1-\frac{T+273.15}{273.15}\right)\\ &\quad -38.2\cdot\left[(T+273.15)\ln\frac{T+273.15}{273.15}+(T_0-T)\right]\end{aligned} \tag{3.17}$$

at standard conditions (i.e. $T_0 = 0$ °C). The temperature is in Celsius. $\Delta H = 6008$ J/mol is a molar enthalpy difference between water and ice at 0 °C and $\Delta C = 38.2$ J/(mol K) = 38.2 J/(mol °C) is the heat capacity difference between supercooled water and ice. The formula shows good agreement with measurements of water and ice pressures (Istomin et al., 2015).

At equilibrium of pore water and bulk ice at $p_0 = 0.1013$ MPa and $T \le T_0$, the difference between chemical potentials of bulk water and pore water is equal the difference between bulk supercooled water and bulk ice; $\Delta\mu_{w,wpor}(w,T) = \Delta\mu_{w,i}(T)$. If the experimental value of $\Delta\mu_{w,wpor}(w,T)$ is known, the equilibrium moisture content w may be calculated as a function of temperature T for $T \le T_0$. From formula 3.11 and 3.17 the following relationship is obtained for activity of water as a function of moisture content w and temperature:

$$\begin{aligned}-R(T+273.15)\ln a &= 6008\cdot\left(1-\frac{T+273.15}{273.15}\right)\\ &\quad -38.2\cdot\left[(T+273.15)\ln\frac{T+273.15}{273.15}+(T_0-T)\right]\end{aligned} \tag{3.18}$$

Formulas 3.17 and 3.18 make it possible to calculate the freezing temperature of pore water if moisture content and water potential or activity is known. Thus, the unfrozen water content can be estimated.

In practice, a more convenient formula is used, relating equilibrium temperature T_{eq} [°C] to pore water activity $a = a(w,T)$:

$$T_{eq} = T_f = 103.25\ln a + 5.57(1-a)^2 \quad [°C] \tag{3.19}$$

where T_f is melting temperature of pore ice, i.e. the equilibrium temperature of saturated porous materials. Equations 3.18 and 3.19 show good correlations and provide almost identical results for $0.6 < a < 1.0$ (Istomin et al., 2017).

At a given moisture content w, the activity of water is only dependent on temperature. For activity values estimated at two temperatures, the activity can be extrapolated to temperatures below 0 °C using $\ln a = b_1 + b_2/T$, where $b_1$and b_2 are empirical constants. Results from experiments

performed by Istomin et al. (2017) shows low temperature dependency of a for porous materials. Only for dry materials, the temperature dependence is not negligible. It can be assumed that $a = a(w)$ for temperatures between - 15 °C and 0 °C.

The formulas above are applied to stable thermodynamic equilibrium of pore water in samples with bulk ice. This is common for natural porous materials, such as frozen sediments and soils. For metastable pore ice - pore water equilibrium, when the chemical potential of pore ice exceeds that of bulk ice, there are practical implications for synthetic porous materials with narrow pore size distributions.

The temperature of freezing T_f of water saturated dispersed media can be found from formula 3.18 and activity of water utilizing equation 3.19. Comparing equilibrium temperature and liquid content under these conditions, makes it possible to determine the equilibrium water content at predetermined negative Celsius temperatures. Unfrozen water content can be found from the moisture content of the tested soil, at different temperatures and water potentials.

The unfrozen pore water content is decreasing in freezing synthetic fine-grained materials (Istomin et al., 2017). It is shown that for glass beads, the decrease is monotonous, and for CPG samples, the decrease is stepwise with plateaus. The stepwise decrease is caused by the different freezing points of water in pores between grains and water in capillaries inside grains. The study shows that the freezing point of capillary water is lower in smaller capillaries. In porous materials free from capillary water, the moisture is found as films on the grains, and the amount correlates to the specific surface area of the grains. The results of thermodynamic calculations correspond well with experimental results from the contact method for negative temperatures of - 20 to - 30 °C. As the sample is cooled, the unfrozen water content decreases.

3.3.4 Thermodynamic Calculations for Finding Nonclathrate Water Content

The procedure of finding the nonclathrated water content is not performed in this master thesis, but the thermodynamic calculations are presented here. The shift of pore ice melting point in a single capillary, freezing shift ΔT_f, is correlated to pore water activity in the range $0.6 \leq a \leq 1.0$ and can be estimated by formula 3.20.

$$\Delta T_f = -85a^4 + 345.93a^3 - 578.46a^2 + 562.18a + 28.501 \tag{3.20}$$

This thermodynamic approach is used in calculating the nonclathrate water content. The shift to lower temperatures of hydrate formation, ΔT_h, is dependent on the moisture content of the sample, and is estimated by formula 3.21, proposed by Korotaev et al. (1973), updated by Najibi et al. (2006) and modified for pore water by Istomin et al. (2015).

$$\Delta T_h = 0.674 \cdot \Delta T_f \tag{3.21}$$

Alternatively formula 3.22, recommended by Istomin et al. (2015, 2017), can be used. $\Delta T_h = T_h - T_0$, where T_0 is the equilibrium temperature of gas hydrate in the system. The constant 68.6 is for methane gas, and the number varies slightly depending on the pressure and hydrate-forming gas.

$$\Delta T_h = 68.6 \cdot \ln a \tag{3.22}$$

The formation of methane hydrate depends on moisture content, and can be estimated from water activity by equation 3.22. At lower moisture contents, the pore water activity decreases, and the hydrate formation conditions shift toward lower temperatures and higher pressures. The determination of gas hydrate formation conditions in porous media depends on the temperature shift, which is correlated to hydrate formation with equilibrium moisture content (nonclathrate water) in fine-grained materials. Similarly to unfrozen water content variations, pore water converts into hydrate in a certain range of temperatures, during freezing in synthetic porous media and natural sediments. The nonclathrate water content depends on grain size, mineralogy, and pore space structure, and decreases monotonically in clay sediments and glass beads, and stepwise in CPG. Clays with larger specific surface area of the grains can contain more nonclathrate water. The nonclathrate water content in kaolinite clay calculated from measured water potential fits good with the content measured directly.

The nonclathrated water can be found using the activity of water and formula 3.20. While temperatures decrease and the pressure increases, the hydrate formation changes and the moisture content is reduced, which results in a lower activity of pore water. The value of the depressing of hydrate forming temperature, ΔT_h, is the most important parameter for determination of gas hydrate formation conditions in porous media. The gas pressure has no appreciable effect on the value, and the the connection between ΔT_h and nonclathrated water content can be investigated. For kaolinite clay, the variations of nonclathrated water content are similar to variations of unfrozen water content. The nonclathrated water content is also determined by grains size and mineral composition of dispersed media, and the pore space structure. For kaolinite clay, the correlation between calculated data of nonclathrated water content using water potential and experimental values obtained by the contact method is good, with a maximum deviation of 0.3 % in the temperature range of - 4 °C to - 17 °C.

3.3.5 Previous Tests and Results

Istomin et al. (2015) and Istomin et al. (2017) tests the procedure on natural kaolinite and polymineral clays, and artificial samples with known particle and pore sizes; controlled pore glass (CPG), a silicia powder consisting of 20 micrometer sized particles with internal porous structure. The porosity of CPG is formed both by empty space inside the particles, and space between particles. The materials and their composition are described more thoroughly in Istomin et al. (2017).

From the measured water potential ψ, Istomin et al. (2017) calculated pore water activity and

difference of chemical potentials for porous fine-grained soils with different moisture contents by equations 3.7 to 3.11. Measurements were carried out at temperatures ranging from 16 °C to 32 °C. The results are summarized in their report (see Istomin et al., 2017, table 3, figures 1 and 2). Results from the test shows that water potential and activity decrease uniformly with decrease of moisture. At high moisture contents the decrease is slow, while it is more rapid at lower moisture contents. The temperature effect on the activity water is within the measurement error.

In more complex materials, such as CPG with fixed sizes of capillaries, the results are less uniform and more intricate. The pore water activity curves are more stepwise with plateaus with insignificant variations within a certain moisture range. The lack of variation is explained by the filling of main capillaries within the CPG particles. At low moisture contents, the pore water is restricted to films, and the activity is reduced as the capillaries become thinner. The Kelvin equation relates activity of capillary water with capillary radius:

$$R(T+273.15)\ln a = \frac{-2\sigma V\cos\theta}{r} \tag{3.23}$$

where r is the capillary radius, T is the temperature [°C], $\sigma = 71.98$ J/m^2 is the liquid surface tension at 25 °C, V is the liquid molar volume, the contact angle between the liquid and solid surface at the pore wall.

Comparisons of values of water activity obtained in the test and from the Kelvin equation performed by Istomin et al. (2017), show good agreement, which implies that the measurements provide reliable estimates of pore water activity in porous materials.

For natural clay samples, the variations of water potential and activity are moisture dependent, like those in glass beads. The decrease is slow in samples with high moisture contents and rapid in samples with low moisture contents. The decrease is uniform due to the broader pore size distribution.

For kaolinite clay, the unfrozen water content is reduced as the temperature in the soil decreases. The test shows good correlation between experimental (contact method) and calculated data, with a maximum deviation of 0.5 %. The decreasing of unfrozen water content is monotonous for the glass beads, and stepwise for the CPG, because of different freezing temperature of pore water and water within grains capillaries. In porous media, there is no capillary water, and the unfrozen film water content correlates with the specific surface area.

From the results of studies performed by Istomin et al. (2015, 2017) it can be concluded that the pore water activity is dependent on moisture content and the pore space structure of the sample. The difference between pore and bulk water increases at drier samples, and correspondingly, the water activity decreases.

Chapter 4

Experiments

4.1 Liquid Limit Determination

4.1.1 Purpose and Theory

In natural state, clay can be defined as liquid, plastic, firm/crumbling, or hard (dry), depending on the water content (Atterberg, 1913). The water contents of a sample distinguishing between the different states are liquid limit w_L, plastic limit w_P, and shrinkage limit w_S. The purpose of the liquid limit determination is to find the water content distinguishing between liquid and plastic state. In this case the information will be used to predict the unfrozen water content for different temperatures of different soils.

4.1.2 Hypothesis

It is believed that the test results will provide diagrams similar to those obtained in Tice et al. (1976), and that they will correlate with results obtained from the water potential testing.

4.1.3 Equipment

The following equipment is used for the test:

- Casagrande apparatus
- Grooving tool
- Clay samples (specified in appendix C)

- Spatula
- Scale
- Distilled water
- Drying oven
- Crucibles or other ovenproof cups

For the test, three different samples of soil is used; clay from Lilleby, Trondheim, clay from UNIS East, Longyearbyen, and soil from the NGTS site in Adventdalen, Longyearbyen, which is apparently sandy silt. Specifications for the clays are given in appendix C. The apparatus is shown in figure 4.1.

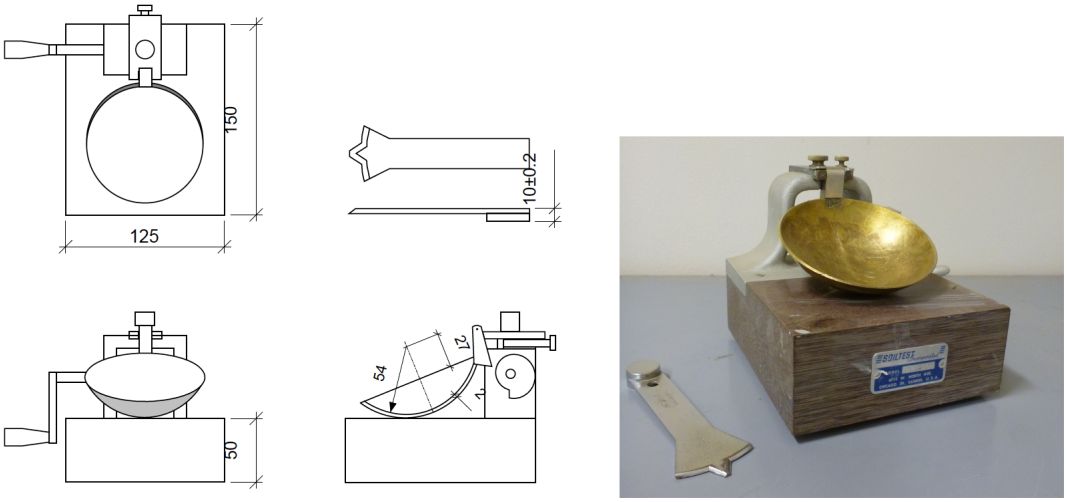

Figure 4.1: Casagrande's liquid limit device (NTNU Geotechnical Division, 2015).

4.1.4 Test Procedure

The liquid limit determination is performed based on the Norwegian Standard procedure (NS 8001, 1982), but the sample preparation differs slightly. Distilled water is added to air-dry samples to form a thick paste. The sample is mixed thoroughly and additional water is added so the water content corresponds with 8 blows on the liquid limit device. The sample is then sealed and stored for one week to equilibrate. Tice et al. (1976) let the samples equilibrate for two weeks, but after discussions with professors at NTNU it was considered that one week was sufficient. Between successive determinations, the sample is exposed to atmosphere to reduce the water content, then mixed and allowed to re-equilibrate for 45 minutes.

The Casagrande aparatus is calibrated in accordance with NS 8001 (1982). Moist, remolded material is placed in the Casagrande cup, shown in figure 4.1. The surface is smoothed and

the thickness of the clay is approximately 1 cm. A groove of width 2.0 mm is established by a grooving tool. The cup is lifted 10 mm by means of a crack and then dropped. This is repeated with ~ 2 drops per second, until the two halves of the soil paste touches each other at a 12.5 mm length in the bottom of the groove. The procedure is performed until the number of drops N equals exactly 25 and then 100 at the closing of the groove.

Alternatively, linear regression can be utilized for determining liquid limit w_L (NTNU Geotechnical Division, 2015). Three determinations with different water contents are carried out. For each determination, the number of drops needed to close the groove over a 12.5 mm distance are found. The number of drops should vary with approximately 5 drops and be within the following intervals: 15 - 25, 20 - 30 and 25 - 35. Corresponding values of water content and number of drops are presented in a diagram. A straight line is drawn through the points, and the liquid limit water content w_L is determined at the intersection of 25 drops. The same procedure can be used to find the water content at N = 100, $w_{N=100}$. Number of drops varies in the intervals 90 - 100, 95 - 105, and 100 - 110. A straight line is drawn and $w_{N=100}$ is found at the intersection of 100 drops. The last method is used in this thesis.

The test is performed for all four soil samples and the results are presented in table 5.1 and the interpretation of the results are showed in equations 5.1 - 5.4, and in figures 5.2 - 5.5. The procedures of linear regression for finding $w_{N=25}$ and $w_{N=100}$ are shown in appendix D.

4.2 Water Potential Determination

4.2.1 Purpose and Theory

The main purpose av this test is to investigate the possibilities of using the water potential determination method for calculating unfrozen water content in frozen soil. The method is proposed by Istomin et al. (2017, 2015), but has not yet been established as an accepted method. More testing remains. The theory behind the test is further described in chapter 3.

4.2.2 Hypothesis

It is believed that the test results will provide diagrams similar to the results presented in Istomin et al. (2017). Furthermore, it is expected that the values for unfrozen water content will match the results obtained in the liquid limit determination method.

4.2.3 Equipment

The following equipment was used for the test:

- Dewpoint PotentiaMeter WP4C (from Decagon Devices)
- Plastic/steel cups, an appurtenance to the WP4C device (from Decagon Devices)
- Clay samples (specified in appendix C)
- Spatula
- Scale
- Distilled water
- Drying oven
- Crucibles or other ovenproof cups

For the test, three different samples of soil is used; clay from Lilleby, Trondheim, clay from UNIS East, Longyearbyen, and soil from the NGTS site in Adventdalen, Longyearbyen, apparently sandy silt. Specifications for the clays are given in appendix C.

4.2.4 Test Procedure

The WP4C device is turned on and set at the preferred testing temperature. Clay samples of ~ 50 g are prepared in a cup. When obtaining the right moisture content, by adding distilled water, a small part of the sample is placed in one of the small plastic or steel cups. For this experiment, plastic cups were used. The cup is filled half full (15 ml), and the bottom is completely covered. The rest of the sample is weighed and put in a drying cabinet for 24 hours. When the plastic cup is placed in the WP4C device, the sample temperature T_s should be less than the temperature inside the WP4C device T_b. Thus, the measured $T_s - T_b$ should be negative. When the temperature difference is less than 1 °C, the measurement is started. The measured water potential and sample temperature is used for further calculations. The tested samples is put in an ovenproof cup, weighed and placed in the drying cabinet for 24 hours. After the samples has dried for 24 hours, the water content is calculated.

The procedure is repeated for samples with different moisture content and for two temperatures. In total, between 12 and 21 samples were tested at 15 °C and then at 25 °C for each soil type. The soil from the NGTS site was two different samples, one was tested at 15 °C and one at 25 °C. The results are presented in figures 5.6 - 5.8.

Chapter 5

Analysis and Results

5.1 Liquid Limit Determination

The graph for unfrozen water content obtained by liquid limit determination is obtained from equation 3.4, and the constants α and β is found from the liquid limit testing described in chapter 4.1. The parameters $w_{N=25}$ and $w_{N=100}$ are found from linear regression, see appendix D. $w_{u,\theta=1}$ and $w_{u,\theta=2}$ are found from equations 3.5 and 3.6. The results are presented in table 5.1 and figure 5.1. Below, the equations for unfrozen water content with corresponding graphs are presented for each soil sample.

Table 5.1: Results from liquid limit determination

Soil Type	$w_{N=25}$	$w_{N=100}$	$w_{u,\theta=1}$	$w_{u,\theta=2}$	α	β
Lilleby	32.9 %	27.1 %	8.3734 %	5.4398 %	8.3734	-0.6223
UNIS East	25.1 %	22.8 %	5.6746 %	3.9864 %	5.6746	-0.5094
AD-d-4-4	31.4 %	25.5 %	7.8544 %	4.8990 %	7.8544	-0.6810
AD-d-2-4	27.0 %	23.2 %	6.3320 %	4.1216 %	6.3320	-0.6195

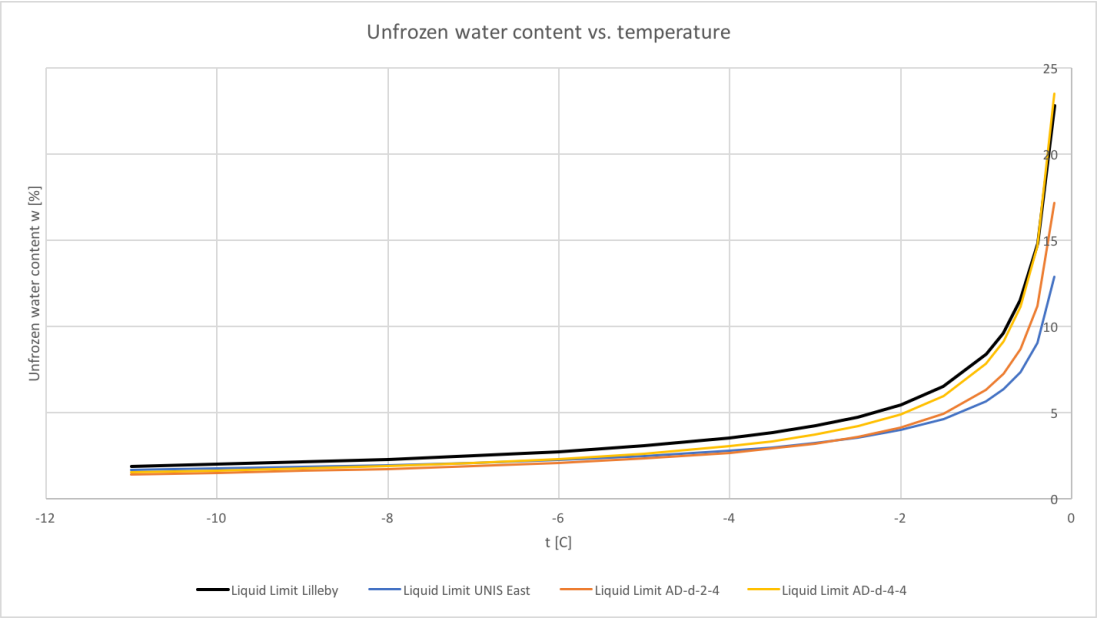

Figure 5.1: Unfrozen water content - temperature curve from liquid limit determination

5.1.1 Lilleby

$$w_u = 8.3734 \cdot \theta^{-0.6223} \quad [\%] \tag{5.1}$$

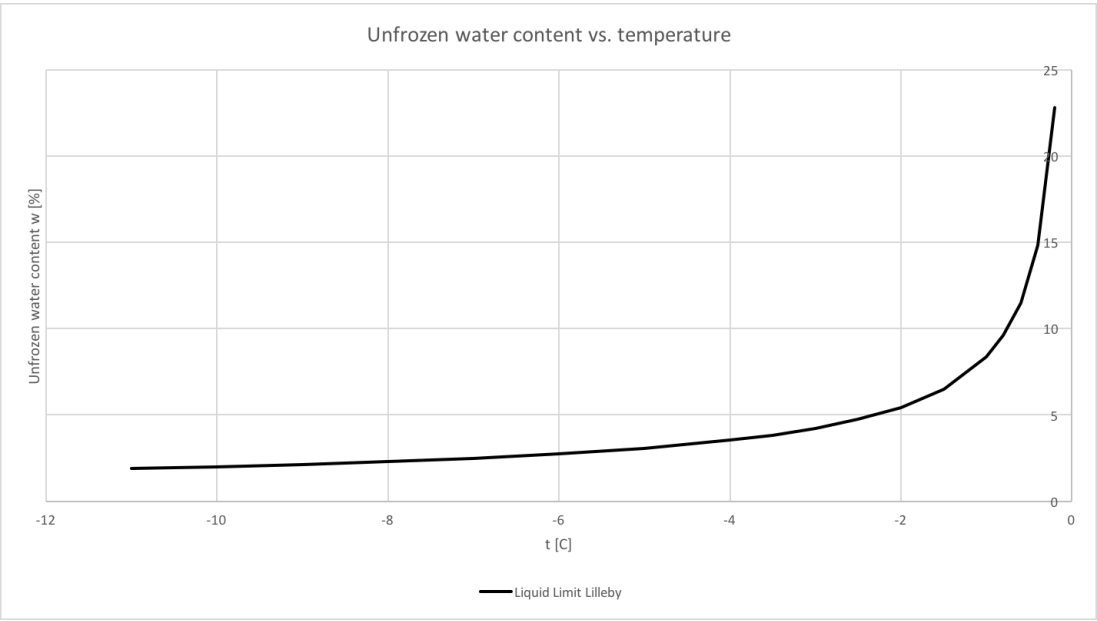

Figure 5.2: Unfrozen water content - temperature curve from liquid limit determination, Lilleby

5.1.2 UNIS East

$$w_u = 5.6746 \cdot \theta^{-0.5094} \quad [\%] \tag{5.2}$$

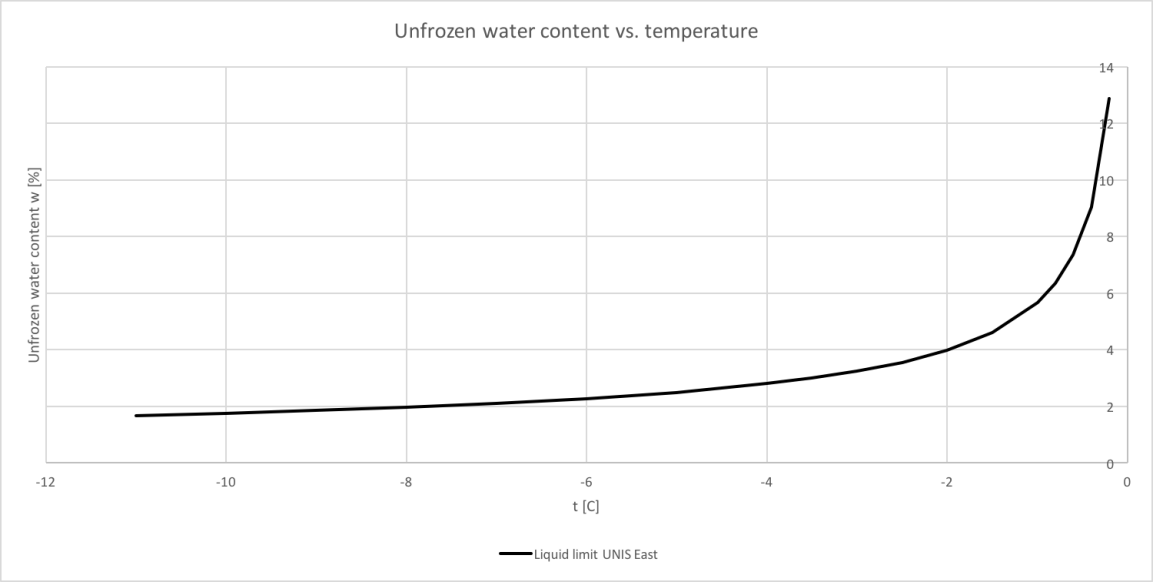

Figure 5.3: Unfrozen water content - temperature curve from liquid limit determination, UNIS East

5.1.3 NGTS: AD-d-4-4

$$w_u = 7.8544 \cdot \theta^{-0.6810} \quad [\%] \tag{5.3}$$

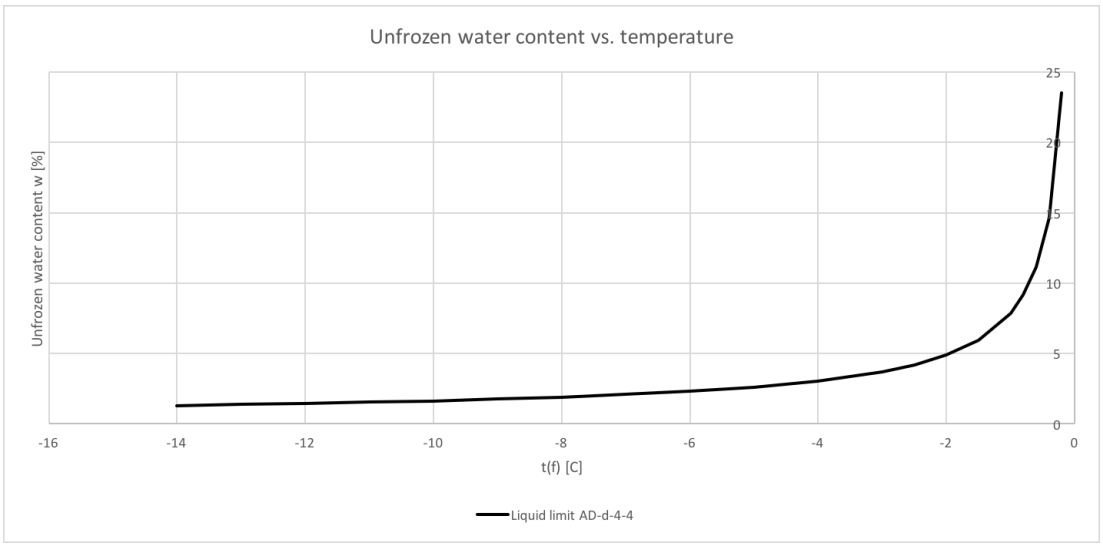

Figure 5.4: Unfrozen water content - temperature curve from liquid limit determination, NGTS: AD-d-4-4

5.1.4 NGTS: AD-d-2-4

$$w_u = 6.3320 \cdot \theta^{-0.6195} \quad [\%] \tag{5.4}$$

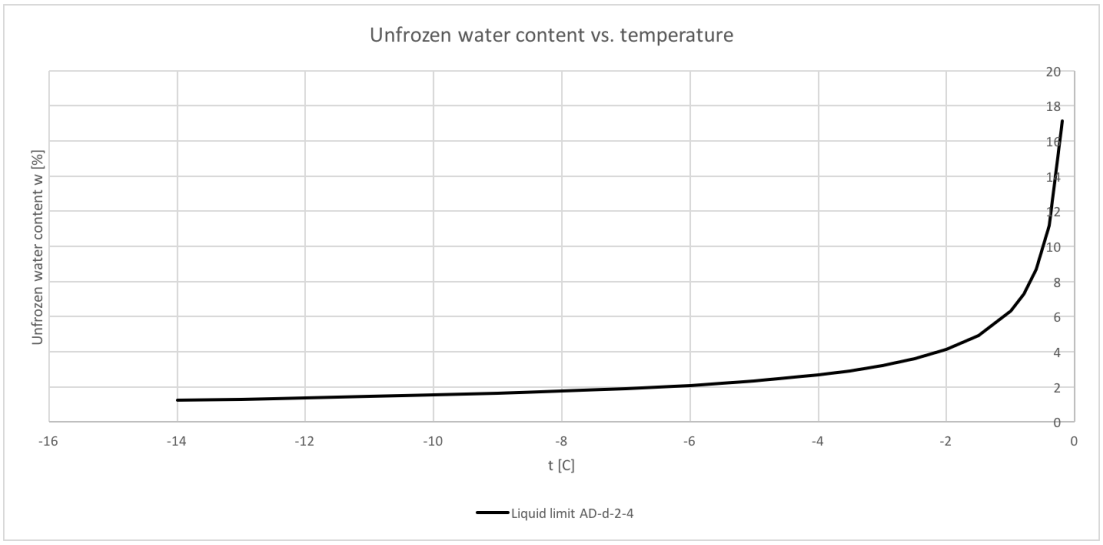

Figure 5.5: Unfrozen water content - temperature curve from liquid limit determination, NGTS: AD-d-2-4

5.2 Water Potential Determination

Figures 5.6, 5.7, and 5.8 present the resulting graphs of unfrozen water content versus temperature below 0 °C from the water potential testing performed with WP4C at UNIS. 15 denotes test temperature of 15 °C, and 25 test temperature of 25 °C. AD-d-2-4 was only tested on 25 °C, and AD-d-4-4 on 15 °C. Based on the results, it seems reasonable to conclude that the testing temperature does not affect the results considerably.

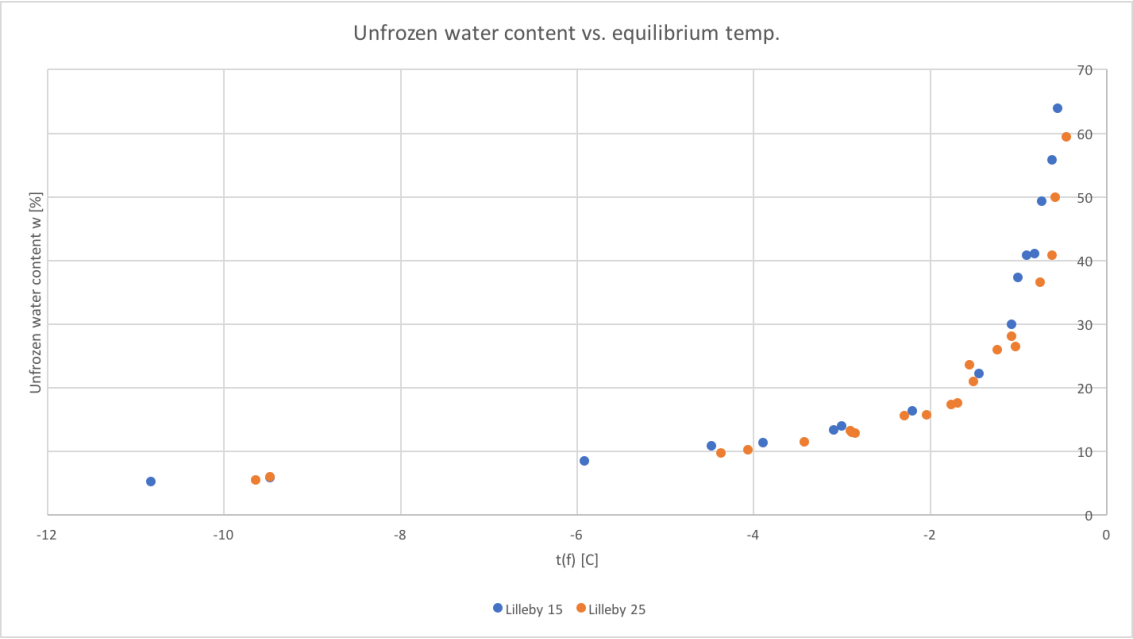

Figure 5.6: Results of water potential testing at 15 and 25 °C, Lilleby clay

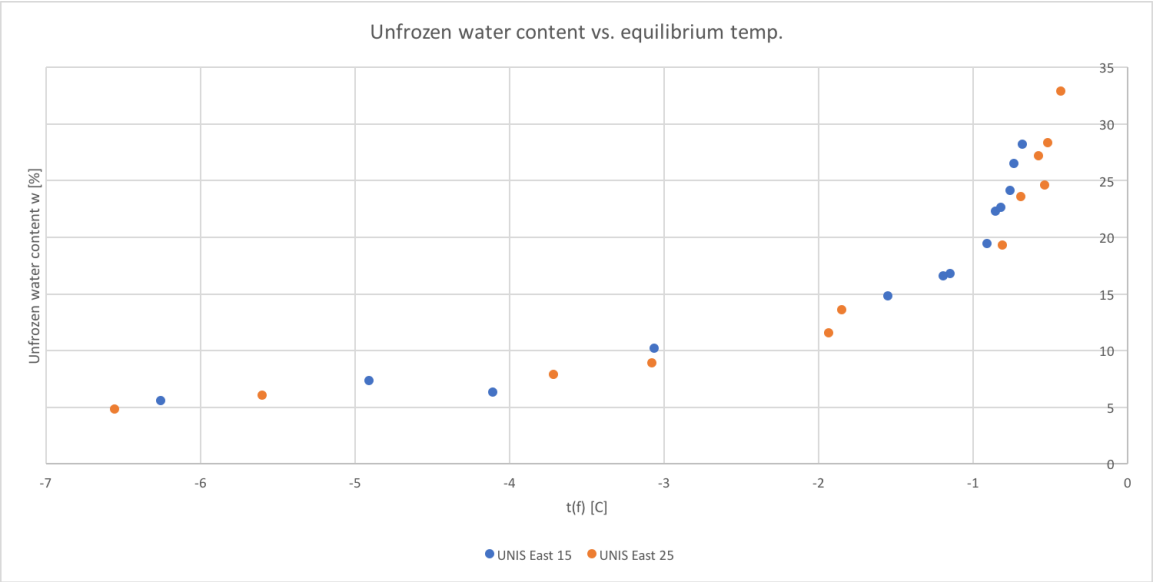

Figure 5.7: Results of water potential testing at 15 and 25 °C, UNIS East clay

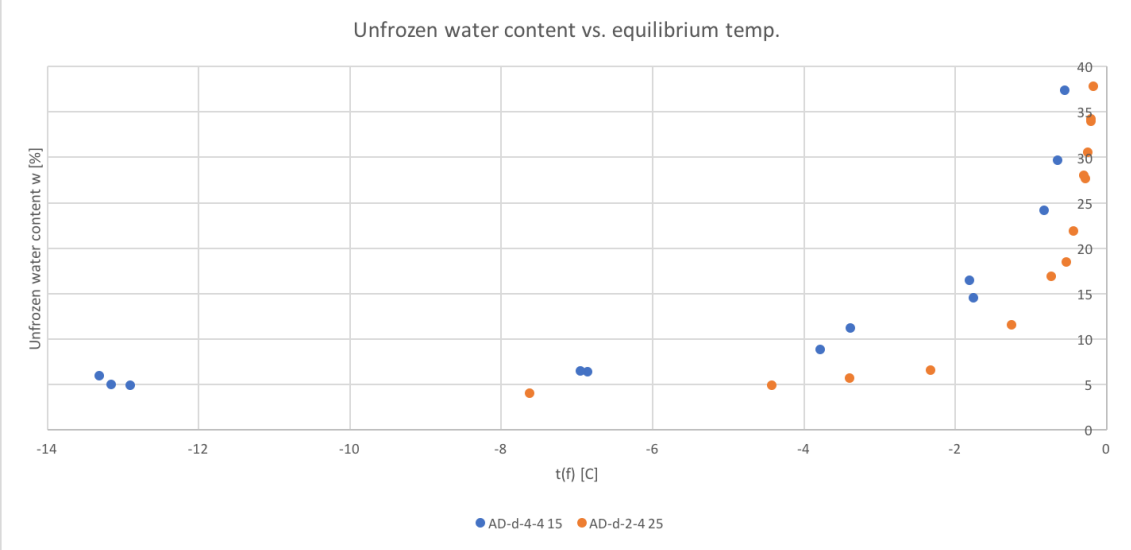

Figure 5.8: Results of water potential testing at 15 and 25 °C, soil from NGTS site

The two soil samples from the NGTS site, AD-d-4-4 and AD-d-2-4, probably differs in composition, which explains the greater deviation between the two graphs.

5.3 Comparisons of the Results

To obtain a better view of the results obtained in the previous tests, the results from both tests for each soil type is presented in the same curve, shown in figures 5.9 - 5.11. As can be seen from the graphs, the unfrozen water content obtained by liquid limit determination is consistently lower than the value from water potential testing.

5.3.1 Lilleby

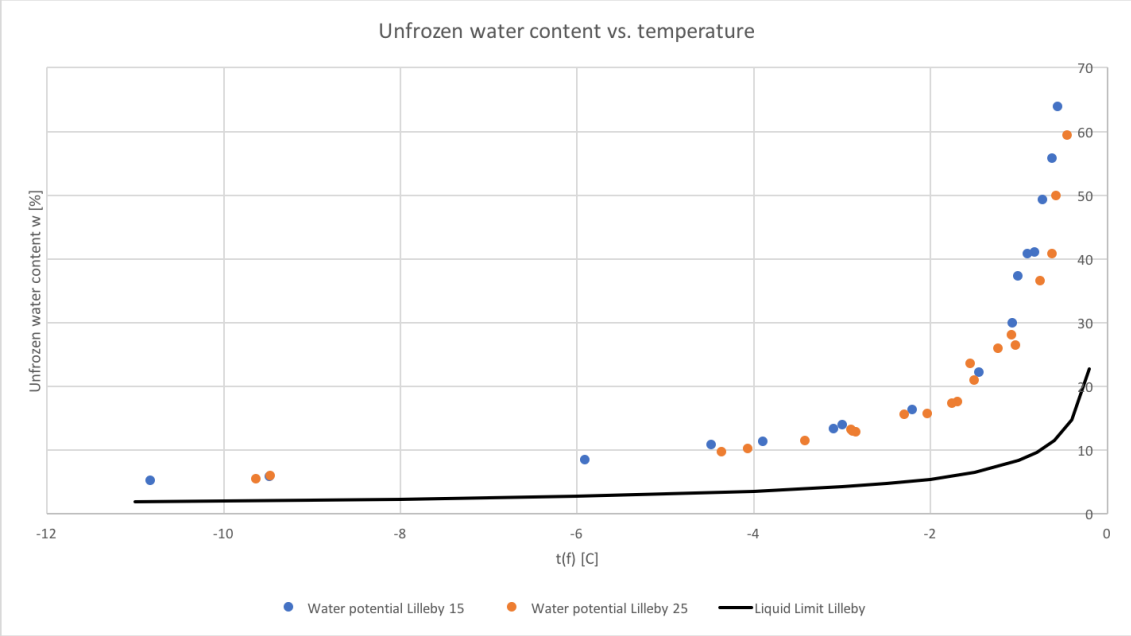

Figure 5.9: Unfrozen water content vs. temperature found by liquid limit determination and water potential determination, Lilleby

5.3.2 UNIS East

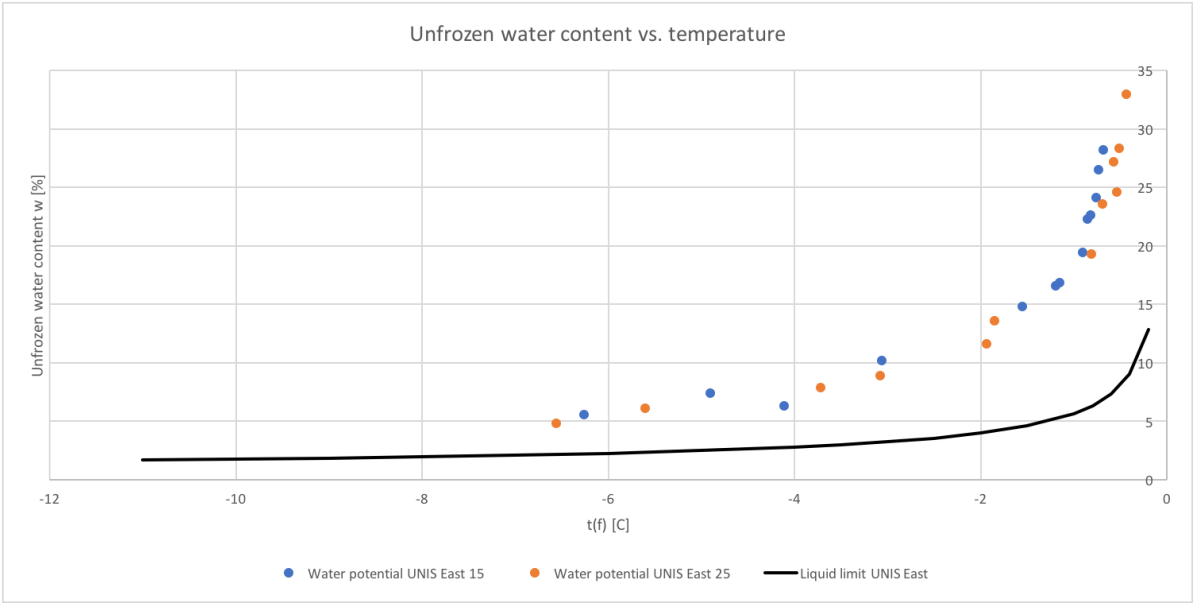

Figure 5.10: Unfrozen water content vs. temperature found by liquid limit determination and water potential determination, UNIS East

5.3.3 NGTS: AD-d-4-4 and AD-d-2-4

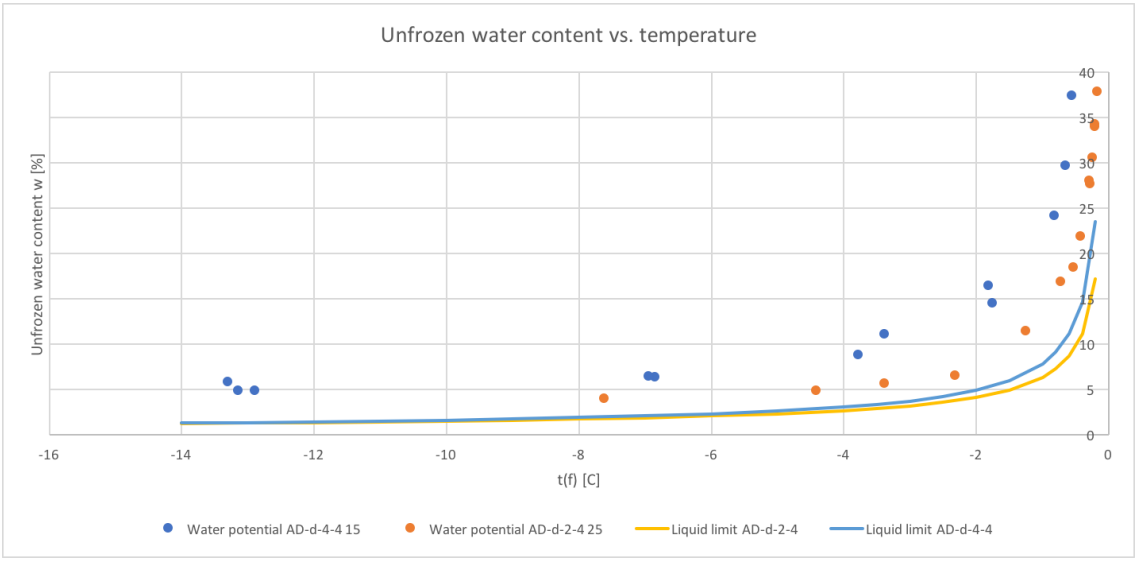

Figure 5.11: Unfrozen water content vs. temperature found by liquid limit determination and water potential determination, NGTS site

5.4 Discussion

As can be seen from the graphs above, the unfrozen water content graph from the liquid limit testing is below the graph from the water potential testing. The water potential testing is based on thermodynamic calculations for temperature-dependent unfrozen water in equilibrium with bulk ice systems. The method measures moisture and temperature dependent pore water potential and water activity. Water potential and water activity can be converted into the difference of chemical potentials between bulk water and pore water, depending on moisture content and temperature. At equilibrium of pore water and bulk ice at $p_0 = 0.1013$ MPa and $T \leq T_0 = 0$ °C, the difference between chemical potentials of bulk water and pore water is equal the difference between bulk supercooled water and bulk ice; $\Delta\mu_{w,wpor}(w,T) = \Delta\mu_{w,i}(T)$. The unfrozen water content at a given temperature can be described as pore water – bulk ice equilibrium. By assuming atmospheric pressure, empirical moisture and temperature dependencies of water potential is obtained for the samples. Hence, the water potential method provides the soil dependent curve for unfrozen water content at different temperatures.

The liquid limit determination is an empirical method that has given good results for the estimated unfrozen water content for several soils (Tice et al., 1976). However, from these results it seems that the method does not fit very well for Norwegian soils. The results obtained from this test provide an unfrozen water content that is lower than the actual amount of unfrozen water. Thus, the predicted settlements will be too small, which may have significant impact on potential structures on the site. Furthermore, the method is somewhat time-consuming and cumbersome, and it is hard to prepare drier samples in the Casagrande cup without the soil to be hooked to the grooving tool. This tendency applies to the soil from Longyearbyen in particular. However, the method is accessible in most laboratories and based on the results, a more appropriate empirical formula for Norwegian soils is suggested. The procedure is shown in chapter E in the appendix.

Table 5.2 shows the parameters for equation 3.5 and 3.6, obtained for the different soils, corresponding with the water potential results. The obtained parameters for the liquid limit determination are adapted to fit the curve from the water potential testing. Parameters in the formulas are named $w_{u,\theta=1,1}$, $w_{u,\theta=1,2}$, $w_{u,\theta=2,1}$, and $w_{u,\theta=2,2}$, when writing the formulas $w_{u,\theta=1} = w_{u,\theta=1,1} \cdot w_{N=25} - w_{u,\theta=1,2}$ and $w_{u,\theta=1} = w_{u,\theta=2,1} \cdot w_{N=100} - w_{u,\theta=2,2}$. The formula for the temperature dependent unfrozen water content is still written as $w_u = \alpha\theta^{\beta}$.

Table 5.2: Adapted parameters for liquid limit determination formulas

Soil Type	$w_{u,\theta=1,1}$	$w_{u,\theta=1,2}$	$w_{u,\theta=2,1}$	$w_{u,\theta=2,2}$	α	β
Lilleby	1.27	8	0.85	3.9	33.78	-0.82
UNIS East	0.83	2	0.65	3	18.83	-0.67
AD-d-4-4	0.75	1	0.72	4	22.55	-0.65
AD-d-2-4	0.53	2	0.6	6	12.31	-0.62

From the table, it is clear that the Lilleby parameters deviate from the parameters obtained for

the soil from Svalbard. Hence, it is reasonable to believe that the liquid limit determination of unfrozen water content should be adapted to different soil types. Choosing the average values for the parameters found for the soil types from Svalbard, the following equations are proposed.

$$w_{u,\theta=1} = 0.703 \cdot w_{N=25} - 1.67 \tag{5.5}$$

$$w_{u,\theta=2} = 0.657 \cdot w_{N=100} - 4.33 \tag{5.6}$$

Using the adapted formulas for liquid limit determination, equations 5.7, 5.8, and 5.9 are obtained for the soils from Svalbard. The graphs are shown in figures 5.12, 5.13, and 5.14.

AD-d-2-4:

$$w_u = 17.32 \cdot \theta^{-0.6595} \quad [\%] \tag{5.7}$$

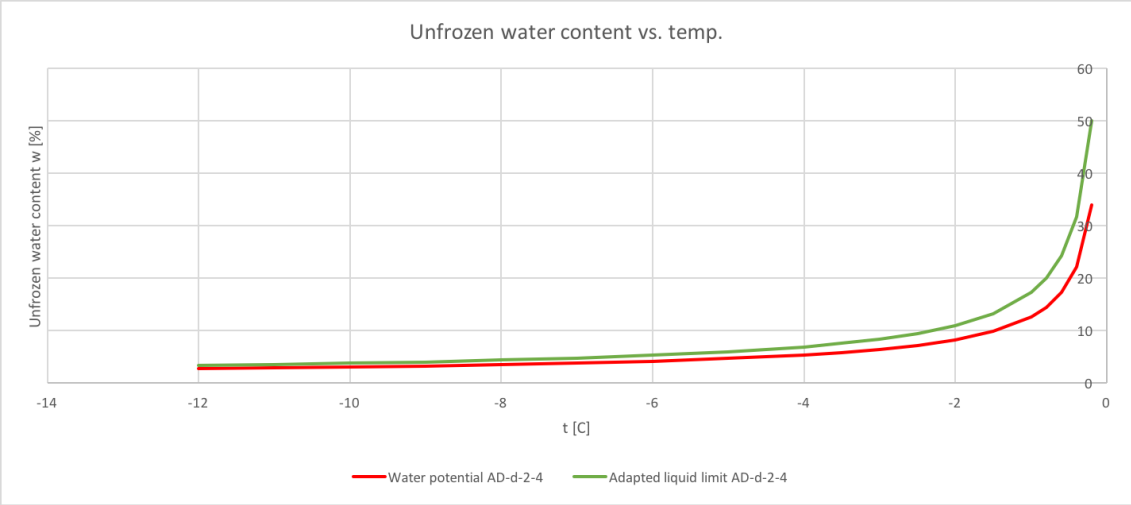

Figure 5.12: Unfrozen water content vs. temperature found by water potential determination and adapted liquid limit determination, AD-d-2-4. $w_{u,\theta=1} = 17.32$, $w_{u,\theta=2} = 10.97$.

AD-d-4-4:

$$w_u = 20.42 \cdot \theta^{-0.7181} \quad [\%] \tag{5.8}$$

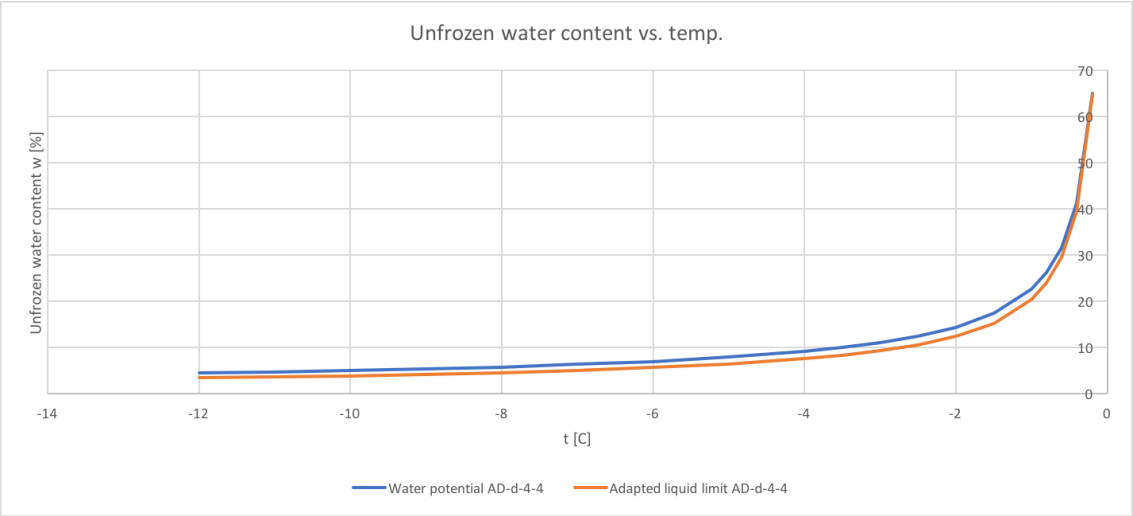

Figure 5.13: Unfrozen water content vs. temperature found by water potential determination and adapted liquid limit determination, AD-d-4-4. $w_{u,\theta=1} = 20.42$, $w_{u,\theta=2} = 12.41$.

UNIS East:

$$w_u = 15.99 \cdot \theta^{-0.5876} \quad [\%] \tag{5.9}$$

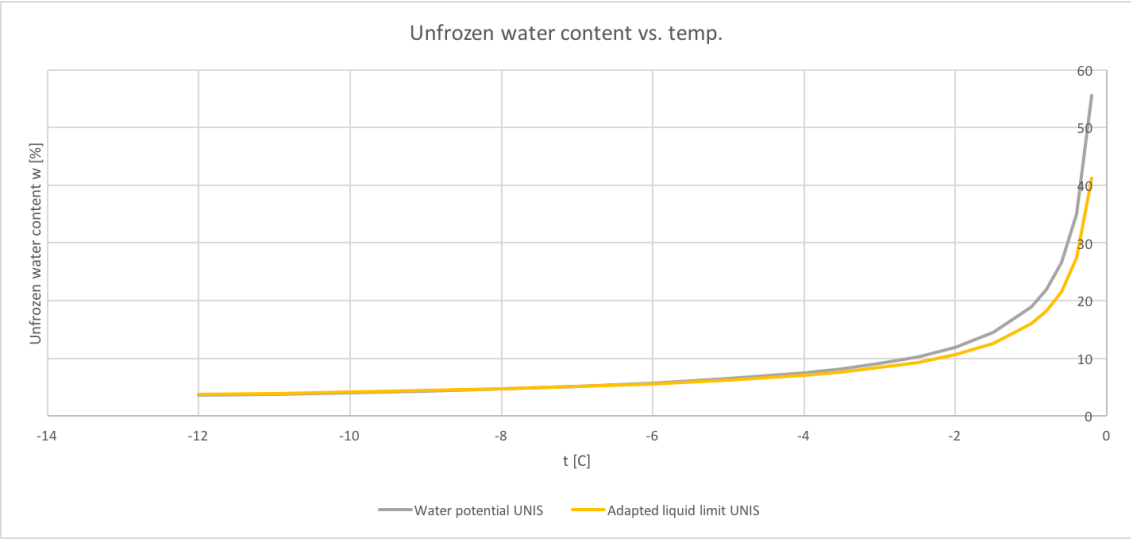

Figure 5.14: Unfrozen water content vs. temperature found by water potential determination and adapted liquid limit determination, UNIS East. $w_{u,\theta=1}$ = 15.99, $w_{u,\theta=2}$ = 10.64.

The adapted liquid limit formulas for unfrozen water content provide graphs much closer to the graph obtained from water potential testing. Also for the Lilleby clay the adapted formula will give a better fit. This is shown in figure 5.15, with the corresponding equation 5.10. However, a formula adapted to Norwegian clay from the mainland should be developed based on data from several soils.

$$w_u = 21.47 \cdot \theta^{-0.6736} \quad [\%] \tag{5.10}$$

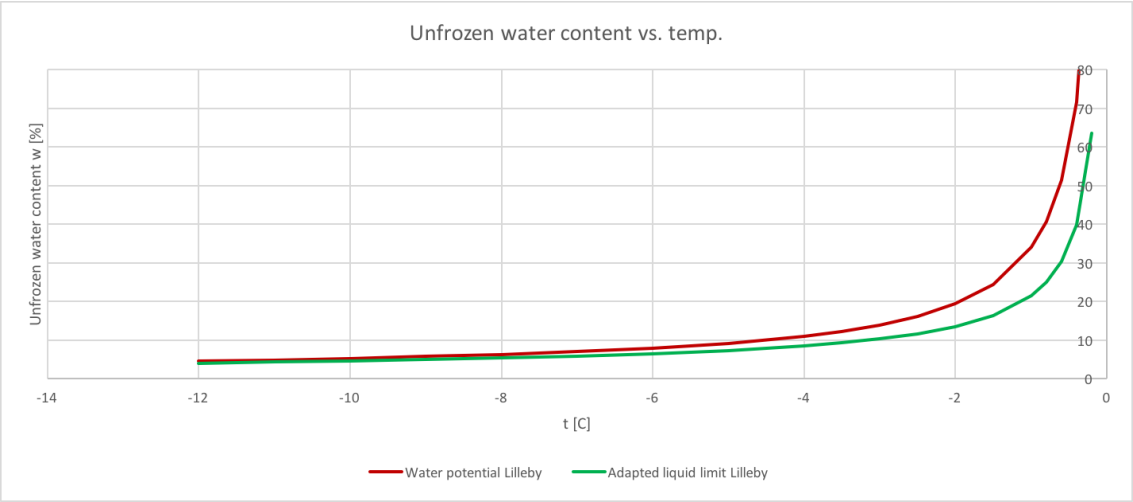

Figure 5.15: Unfrozen water content vs. temperature found by water potential determination and adapted liquid limit determination, Lilleby

Chapter 6

Geothermal Model Proposition

A one-dimensional geothermal model is proposed to investigate the effect of unfrozen water content on heat flows in the tested soils. The model presents a downward temperature curve based on phase changes and ground surface temperatures, and compares the heat flows based on results from liquid limit and water potential testing. The model is created using Plaxis 2D Thermal. Plaxis 2D is a two-dimensional finite element program analyzing deformation, stability and groundwater flow in geotechnical engineering. Plaxis 2D Thermal investigates the effects of heat flow on hydraulic and mechanical behaviour of soils and structures in geotechnical designs. The program is convenient when investigating how climate changes affect structures and foundations, optimizing freezing pipes, and analyzing stress responses due to temperature changes. The results from the Plaxis model is compared to results from hand calculations performed based on the Stefan and Berggren modified equations.

6.1 Heat Flow in Soils

The temperature in the ground affects soil engineering behavior, and is an important factor in the design of frozen ground constructions. The temperature in the ground depends on ground surface temperature, the geothermal gradient, and construction activity. Additionally, soil factors, such as soil latent heat, thermal conductivity, and heat capacity of the soil affects the temperature. The mean annual ground surface temperature differs from the mean annual air temperature. The difference depends on surface factors, such as vegetation, snow cover, and drainage. For seasonal thawing and freezing problems, ground surface indices for air thawing I_{at} and air freezing I_{af} are used. They are estimated empirically by n-factors defined in equations 6.1 and 6.2.

$$n_f = \frac{I_{sf}}{I_{af}} \tag{6.1}$$

$$n_t = \frac{I_{st}}{I_{at}} \tag{6.2}$$

where I_{sf} is the ground surface freezing index, and I_{st} is the ground surface thawing index. Approximate n-factors for different surface types are tabulated (e.g., see Andersland and Ladanyi, 1994, Chap. 3), and may change from year to year.

6.1.1 Frost Depth

Freezing, thawing, and redistribution of water in the ground during temperature changes cause variations in soil properties and thus, ground responses. The depth of affected soil depends on the seasonal frost penetration. Methods for finding the frost penetration depth in nonuniform soils often refer to the Stefan equation and the modified Berggren equation. The Stefan equation is based on the assumption that only the latent heat of soil moisture must be removed when freezing the soil, resulting in equation 6.3.

$$Y = \sqrt{\frac{48 k I_{sf}}{L}} \tag{6.3}$$

where Y [ft] is the depth, k [Btu/(hr-ft-°F)] is the soil thermal conductivity, L [Btu/ft^3] is the soil latent heat, I_{sf} [°F-days] is the absolute value of of the freezing index, and 48 represents $2 \cdot dt = 2 \cdot (24\ \text{h/day})$. As volumetric heat of the soil is neglected, the Stefan equation overestimates the frost depth. The modified Berggren equation is more realistic, introducing a correction coefficient λ, as can be seen in equation 6.4.

$$Y = \lambda \sqrt{\frac{2 k v_s t}{L}} \tag{6.4}$$

where $v_s = I_{sf}/t$ is the difference between the ground surface temperature and the freezing temperature of the soil moisture, and t is the time. In SI units, equation 6.4 becomes

$$\begin{aligned} Y &= \lambda \sqrt{2 \cdot (3600\ \text{s/h}) \cdot 24\ \text{h/day} \cdot \frac{k[\text{J/(sm°C)}]\, I_{sf}[\text{°C} \cdot \text{days}]}{L[\text{MJ/m}^3]}} \\ &= \lambda \sqrt{172800 \cdot \frac{k I_{sf}}{L}} \end{aligned} \tag{6.5}$$

λ [-] is given by two dimensionless parameters, α and β (μ in the figure), in figure 6.1. The thermal ratio α and the fusion parameter β are given in formulas 6.6 and 6.7.

$$\alpha = \frac{v_0}{v_s} = \frac{v_0 t}{I_{sf}} \tag{6.6}$$

$$\beta = \frac{c_v}{L} \cdot v_s = \frac{c_v I_{sf}}{Lt} \tag{6.7}$$

where v_0 is the initial surface temperature, c_v [kJ/(m$^3 \cdot$°C)] is the soil volumetric heat capacity, and L [kJ/m^3] is the volumetric latent heat. For soils containing unfrozen water content w_u, equation 6.8 satisfactory defines L. Other terms are as defined above.

$$L = \rho_d L' \frac{w - w_u}{100} \tag{6.8}$$

$L' = 333.7$ kJ/kg is the mass latent heat for water, ρ_d [kg/m^3] is the dry soil density, w the total water content, and w_u the unfrozen water content of the frozen soil.

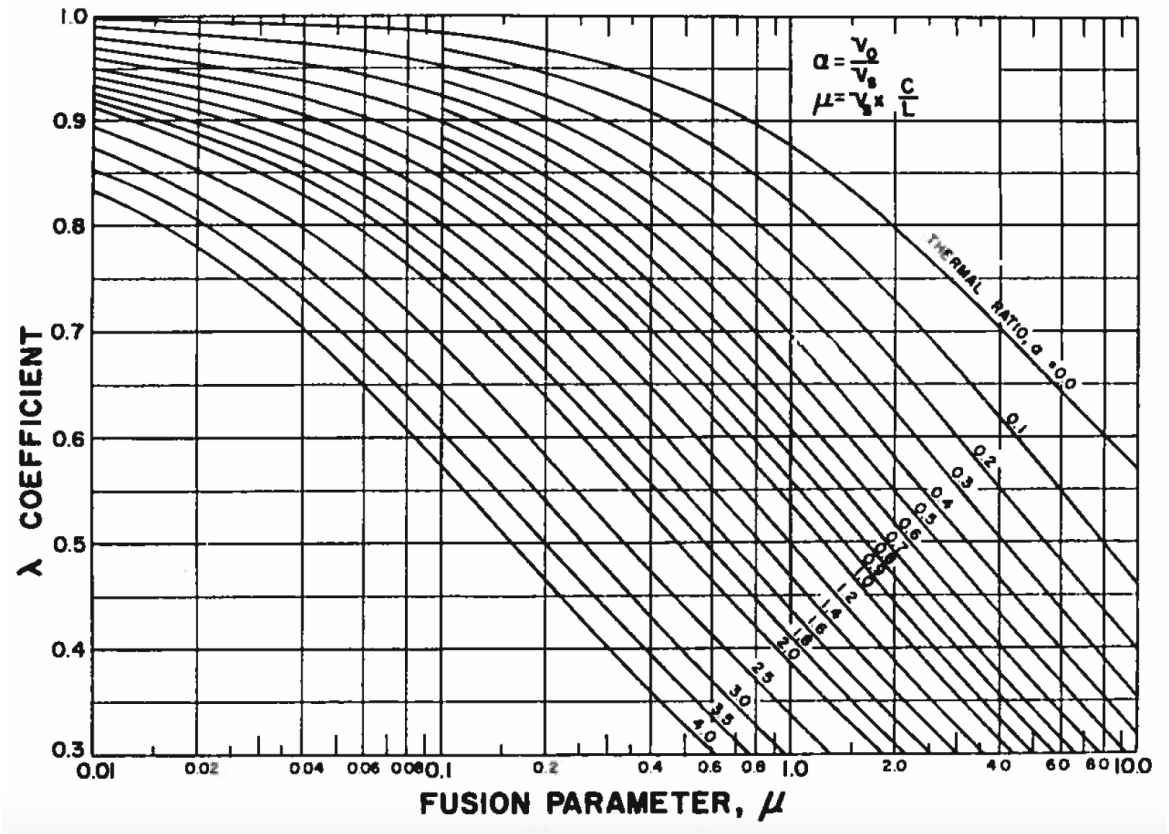

Figure 6.1: Correction coefficient λ in the modified Berggren equation (Andersland and Ladanyi, 1994)

6.1.2 Thawing of Frozen Soil

Thaw settlement problems are connected to the amount of soil thawed and the liberation of excess pore fluids. Assuming that the soil properties in frozen and thawed regions of the soil are homogeneous and independent of temperature, and that latent heat is liberated at 0 °C, the following relationship is established for thaw depth Y [m].

$$Y = \alpha\sqrt{t} \tag{6.9}$$

where t [s] is the time and α [m/$\sqrt{\text{s}}$] is approximated by equation 6.10 when temperature distribution in the frozen zone is assumed not to affect the rate of thaw.

$$\alpha = 2\sqrt{\alpha_u}\left(\frac{\text{Ste}}{2}\right)^{1/2}\left(1-\frac{\text{Ste}}{8}\right) \tag{6.10}$$

α_u is the unfrozen soil thermal diffusivity, Ste = $c_{vu}T_s(L)^{-1}$ is the Stefan number, c_{vu} the unfrozen volumetric heat capacity, T_s the applied constant surface temperature, and L the volumetric latent heat of the soil. By assuming linear temperature distribution in the thawed soil and ground temperature $T_g \approx 0$ °C in the frozen soil, Nixon and McRoberts (1973) obtained the following solution for the predicted thaw depth.

$$Y = \left(\frac{2k_u T_s}{L}\right)^{1/2}\sqrt{t} \tag{6.11}$$

where k_u is the unfrozen thermal conductivity.

6.2 Plaxis Model

The model is generated using the plain strain model and linear elastic material model. Undrained (A) is chosen as the drainage type and water flow boundaries are closed to exclude water flow. The soil polygon is 1 m wide and 10 m high. Mechanically, the vertical lines of the soil polygon are normally fixed, and the lower horizontal line is fully fixed. The upper horizontal line is free for vertical displacement. No loads or water flow is applied. The temperature at the bottom of the soil polygon is set to 275 K = 1.85 °C. The calculation is run twice for each soil type, with ground surface temperature set to −3 °C and −10 °C. The model is only run on materials representing clay from Lilleby and UNIS East due to absent information about the NGTS soil.

The model consists of three phases; the initial phase, a cooling phase, and a phase for the temperature change. Fully coupled flow-deformation is chosen as the calculation type. Thermal,

the temperatures are from the previous phase. In the initial phase, the ground surface temperature is set to 1.85 °C. The duration of the cooling phase is 1 day, and the temperature at ground surface is lowered to the chosen surface temperature T_s. The duration of the temperature change phase is 500 days, to obtain steady state for the temperature distribution, as this process is slowed down when drainage and water flow is excluded.

6.2.1 Choice of Parameters

General and mechanical parameters used in the model are chosen based on index testing performed at NTNU and UNIS, see appendix C. For the clay from Lilleby, the Poissons ratio ν is calculated from Young's modulus E, which is assumed to equal the average stiffness E_{50} from triaxial testing. Young's modulus E for the UNIS East clay is found from the diagram in figure 6.2, assuming that $E \approx E_u$ and overconsolidation ratio OCR ≈ 1.5. The values of the void ratio e are from the index testing. Poisson's ratio is assumed to be 0.33. In reality, stiffness varies with stress level and how close the material is to failure. Additionally, stiffness depends on loading or unloading. In the model, the purpose is to see the effect of the unfrozen water content, and the choice of stiffness parameters are considered to be of less importance. The mechanical parameters are shown in table 6.1.

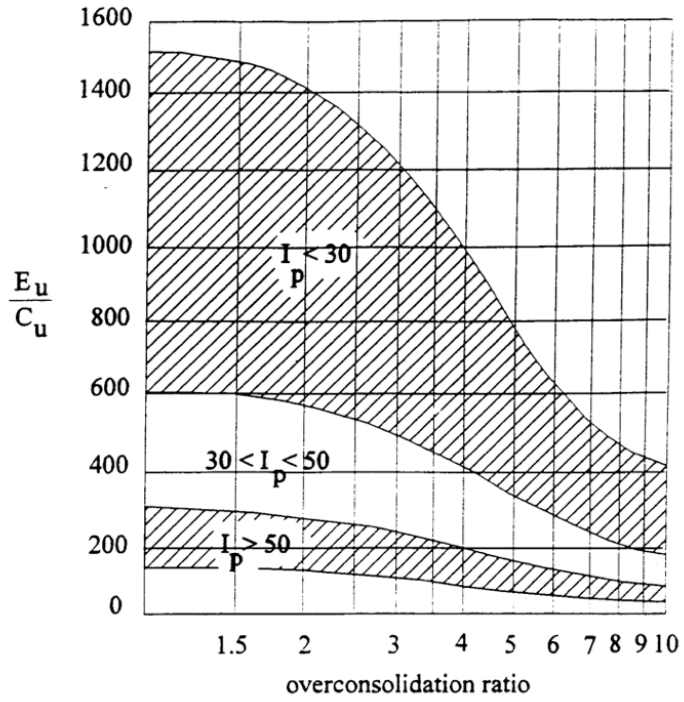

Figure 6.2: Relationship between undrained shear strength $s_u(c_u)$ and undrained Young's modulus E_u (Sture, 2004)

Table 6.1: General and mechanical parameters in Plaxis model

Soil Type	$\gamma_{unsat} = \gamma_{sat}$	E'	ν'	e
Lilleby	19.70 kN/m^3	4630 kN/m^2	0.35	0.83
UNIS East	20.40 kN/m^3	27300 kN/m^2	0.33	0.63

Thermal parameters used in the model are retrieved from average values for clay (e.g., see The Engineering Toolbox, 2017). Temperature dependent unfrozen water content is applied from the results of the liquid limit determination and the water potential testing. The thermal parameters are shown in table 6.2, where c_s is the specific heat capacity, λ_s the thermal conductivity, α the thermal expansion, and ρ_s the density of solids.

Table 6.2: Thermal parameters in Plaxis model

Soil Type	c_s	λ_s	$\alpha_x = \alpha_y = \alpha_z$	ρ_s
Lilleby	1381 kJ/t/K	$1.3 \cdot 10^{-3}$ kW/m/K	$0.04 \cdot 10^{-3}$ K^{-1}	2.83 t/m^3
UNIS East	1381 kJ/t/K	$1.3 \cdot 10^{-3}$ kW/m/K	$0.04 \cdot 10^{-3}$ K^{-1}	2.71 t/m^3

For the rest of the parameters, default values are used.

6.2.2 Results

The Plaxis model is run on soils representing clay materials from Lilleby and UNIS East for two different ground surface temperatures. The unfrozen water contents from both water potential testing and liquid limit determination are added at different runs, and the results are compared. All the results are presented in appendix F. The results from runs with surface temperature $T_s = -3$ °C are presented in figures F.1 - F.3, and results from surface temperature $T_s = -10$ °C are presented in figures F.4 - F.6.

The heave seen in figures F.1 and F.4 is caused by the phase change, and not segregation, as there is no water supply or drainage. As can be seen in figures F.2 and F.5, the temperature varies from 2 °C at the bottom of the soil polygon, to the applied surface temperature in the top. The temperature is evenly distributed in the soil.

Figures 6.3 and 6.4 present the saturation of ice with frost depths, indicated by the white horizontal line, obtained in the model. Values of ice saturation are found in figures F.3 and F.6 in the appendix. As seen in the figures, the model provides a significantly higher amount of ice in the soil polygons where the unfrozen water content is based on the results from the liquid limit determination. This is the opposite result of what is expected, as low unfrozen water content should result in low frost penetration due to the energy required for the phase change from water to ice. Liquid water has more energy than frozen water, and some of the energy, known as latent heat of freezing, is released when the state of water is changed from liquid to solid. Hence,

the released heat energy will slow down the temperature decrease, and thus, the freezing process. This is also explained in chapter 2.4, see figure 2.4. Therefore, the low unfrozen water content results in more released energy keeping the temperature constant, giving a smaller frost penetration depth.

Plaxis does not normally take latent heat of fusion into account, but when the unfrozen water content is activated, latent heat is supposed to be incorporated in the model. The time after the cooling phase is chosen to be 500 days, which may be enough time for the latent heat to be released and thus result in a deeper frost penetration for the soil containing low unfrozen water content. Additionally, the thermal conductivity will change with time as the water - ice ratio changes. It is not known if the Plaxis model includes this. After several adjustments and discussions, attempting to identify the error, it is still unknown why these results are obtained.

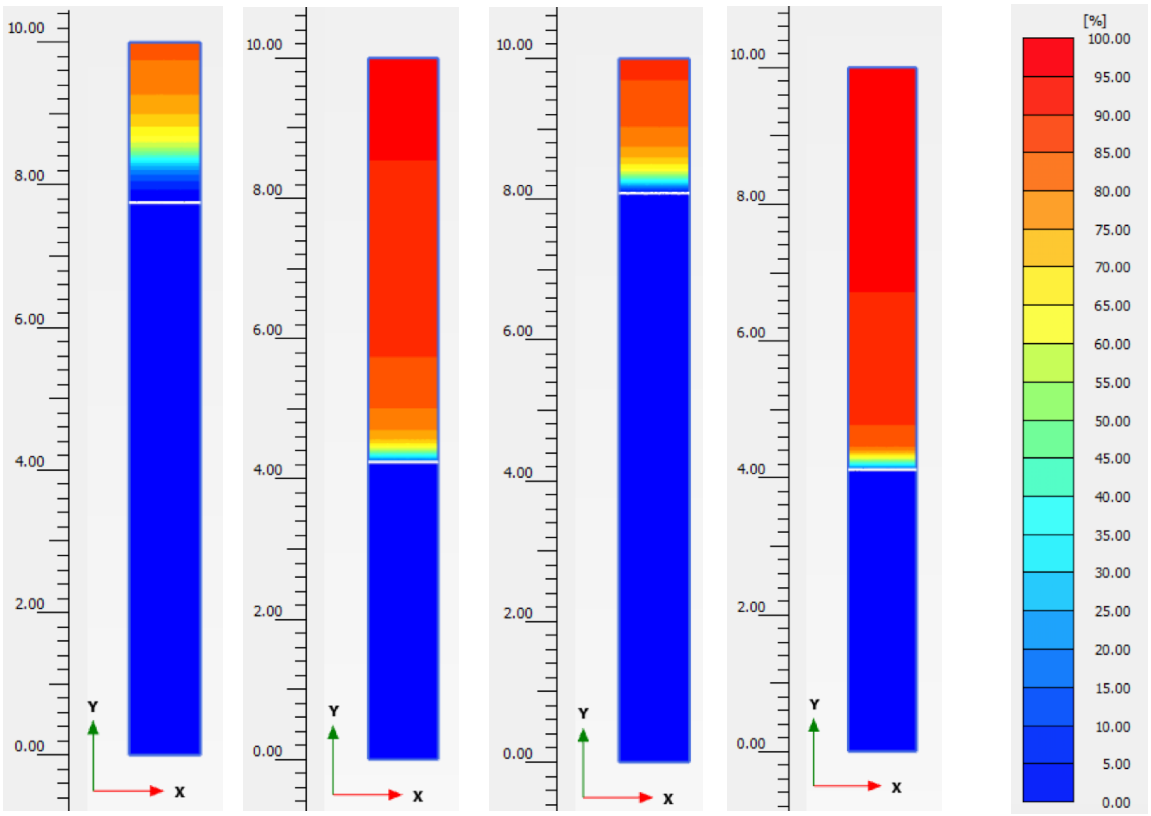

Figure 6.3: Saturation of ice with frost depths Plaxis model, −3 °C. From the left: Lilleby WP ($Y \approx 2.3$ m) and LL ($Y \approx 5.8$ m), UNIS East WP ($Y \approx 1.9$ m) and LL ($Y \approx 5.9$ m)

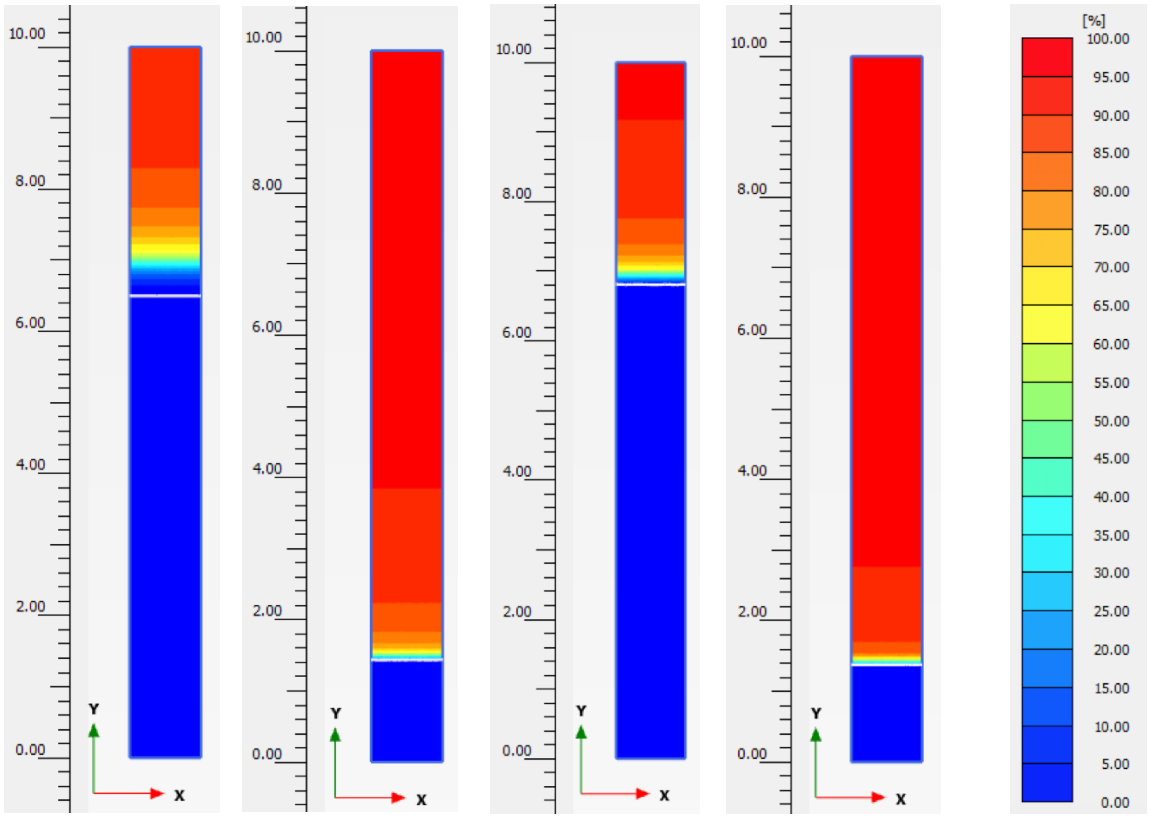

Figure 6.4: Saturation of ice with frost depths Plaxis model, −10 °C. From the left: Lilleby WP ($Y \approx 3.5$ m) and LL ($Y \approx 8.6$ m), UNIS East WP ($Y \approx 3.2$ m) and LL ($Y \approx 8.6$ m)

For permafrost engineering, the opposite problem is more relevant when considering climate changes. That is to say, an initial frozen soil profile exposed to increased temperatures and estimation of the maximal thawing depth. The expected result is then increased thaw depth for soils containing more unfrozen moisture. This can be tested in the geothermal model by changing temperature conditions.

6.3 Hand Calculations

To investigate the importance of the unfrozen water content on heat flows in frozen soils, equation 6.5 is used. As surface temperatures are used in the Plaxis model, the ground surface freezing index I_{sf} is found directly from $I_{sf} = t \cdot v_s$, with $t = 500$ days and $v_s = T_s$ in the Plaxis model.

6.3.1 Thermal Parameters

Dry density ρ_d is found from the relationship $\rho_d = \frac{\rho}{1+w}$, assuming that the saturation $S_r \approx 1$. The soil thermal conductivity k [W/(m K)] can be found from equations 6.12 - 6.15. The equations

for dry conductivity k_{dry}, saturated conductivity k_{sat} (for saturated frozen soils containing w_u), and thermal conductivity of soil constituents k_s are based on the studies of Johansen (1975). When $S_r = 1$, the Kersten number $K_e = 1.0$ for frozen soils.

$$k = k_u = (k_{sat} - k_{dry})K_e + k_{dry} = k_{sat} \tag{6.12}$$

$$k_{dry} = \frac{0.137\rho_d + 64.7}{\rho_s - 0.947\rho_d} \pm 20\% \tag{6.13}$$

$$k_{sat} = k_s^{1-n} \cdot k_i^{n-w_u} \cdot k_w^{w_u} \tag{6.14}$$

$$k_s = k_q^q \cdot k_o^{1-q} \tag{6.15}$$

where ρ_d [kg/m^3] is the dry density. Thermal conductivity of ice $k_i = 2.2$ W/(m K), and thermal conductivity of water $k_w = 0.57$ W/(m K). k_q and k_o are the thermal conductivities of quartz and other minerals, respectively. q is the quartz fraction of the total solids content. Johansen (1975) uses the following values: $k_q = 7.7$ W/(m K) and $k_o = 2.0$ W/(m K).

Table 6.3 presents the parameters used for the different soils in the calculations. Due to the lack of index testing of the soil samples from the NGTS site on Svalbard, they are not studied in the geothermal model. To be able to compare the results from the geothermal models, the unfrozen thermal conductivity k_s is assumed to be equal to the thermal conductivity of the solid material λ_s in the Plaxis model.

Table 6.3: Parameter used in the model for heat flow

Soil Type	ρ_s	w	n	ρ_d	k_s
Lilleby	2.83 g/cm^3	30.3 %	48.3 %	1.54 g/cm^3	1.3 W/mK
UNIS East	2.71 g/cm^3	25.22 %	38.7 %	1.66 g/cm^3	1.3 W/mK

6.3.2 Calculations and Results

The initial temperature $v_0 = 2$ °C and the soil heat capacity $c_s = 1.381$ kJ/kg°C, as in the Plaxis model. The volumetric soil heat capacity can be found by multiplying the specific heat capacity by the density of the material. Thus, $c_v = 2775.8$ kJ/m^3°C for Lilleby clay and $c_v = 2872.5$ kJ/m^3°C for UNIS East clay. The unfrozen water content w_u is temperature dependent, and thus depth and time dependent, as well. The used values of the unfrozen water contents are conservatively chosen to be equal to the results from the laboratory testing performed at UNIS. The ground surface temperatures $v_s = T_s$ are from the Plaxis model. Thus, thaw depth is calculated for $v_s = -3°$ C and $v_s = -10°$ C. Table 6.4 shows the unfrozen water contents found for liquid limit

determination (LL) and water potential testing (WP), and the associated calculated values used in the model. It is assumed that k_i = 2.25 W/mK at −5° C and k_w = 0.574 W/mK at 4.4 °C (The Engineering Toolbox, 2017).

Table 6.4: Calculated values in heat flow model

Parameter	**Lilleby**				**UNIS East**			
c_v [kJ/m^3°C]	2775.8				2872.5			
v_s [°C]	−3		−10		−3		−10	
I_{sf} [°C · days]	− 1 500		− 5 000		− 1 500		− 5 000	
Method	WP	LL	WP	LL	WP	LL	WP	LL
w_u [%]	13.9	4.2	5.2	2.0	9.1	3.2	4.1	1.8
k [W/m°C]	1.40	1.60	1.58	1.65	1.42	1.54	1.52	1.57
L [kJ/m^3]	84 279	134 127	128 988	145 433	89 295	121 978	116 993	129 733
α [−]	0.667	0.667	0.2	0.2	0.667	0.667	0.2	0.2
β [−]	0.099	0.062	0.215	0.191	0.097	0.071	0.246	0.221
λ [−]	0.88	0.91	0.92	0.93	0.88	0.91	0.92	0.92
Y [m]	1.83	1.60	2.99	2.91	1.79	1.65	3.08	2.97

As expected, the frost penetration depth Y is higher for high unfrozen water content (from water potential testing).

6.4 Discussion and Conclusions

The results from the two methods, Plaxis geothermal model and hand calculation, for finding frost penetration depth differs. The same soil and heat parameters are used in both methods. As explained, it is expected that the frost penetration depth for low unfrozen water content is smaller than for high unfrozen water content. The distinction in the results is explained by an error in the Plaxis model, that has not been able to define. Comparing the results for soil with unfrozen water content obtained from water potential testing, it may seem that the frost penetration depth obtained in Plaxis is not too wrong, differing ~ 0.1 m at −3 °C and ~ 0.5 m at −10 °C. The obtained frost penetration depth is greater for the Plaxis model. The divergence in the Plaxis model for the steep freezing curve in liquid limit determination may be improved by using a finer mesh and smaller time steps. The steep curve with the used mesh and time steps seems to exclude the transition zone in the process of water freezing to ice. In the hand calculations, the change in thermal conductivity with time, because of the changed water - ice ratio, is not accounted for. It is unknown if this is implemented in the Plaxis model.

However, from the results of the hand calculations, it can be seen that the frost penetration depth for a soil changes based on the temperature dependent unfrozen water content. Consequently, the frost penetration depth based on unfrozen water content from liquid limit determination will be considered too small, due to the apparent lower unfrozen water content. This will

influence the outcome of designs in permafrost areas, designing for a too small frost penetration depth. The same applies for the thawing depth, which is more relevant in permafrost areas. An underestimated unfrozen water content will result in a thawing depth too small, possibly causing problems for geotechnical design considerations.

Chapter 7

Summary and Recommendations for Further Work

7.1 Summary and Conclusions

Methods for determining unfrozen water content in fine grained soils have been investigated, liquid limit determination and water potential testing in particular. Methods vary in complexity, duration, accessibility, and accuracy.

Soil samples from Longyearbyen and Trondheim have been investigated in the laboratories of UNIS and NTNU. Liquid limit determination was performed at NTNU, and water potential testing at UNIS. As can be seen in the graphs presented in chapter 5.3, the unfrozen water content obtained by liquid limit determination is consistently lower than the values found from water potential testing.

Liquid limit determination is an accessible, but time-consuming and cumbersome method, and the results depend on human accuracy. The results of the tests indicate that the parameters in the model do not fit Norwegian clays very well. More suitable parameters are proposed, based on the results from the soil from Longyearbyen. The adapted formulas for $w_{u,\theta=1}$ and $w_{u,\theta=2}$ are:

$$w_{u,\theta=1} = 0.703 \cdot w_{N=25} - 1.67 \tag{7.1}$$

$$w_{u,\theta=2} = 0.657 \cdot w_{N=100} - 4.33 \tag{7.2}$$

The water potential testing is based on thermodynamic calculations for temperature dependent unfrozen water in equilibrium with bulk ice. Moisture and temperature dependent pore water

potential and activity are measured, and the corresponding unfrozen water content is considered to be very accurate for the tested soil. As stated by Istomin et al. (2017), it can be seen from the results for clay from Lilleby and UNIS East (figures 5.6 and 5.7), that test temperature does not considerably affect the unfrozen water content for porous materials in the tested temperature range.

The results display that liquid limit determination clearly underestimates the amount of unfrozen water, and thus settlements of the soil. It can be concluded that the water potential method is a more efficient and accurate method for finding the unfrozen water content of a soil.

In chapter 6, a geothermal Plaxis model for finding thermal properties, including frost penetration, based on the unfrozen water content, is proposed and tested on the soils. The frost penetration depth is also predicted by hand calculations using the modified Berggren equation. In the Plaxis model, lower unfrozen water content gives deeper frost penetration, while the opposite result is obtained by hand calculations. The Plaxis model provides results opposite of what is expected. A high amount of thermal energy is required for the phase change of water to ice, resulting in a smaller frost penetration for low unfrozen water content. The Plaxis error has not been successfully identified in this master thesis.

Hand calculations show that frost penetration is increased between 0.1 and 0.25 m when the unfrozen water content from water potential testing is applied instead of liquid limit determination. This is an increase of $\sim 2.75 - 14.4\%$. The difference is most prominent for the tests ran at -3 °C.

7.2 Discussion

For geotechnical designs in permafrost, the unfrozen water content is an important parameter to determine. The parameter influences the settlement and creep calculations. An underestimation of the unfrozen water content will give too small calculated settlement values, making the structure unstable and possibly harmful for nearby infrastructure. Additionally, a too low unfrozen water content will give a too small frost penetration depth influencing decisions on cooling structures and soil.

The testing in this thesis was performed on three soils from Longyearbyen, and one from the Trondheim area. The testing shows the same trend for all the soils. However, the proposed adapted parameters for the liquid limit model indicates how to adapt the formulas to Norwegian soils, but they are not reliable as more soils should be tested. The geothermal models were not tested on the soil types from the NGTS site. Thus, the results and conclusions are only based on testing of two different soil types. It is still obviously an error in the Plaxis model, that should be investigated further.

7.3 Recommendations for Further Work

For further work within the topic, the following is recommended to be performed:

- For further improvement of the liquid limit determination of unfrozen water content, extensive testing should be performed on Norwegian fine grained soils. Formulas for $w_{u,\theta=1}$ and $w_{u,\theta=2}$ adapted to Norwegian soils could then be proposed with more reliability.
- The water potential testing should be the main method for finding unfrozen water content. It requires routines to be formed and established.
- The geothermal model in Plaxis needs to be investigated more. To find the error in the model, testing and adjustments are required. Changes in thermal conductivity with time should be included in hand calculations and the Plaxis model.
- The Plaxis model can be a useful tool in geotechnical designs in permafrost areas by including other factors such as water flow, creep, and mechanical loads.

Bibliography

Andersland, O. B. and Ladanyi, B. (1994). *An introduction to Frozen Ground Engineering*. Chapman & Hall.

Anderson, D. and Tice, A. (1973). Physical aspects of soil water and salts in ecosystems. *Ecological Studies*, 4:107–124. Springer Verlag.

Anderson, D. M. and Morgenstern, N. R. (1973). Physics, chemistry, and mechanics of frozen ground: A review. In *North American Contribution, Second International Conference on Permafrost, Yakutsk, USSR*, pages 257–288. National Academy of Sciences, Washington D. C.

Anderson, D.M., T. A. and Banin, A. (1973). The water-ice phase composition of clay-water systems. Part I. The kaolinite-water system. *Proceedings, Soil Science Society of America*, 37(6).

ASTM D4318 - 05 (2005). Standard Test Methods for Liquid Limit, Plastic Limit, and Plasticity Index of Soils. Standard, ASTM International, West Conshohocken, PA.

Atterberg, A. (1913). Die plastizität und bidigheit liefernden bestandeile der tone. *International Mitteilungen für Bodenkunde*, 3:291–330.

Banin, A. and Anderson, D. (1974). Effects of salt concentration changes during freezing on the unfrozen water content of porous materials. *Water Resources Research*, 10(1):124–128.

Bates, R. E. and Bilello, M. A. (1966). Defining the cold regions of the northern hemisphere. Technical report, U. S. Amy Cold Reg. Res. Eng. Lab. Tech. Rep. 178.

Brown, R. J. E., Johnston, G. H., Mackay, J. R., Morgenstern, N. R., and Shilts, W. W. (1981). Permafrost distribution and terrain characteristics. In Johnston, G. H., editor, *Permafrost Engineering Design and Construction*, pages 31–72. Wiley, New York.

Brown, R. J. E. and Kupsch, W. O. (1974). Permafrost terminology. Technical report, Natl. Res. Counc. Can. Tech. Memo. 111.

Campbell, G. S., Smith, D. M., and Teare, B. L. (2007). Application of a dew point method to obtain the soil water characteristic. Technical report, Decagon Devices, Inc., 950 NE Nelson Ct., Pullman WA. USA. doi:10.1007/3-540-69873-6_7.

Carter, M. R. (1993). *Soil Sampling and Methods of Analysis*. Lewis Publishers.

Casagrande, A. (1932). Research on the atterberg limits of soils. *Public Roads*, 13:121–136.

Gilbert, G. L. (2014). Sedimentology and geocryology of an arctic fjord head delta (Adventdalen, Svalbard). Master thesis, University of Oslo.

Hayhoe, H. N., Bailey, W. G., and Topp, G. C. (1983). Measurement of soil water contents and frozen soil depth during a thaw using time-domain reflectometry. *Atmosphere-Ocean*, 21:299–311.

Hivon, E. and Sego, D. C. (1990). Determination of the unfrozen water content of saline permafrost using the time-domain reflectometry (TDR). Technical report, Department of Civil Engineering, University of Alberta, Edmon, Alberta.

Holtz, R. D. and Kovacs, W. D. (1981). *An introduction to Geotechnical Engineering*. Englewood Cliffs, NJ: Prentice Hall.

Istomin, V., Chuvilin, E., Bukhanov, B., and Uchida, T. (2015). A method for determination of water content in real and model porous media in equilibrium with bulk ice or gas hydrate. Technical report, Skolkovo institute of science and technology (Skoltech). Presented at Geo Québec 2015.

Istomin, V., Chuvilin, E., Bukhanov, B., and Uchida, T. (2017). Pore water content in equilibrium with ice or gas hydrate in sediments. *Cold Regions Science and Technology*, 137:60–67.

Johansen, Ø. (1975). *Thermal conductivity of soils*. PhD thesis, Norwegian Technical University, Trondheim. Also: U.S. Army Cold Reg. Res. Eng. Lab. Transl. 637, July 1977.

Korotaev, Y., Kuliev, A., and Musaev, R. (1973). Combatting hydrates during the transportation of natural gas. Technical report, Nedra, Moscow. Russia.

Kurylyk, B. L. and Watanabe, K. (2013). The mathematical representation of freezing and thawing processes in variably-saturated, non-deformable soils. *Advances in Water Resources*, 60:160–117.

Najibi, H., Mohammadi, A., and Tohidi, B. (2006). Estimating the hydrate safety margin in the presence of salt and/or organic inhibitor using freezing point depression data of aqueous solutions. *Industrial Engineering Chemical Research*, 45(12):4441–4446.

NGI (2016). R&D program | NGTS - Norwegian Geo-Test Sites. URL: https://www.ngi.no/eng/Projects/NGTS-Norwegian-Geo-Test-Sites Accessed: 2017-06-07.

Nixon, J. F. and McRoberts, E. C. (1973). A study of some factors affecting the thawing of frozen soils. *Canadian Geotechnical Journal*, 10(3):439–452.

NS 8001 (1982). *Geotechnical testing. Laborathory methods. Percussion liquid limit*. Norges Standardiseringsforbund (NSF), 1st edition.

NTNU Geotechnical Division (2015). *Lecture notes MSc course TBA4110. Geotechnics: Field and Laboratory Investigations*. NTNU Department of Civil and Transport Engineering, Trondheim.

Patterson, D. E. and Smith, M. W. (1983). Measurement of unfrozen water content in saline permafrost using time-domain reflectometry. In *Proceedings: Fourth International Conference on Permafrost. Fairbanks, Alaska*, pages 968–972, National Academy of Sciences, Washington D. C.

Smith, M. and Patterson, D. (1984). Determining the unfrozen water content in soils by time-domain reflectometry. *Atmosphere-Ocean*, 22(2):261–263. DOI: 10.1080/07055900.1984.9649198.

Smith, M. W. and Tice, A. R. (1988). Measurement of the dozen water content of soils. Comparison of NMR and TDR methods. Technical report, U.S. Army Corps of Engineers. CRREL Report 88-18.

Spaans, E. J. A. and Baker, J. M. (1995). Examining the use of time domain reflectometry for measuring liquid water content in frozen soil. *Water Resources Research*, 13(12):2917–2925.

Sture, S. (2004). Determination of soil stiffness parameters. University Lecture, University of Colorado Boulder.

Svensson, M., Zens, P., Zimmermann, A., Marx, F., and Schär, C. (2017). Permafrost UNIS - East parking place for field equipment. Technical report, UNIS, Longyearbyen.

Terzaghi, C. (1926). Simplified soil tests for subgrades and their physical significance. *Public Roads*, 7(8):153.

The Engineering Toolbox (2017). URL: http://www.engineeringtoolbox.com Accessed: 2017-06-13.

Tice, A. R., Anderson, D. M., and Banin, A. (1976). The prediction of unfrozen water contents in frozen soils from liquid limit determinations. Technical report, US Cold Regions Research and Engineering Laboratory. CRREL report 76-8.

Tice, A. R., Black, P. B., and Berg, R. L. (1988). Unfrozen water contents of undisturbed and remolded Alaskan silt as determined by nuclear magnetic resonance. Technical report, U.S. Army Corps of Engineers, Hanover, New Hampshire. CRREL Report 88-19.

Tice, A. R., Burrous, C. M., and Anderson, D. M. (1978). Determination of unfrozen water in frozen soil by pulsed nuclear magnetic resonance. In *Permafrost: Third international Conference, Proceedings*, pages 149–155, N. R. C., Ottawa, Canada.

Topp, G. C., Davis, J. L., and P., A. A. (1980). Electromagnetic determination of soil water content: Measurements in coaxial transmission lines. *Water Resources Research*, 16(3):574–582.

Vikre, A. G., Nybo, M. S., Rognlien, R., and Dahl, M. (2016). Final Report - TBA4110. Technical report, NTNU, Trondheim.

Watanabe, K. and Mizoguchi, M. (2002). Amount of unfrozen water in frozen porous media saturated with solution. *Cold Regions Science and Technology*, 34:103–110.

Williams, P. J. (1964). Unfrozen water content of frozen soils and soil moisture suction. *Géotechnique*, 14(3):231–246.

Yershov, E., Akimov, P., Cheverev, V., and Kuchukov, E. (1979). The phase composition of moisture in frozen soils. Technical report, MSU, Moscow. Russia.

Appendix A

Acronyms

ASTM	American Society for Testing and Materials 1950
CPG	Controlled Pore Glass
DTA	Differential Thermal Analysis
DSC	Differential Scanning Calorimetry
LL	Liquid Limit determination
NGI	Norwegian Geotechnical Institute
NGTS	Norwegian Geo-Test Sites
NS	Norwegian Standard
NSF	Norges Standardiseringsforbund
NMR	Nuclear Magnetic Resonance
NTNU	Norwegian University of Science and Technology
OCR	Overconsolidation ratio
SINTEF	The Foundation for Scientific and Industrial Research
TDR	Time Domain Reflectometry
UNIS	University Centre in Svalbard
WP	Water Potential testing
WP4C	Water Potential Meter 4C

Appendix B

Nomenclature

Latin Symbols

a	Activity of water
A_s	Surface temperature amplitude
C	Heat capacity
c_v	Soil volumetric heat capacity
c_{vu}	Unfrozen volumetric heat capacity
c_s	Specific heat capacity
d	Effective pore diameter
D_{10}	Effective grain size, the sieve size where 10 % of the soil grains pass
e	Void ratio
E'	Effective Young's Modulus
H	Molar enthalpy
h_c	Maximum capillary rise
I_{af}	Air freezing index
I_{at}	Air thawing index
I_L	Liquidity index
I_P	Plasticity index

i_r	Relative ice content
I_{sf}	Ground surface freezing index
I_{st}	Ground surface thawing index
k	Thermal conductivity
k_{dry}	Dry thermal conductivity
K_e	Kersten number
k_i	Thermal conductivity of ice
k_o	Thermal conductivity for other minerals
k_q	Thermal conductivity of quartz
k_s	Thermal conductivity for soil constituents
k_{sat}	Saturated thermal conductivity
k_u	Unfrozen thermal conductivity
k_w	Thermal conductivity of water
L	Latent heat
L'	Mass latent heat of water
M	Total sample mass
M	Molecular weight of water (= 18.015 g/mol)
M_{ad}	Mass of air dry soil
M_i	Mass of ice
M_s	Mass of solids
M_{uw}	Mass of unfrozen water
M_u	Mass of unfrozen water
M_w	Mass of water
N	Number of drops in Casagrande testing
n	Porosity
n_f	Freezing factor
n_t	Thawing factor

p	Period
p_0	Atmospheric pressure
p_w	Saturation vapor pressure of bulk water
p_{wpor}	Water vapor pressure of the air above soil sample
q	Quartz fraction of total solids content
R	Universal gas constant (= 8.314 J/mol K)
r	Capillary radius
S_r	Saturation
$S_{r,ice}$	Saturation of ice
Ste	Stefan number (Ste = $c_{vu} T_s (L)^{-1}$)
t	Time
T	Temperature
T_0	Standard temperature (= 0°C = 273.15 K)
T_b	Temperature inside the WP4C device
T_d	Dew point temperature
T_e	Temperature where all free water and most of the bound water is frozen
T_{eq}	Equilibrium temperature
T_f	Freezing temperature
T_g	Ground temperature
T_h	Tempreature of hydrate formation
T_m	Mean annual temperature
T_s	Sample temperature
T_s	Surface temperature
T_{sc}	Supercooled temperature
$T_{s,t}$	Ground surface temperature
T_z	Temperature at a certain depth
$T_{z,t}$	Ground temperature

V	Total volume
V	Liquid molar volume
V_v	Volume of voids
V_s	Volume of solids
v_0	Initial surface temperature
v_s	Difference between ground surface temperature and freezing temperature of the soil moisture ($v_s = I_{sf}/t$)
w	Water content
w_{ad}	Water content of air dry soil
w_i	Ice content
w_L	Liquid limit
$w_{N=25}$	Water content at 25 drops in the Casagrande apparatus
$w_{N=100}$	Water content at 100 drops in the Casagrande apparatus
w_P	Plastic limit
w_S	Shrinkage limit
w_u	Unfrozen water content
$w_{u,\theta=1}$	Unfrozen water content at −1°C
$w_{u,\theta=2}$	Unfrozen water content at −2°C
X	Frost or thawing depth
z	Depth

Greek Symbols

α	Soil parameter, thermal expansion
α_u	Soil thermal diffusivity
β	Soil parameter
γ	Unit weight soil
λ	Correction coefficient

λ_s	Thermal conductivity
μ_w	Chemical potential of bulk water
μ_i	Chemical potential of bulk ice
μ_{wpor}	Chemical potential of pore water
ν'	Poissons Ratio
ϕ	Phase lag
ψ	Water potential
ρ	Density of water (= 1.0 g/cm^3)
ρ_d	Dry bulk density
ρ_s	Bulk density of solids
σ	Liquid surface tension
θ	Temperature in Celcius below freezing
θ	Temperature (in DTA)

Appendix C

Soil Samples

Soil samples tested were extruded at Lilleby, UNIS East, and the NGTS site at Svalbard. Information about the samples is given below.

C.1 Lilleby

Clay samples from Lilleby construction site in Trondheim were extruded during the field work of the NTNU MSc course *TBA4110 Geotechnics - Field and Laboratory Investigations* in September 2016. The laboratory investigations were performed at the NTNU Geotechnical Engineering Laboratory in October 2016. The soil is characterized as medium stiff clay with undrained shear strength increasing with depth. The friction angle α is represented by $\tan\phi \approx 0.577$. The clay has low sensitivity and shows no sign of having quick or sensitive behaviour (Vikre et al., 2016). The clay is classified as uniformly graded based on the coefficient of uniformity $C_u = 4.6$. More information is given in figure C.1 and table C.1, and in Vikre et al. (2016).

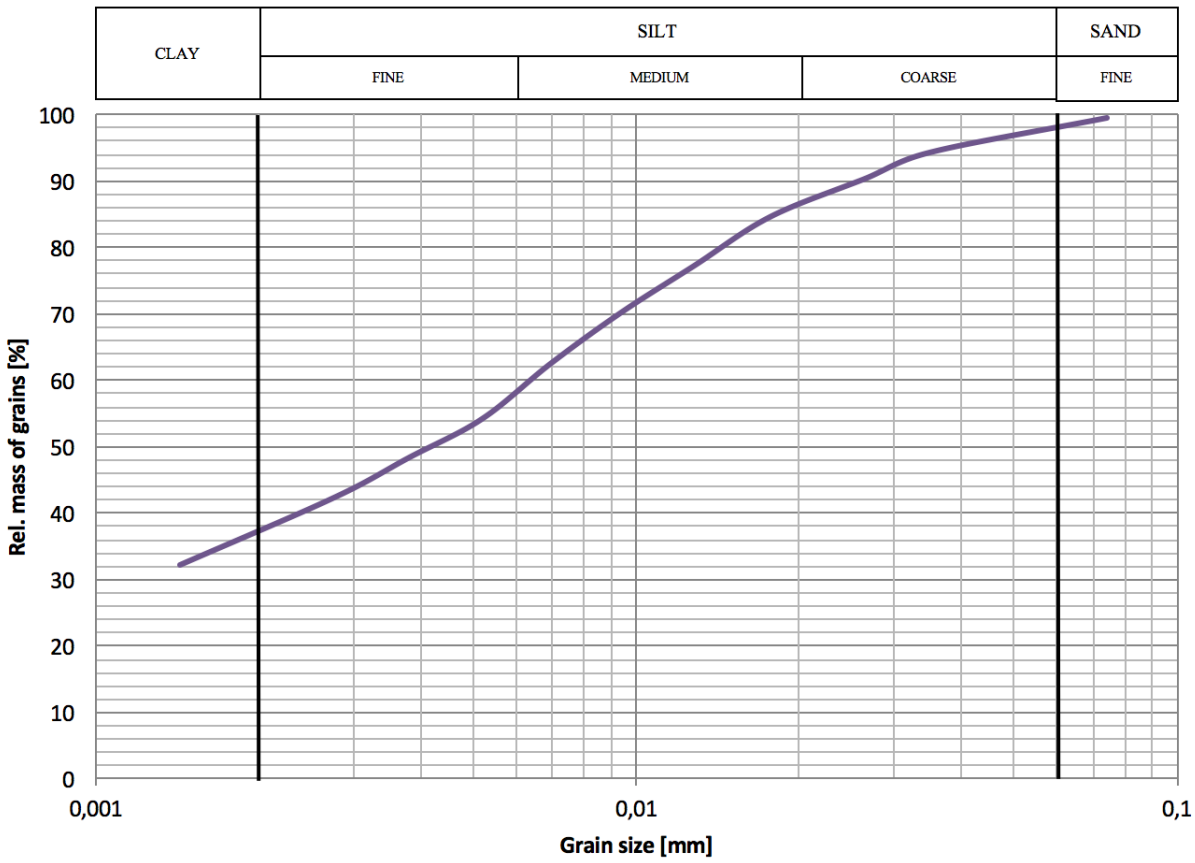

Figure C.1: Grain Size Distribution Lilleby Clay (Vikre et al., 2016).

Table C.1: Design Parameters Lilleby (Vikre et al., 2016)

Parameter	**Symbol**	**Value**
Undrained Shear Strength	s_u	28 + 2.875z kPa
Attraction	a	10 kPa
Friction factor	$\tan\phi$	0.577
Cohesion	c	5.77 kPa
Stiffness	E_{50}	4.63 MPa
Sensitivity	S_t	Low
Preconsolidation Stress	σ'_c	150 - 200 kPa
Modulus Number	m	22.5
Modulus	M	5 - 10 MPa
Unit Weight	γ	19.7 kN/m^3
Grain Density	ρ_s	2.83 g/cm^3
Density	ρ	2.01 g/cm^3
Water Content	w	30.3 %
Liquid Limit	w_L	33.5 %
Plastic Limit	w_P	20.4 %
Plasticity Index	I_P	13.1 %
Liquidity Index	I_L	0.756
Saturation	S_r	95.9 %
Porosity	n	48.3 %
Void Ratio	e	0.83

C.2 UNIS East

The clay sample from UNIS east was extruded during the UNIS course *AT-329 Cold Region Field Investigations* in February 2017. Laboratory work was performed at UNIS Teaching Laboratory in February 2017 (Svensson et al., 2017). The soil is characterized as silty, sandy clay. Shear strength is obtained only from the falling cone test, and the value classifies the clay as medium stiff. According to the values for undrained and remolded shear strength, the sample has low sensitivity. The undisturbed tests were performed on partly frozen samples, which gives a higher shear strength than for the unfrozen sample. The clay is classified as well-graded based on the coefficient of uniformity C_u = 154. More information is given in figure C.2 and table C.2, and in Svensson et al. (2017).

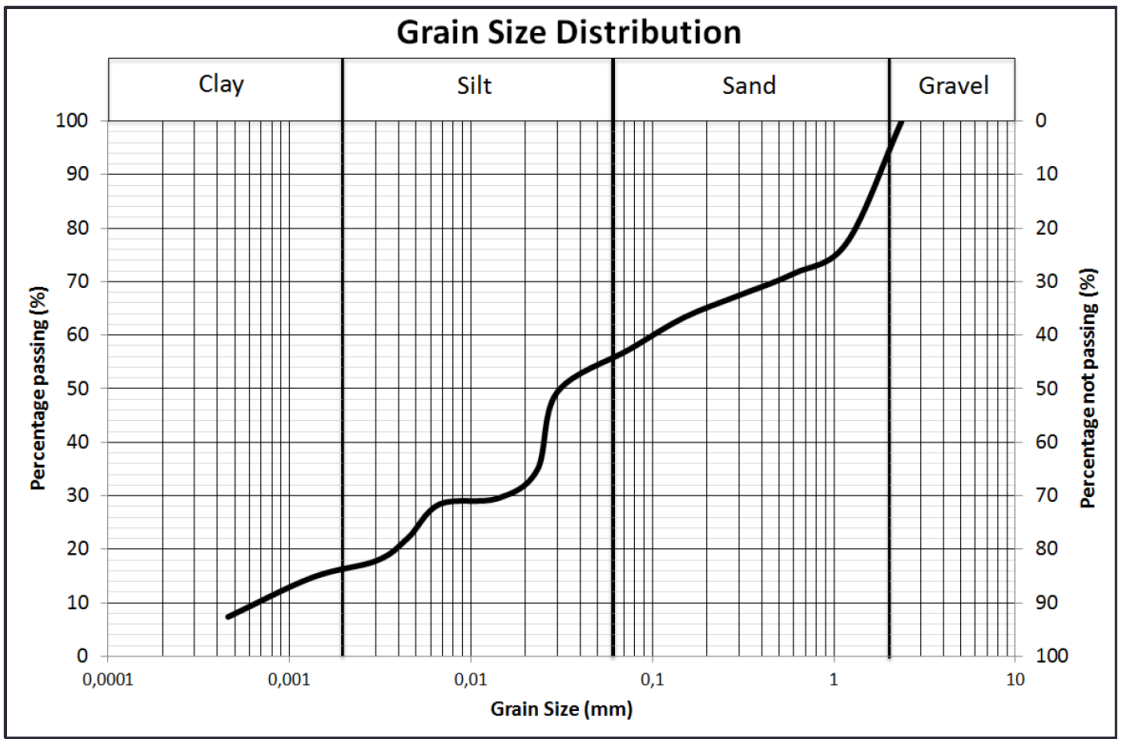

Figure C.2: Grain Size Distribution UNIS East Clay (Svensson et al., 2017).

Table C.2: Design Parameters UNIS East (Svensson et al., 2017)

Parameter	**Symbol**	**Value**
Undrained Shear Strength	s_u	26.0 kPa
Remolded Shear Strength	s_r	8.44 kPa
Sensitivity	S_t	Low
Unit Weight	γ	20.40 kN/m^3
Grain Density	ρ_s	2.71 g/cm^3
Density	ρ	2.08 g/cm^3
Water Content	w	25.22 %
Liquid Limit	w_L	26.75 %
Plastic Limit	w_P	19.06 %
Plasticity Index	I_P	7.69 %
Liquidity Index	I_L	0.80
Porosity	n	38.7 %
Void Ratio	e	0.63

C.3 NGTS site: AD-d-2-4 and AD-d-4-4

The soil samples from NGTS test site is from the upper 10 m of the ground, extruded in Adventdalen, Longyearbyen. The soil has not yet been tested in laboratories, but Gilbert (2014) has performed tests on samples from a bore hole ~ 100 m from the NGTS site, see map in figure C.3. Based on his investigations, the soil is assumed to be sandy silt. Figures C.4 and C.5 show results from the investigations.

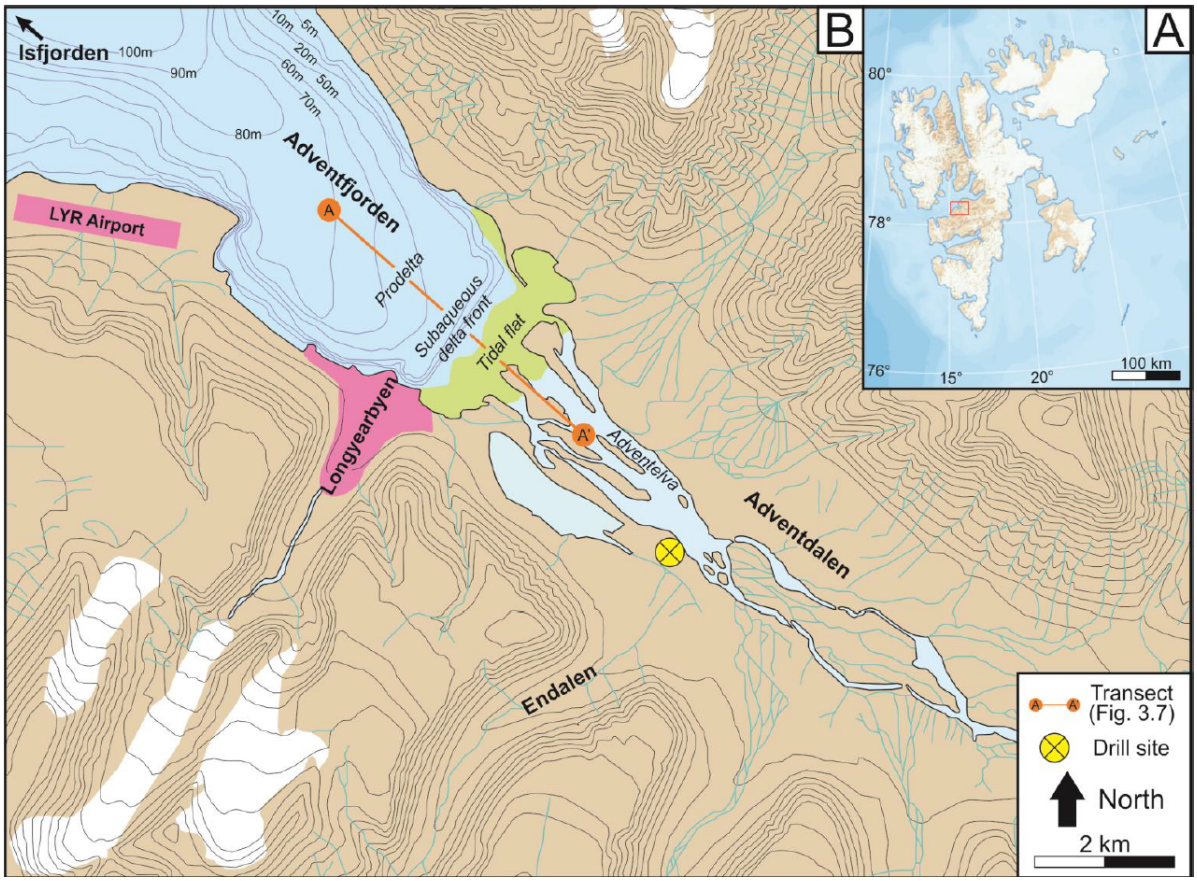

Figure C.3: A: Overview map of the Svalbard Archipelago (study area denoted by red box). B: The Adventdalen area with drill site marked for investigations performed by Graham L. Gilbert (Gilbert, 2014, fig. 1.1)

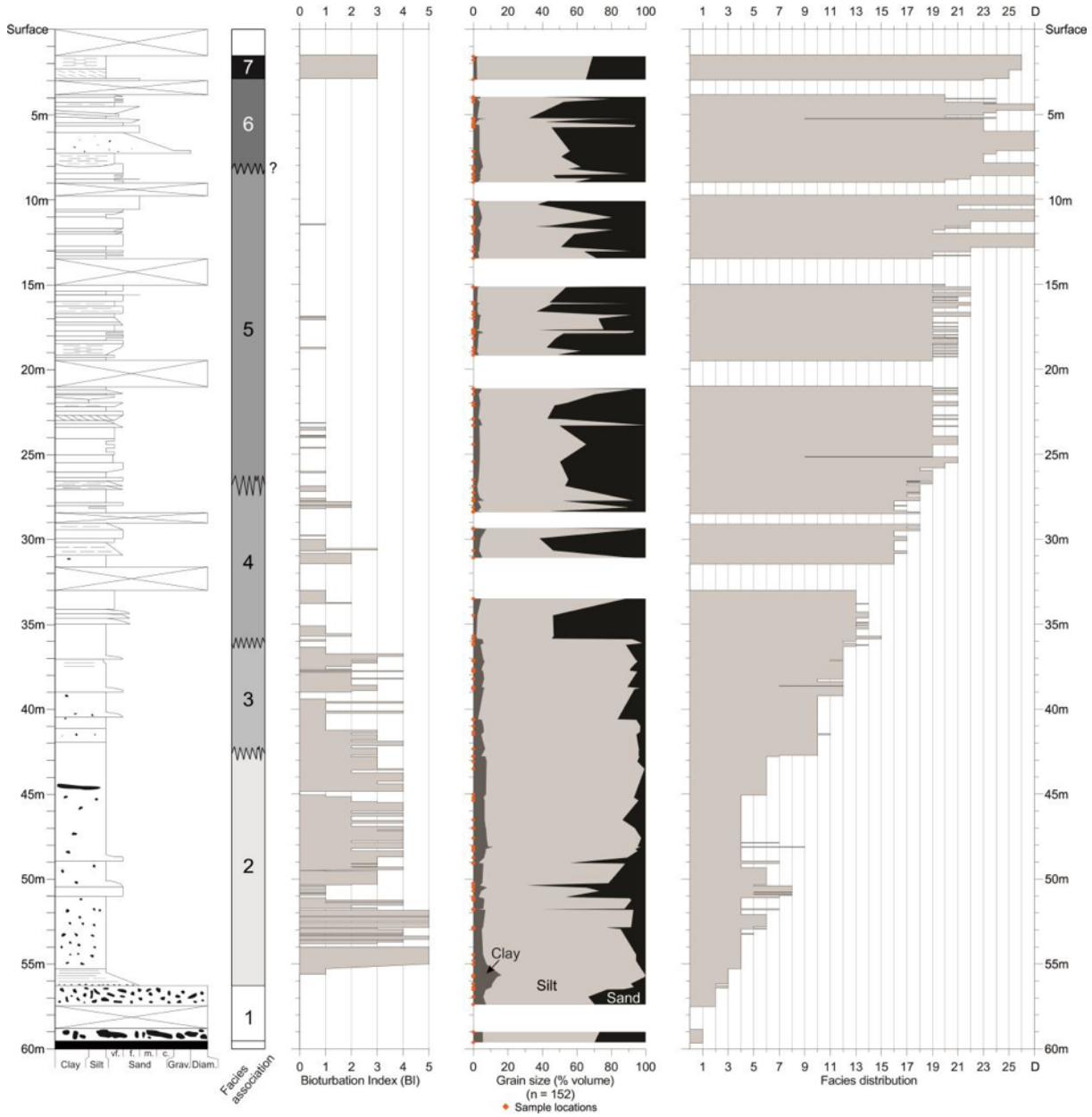

Figure C.4: Simplified sedimentary log with facies and facies association distributions (Gilbert, 2014, fig. 5.1)

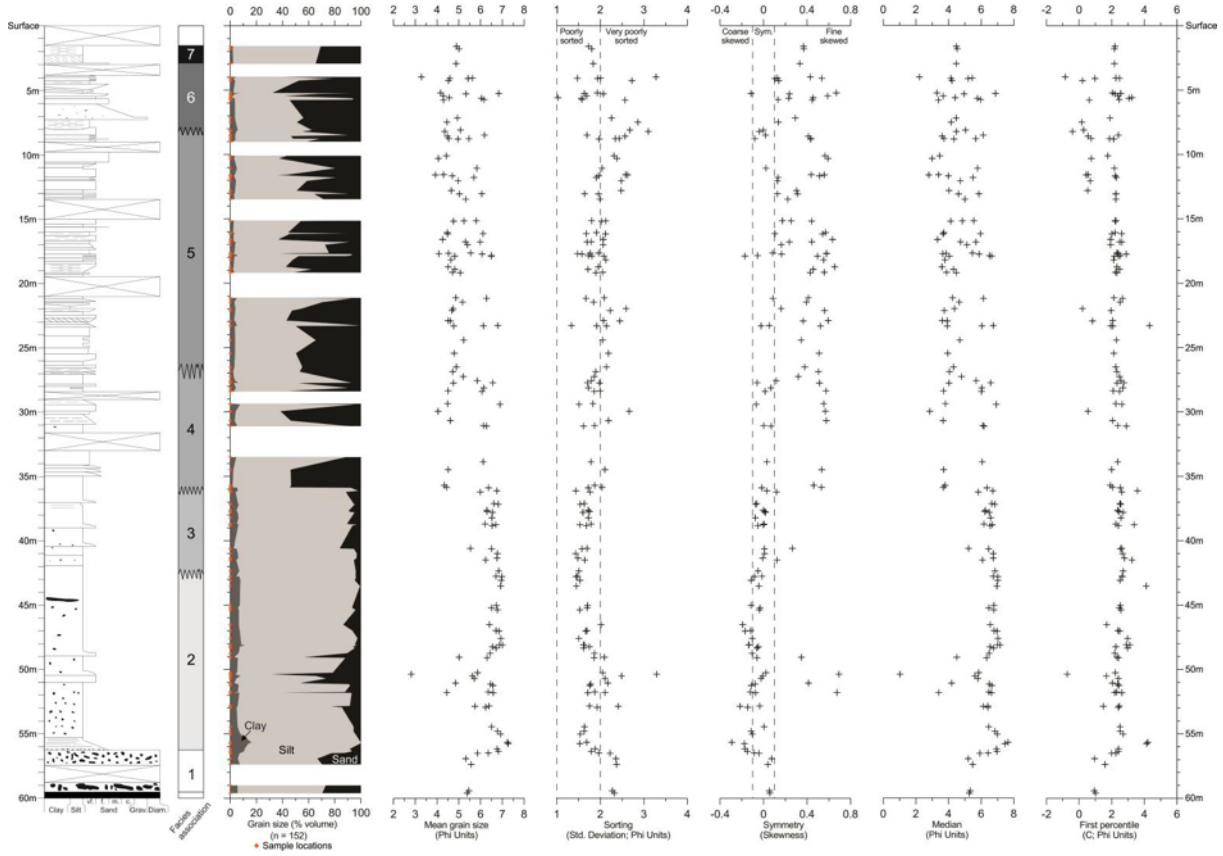

Figure C.5: Distribution of grain size parameters including sedimentary composition, mean grain size, sorting, symmetry, median, and the first percentile (Gilbert, 2014, fig. 5.3).

The results from the tests performed by Gilbert (2014) indicate that silt is the dominant particle size in the cored sediments, though sand increases in dominance towards the ground surface. In other words, mean grain size increases in the upper layers of the sample. Clay particles are present in all samples, ranging from 1 to 16 % of the total sample volume. Gravimetric moisture contents are showed in Gilbert (2014, table F.1). Shear strength parameters were not a part of the study. More information is found in Gilbert (2014).

Appendix D

Liquid Limit Linear Regression

Liquid limit determination for finding $w_{N=25}$ and $w_{N=100}$ was performed using linear regression. The graphs from the testing of 25 drops are presented in figures D.1 - D.4, and graphs from the 100 drops tests are presented in figures D.5 - D.8.

D.1 Linear Regression for Finding Water Content at 25 drops

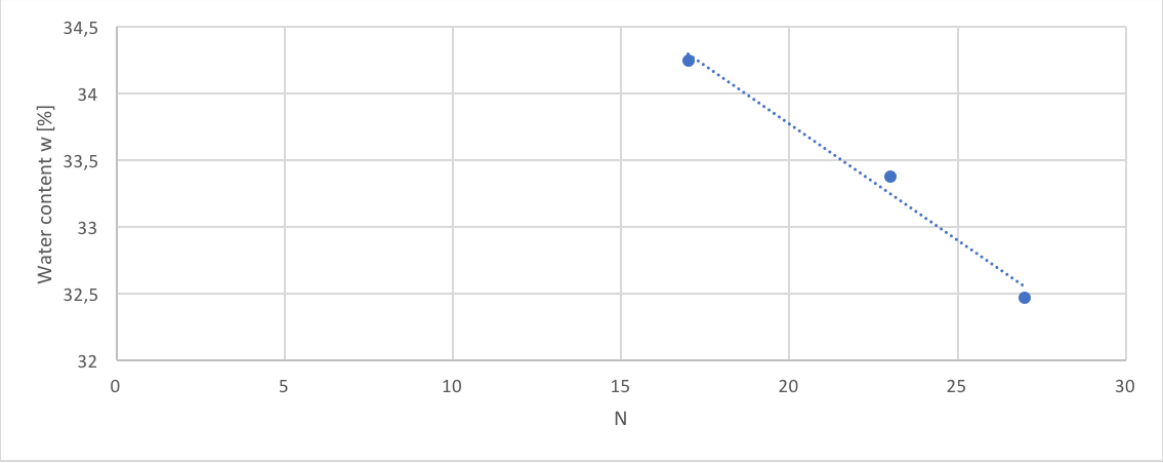

Figure D.1: Linear regression Lilleby, $w_{N=25} = 32.9$ %

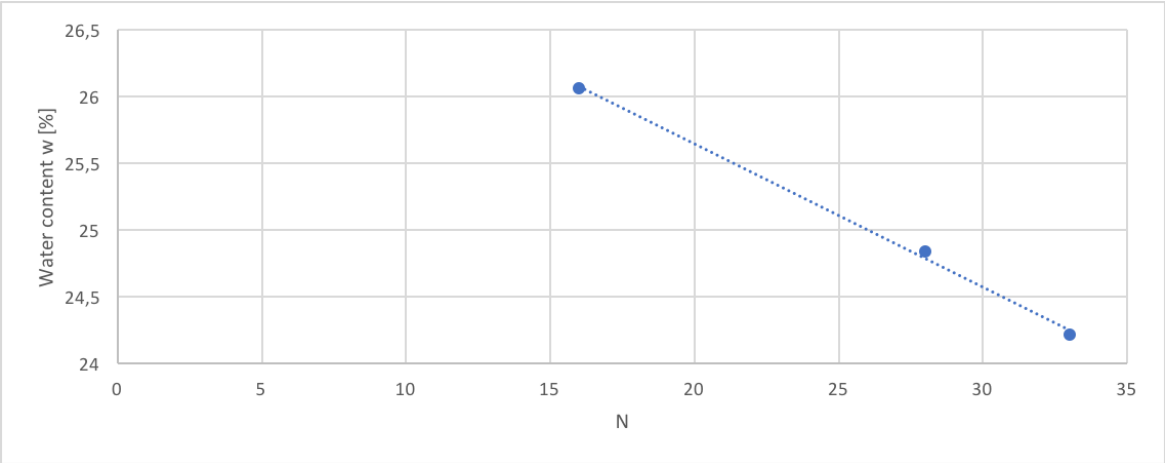

Figure D.2: Linear regression UNIS East, $w_{N=25} = 25.1$ %

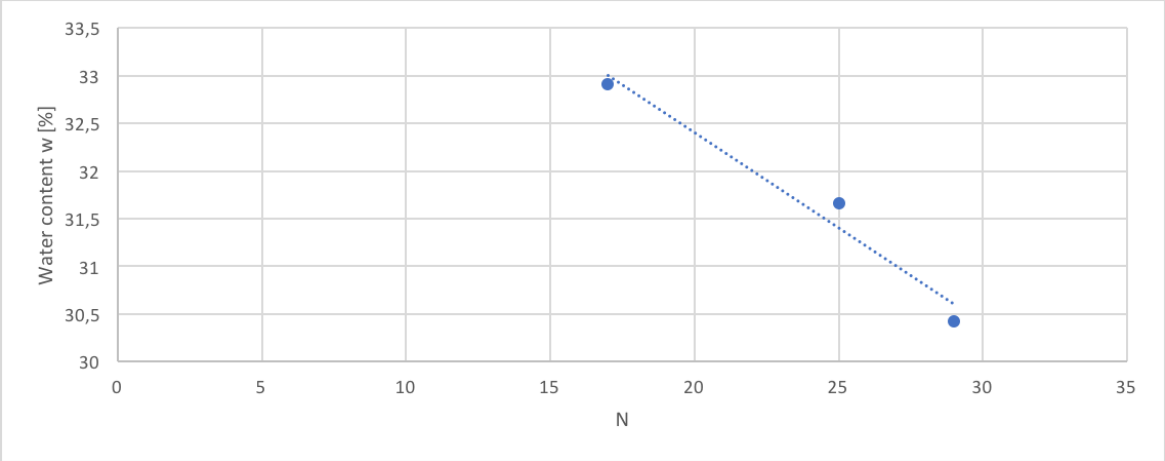

Figure D.3: Linear regression NGTS: AD-d-4-4, $w_{N=25} = 31.4$ %

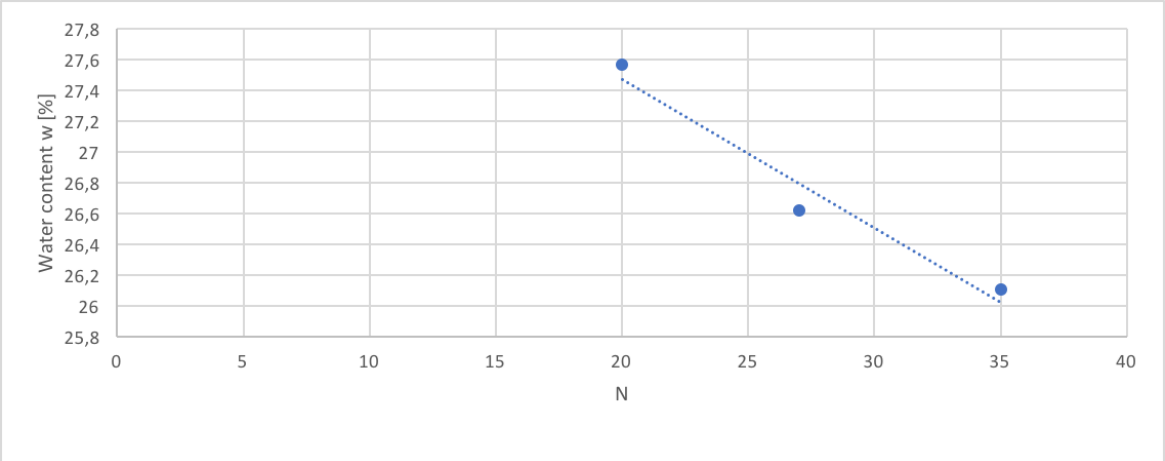

Figure D.4: Linear regression NGTS: AD-d-2-4, $w_{N=25} = 27.0$ %

D.2 Linear Regression for Finding Water Content at 100 drops

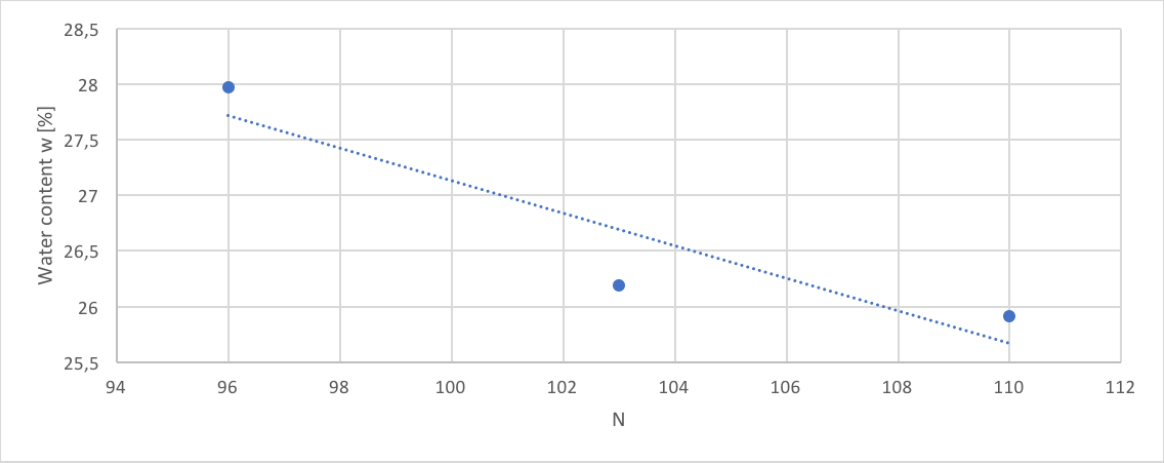

Figure D.5: Linear regression Lilleby, $w_{N=100} = 27.1$ %

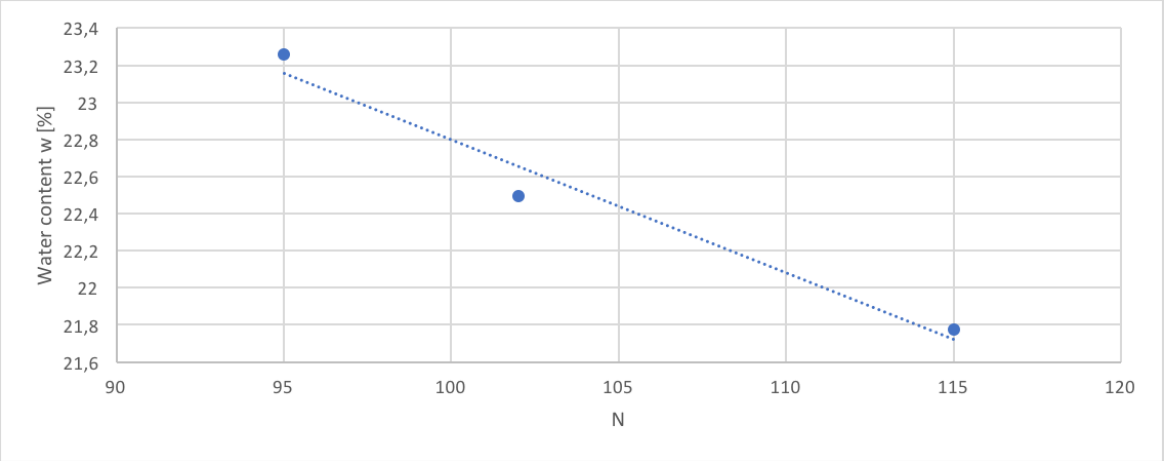

Figure D.6: Linear regression UNIS East, $w_{N=100} = 22.8$ %

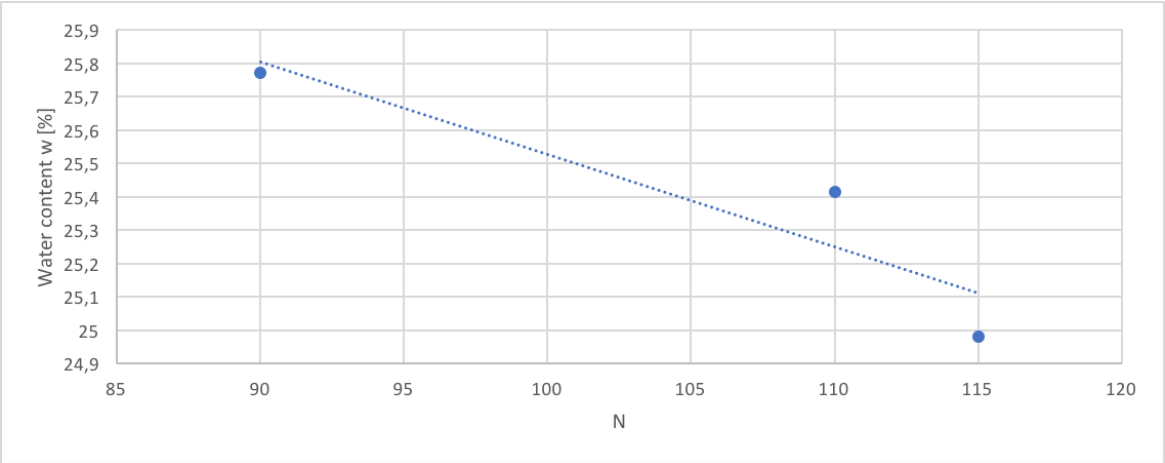

Figure D.7: Linear regression NGTS: AD-d-4-4, $w_{N=100} = 25.5$ %

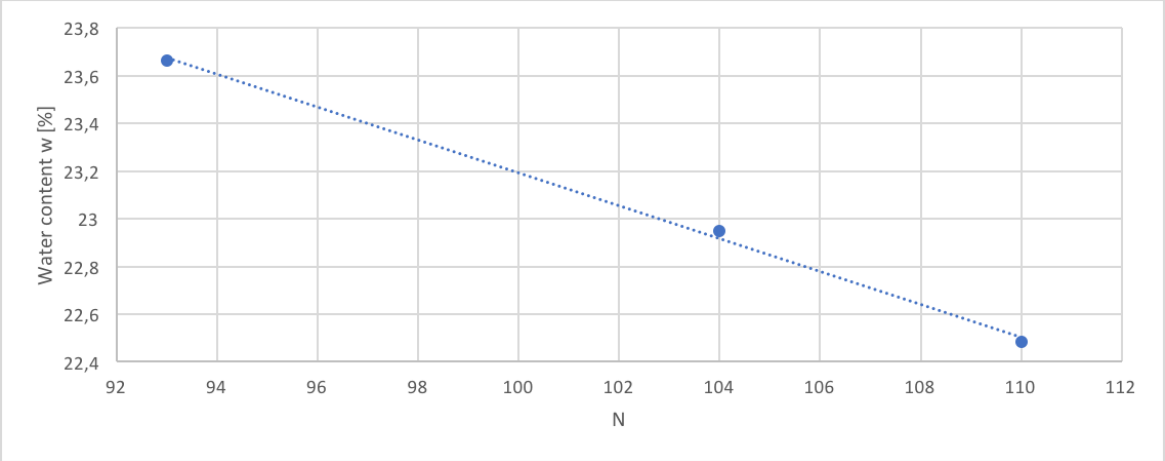

Figure D.8: Linear regression NGTS: AD-d-2-4, $w_{N=100} = 23.2$ %

Appendix E

Adapted Parameters for Liquid Limit Determination

This chapter shows the procedure followed for finding parameters adapted to Norwegian soils, for liquid limit determination. For AD-d-2-4, equations E.1 and E.2, resulting in equation E.3, for the liquid limit determination, gives almost exact match with the results obtained in the water potential determination. The curves are shown in figure E.1.

$$w_{u,\theta=1} = 0.53 \cdot w_{N=25} - 2.0 \tag{E.1}$$

$$w_{u,\theta=2} = 0.60 \cdot w_{N=100} - 6.0 \tag{E.2}$$

$$w_u = 12.31 \cdot \theta^{-0.62} \ \ [\%] \tag{E.3}$$

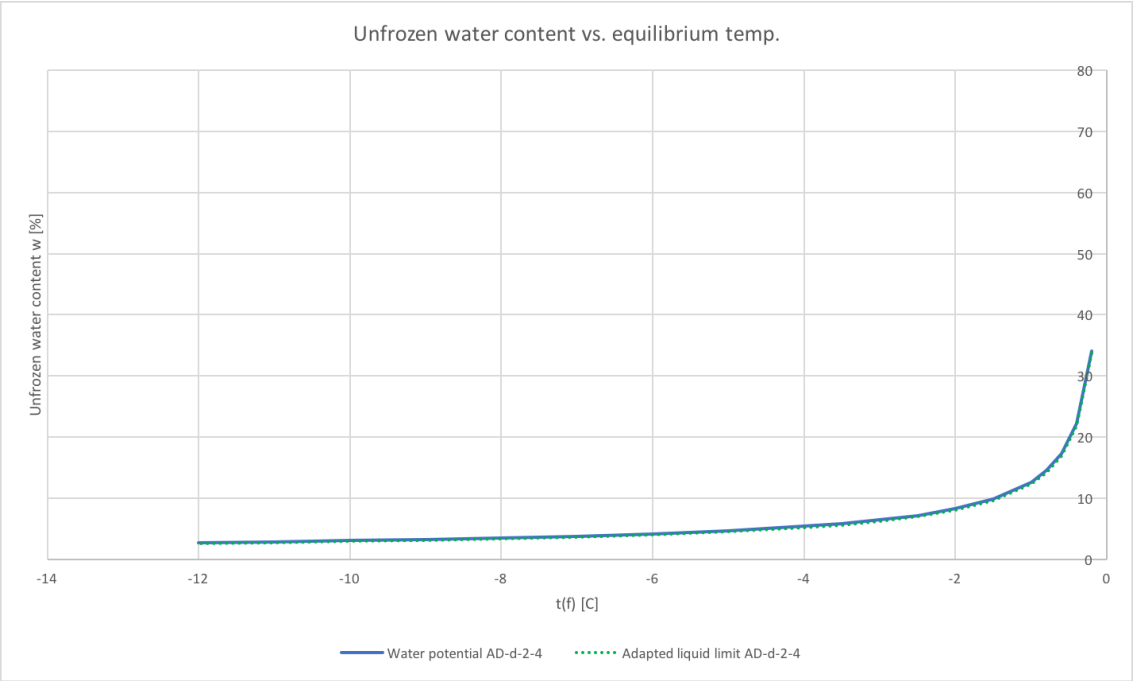

Figure E.1: Unfrozen water content vs. temperature found by water potential determination and adapted liquid limit determination, AD-d-2-4

Equations E.4, E.5 and E.6 describe the adapted liquid limit determination graph for AD-d-4-4. The graph is shown with in figure E.2.

$$w_{u,\theta=1} = 0.75 \cdot w_{N=25} - 1.0 \tag{E.4}$$

$$w_{u,\theta=2} = 0.72 \cdot w_{N=100} - 4.0 \tag{E.5}$$

$$w_u = 22.55 \cdot \theta^{-0.65} \ \ [\%] \tag{E.6}$$

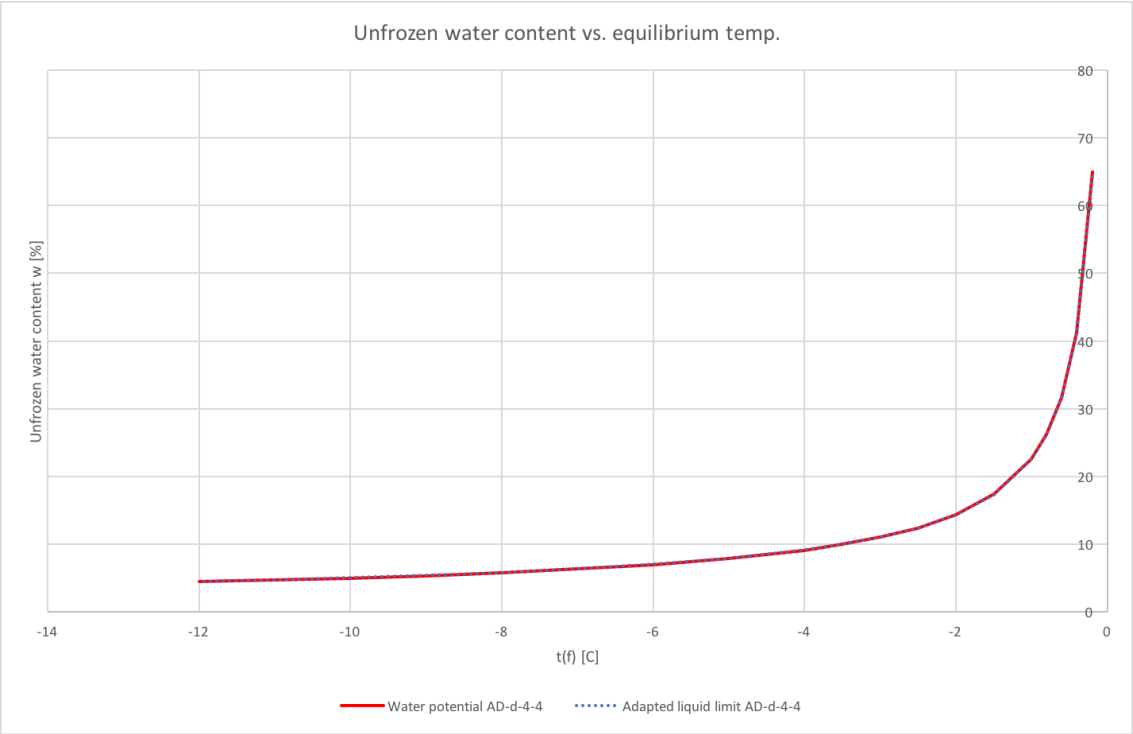

Figure E.2: Unfrozen water content vs. temperature found by water potential determination and the adapted liquid limit graph, AD-d-4-4

For the Lilleby Clay, the adapted liquid limit method is described by equations E.7 - E.9. Graphs are shown in figure E.3.

$$w_{u,\theta=1} = 1.27 \cdot w_{N=25} - 8.0 \tag{E.7}$$

$$w_{u,\theta=2} = 0.85 \cdot w_{N=100} - 3.9 \tag{E.8}$$

$$w_u = 33.78 \cdot \theta^{-0.82} \quad [\%] \tag{E.9}$$

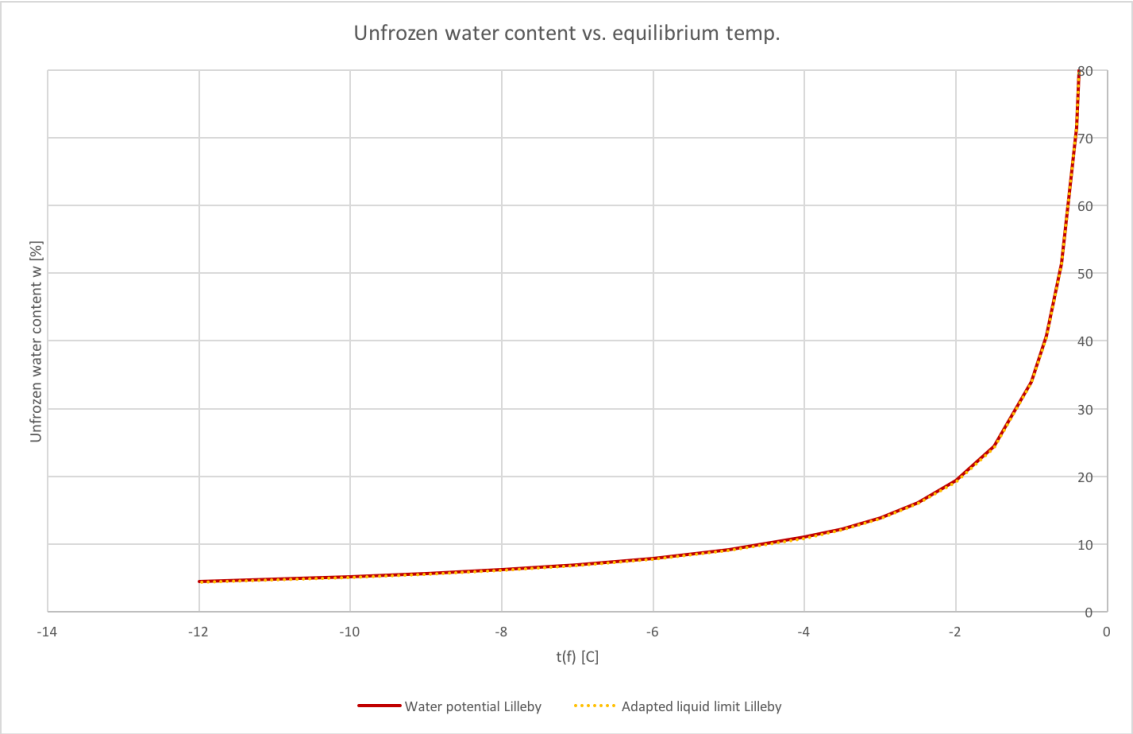

Figure E.3: Unfrozen water content vs. temperature found by water potential determination and the adapted liquid limit graph, Lilleby

For the soil from UNIS East, the adapted liquid limit graph is described by equations E.10, E.11, and E.12. The curves are shown in figure E.4.

$$w_{u,\theta=1} = 0.83 \cdot w_{N=25} - 2.0 \tag{E.10}$$

$$w_{u,\theta=2} = 0.65 \cdot w_{N=100} - 3.0 \tag{E.11}$$

$$w_u = 18.83 \cdot \theta^{-0.67} \quad [\%] \tag{E.12}$$

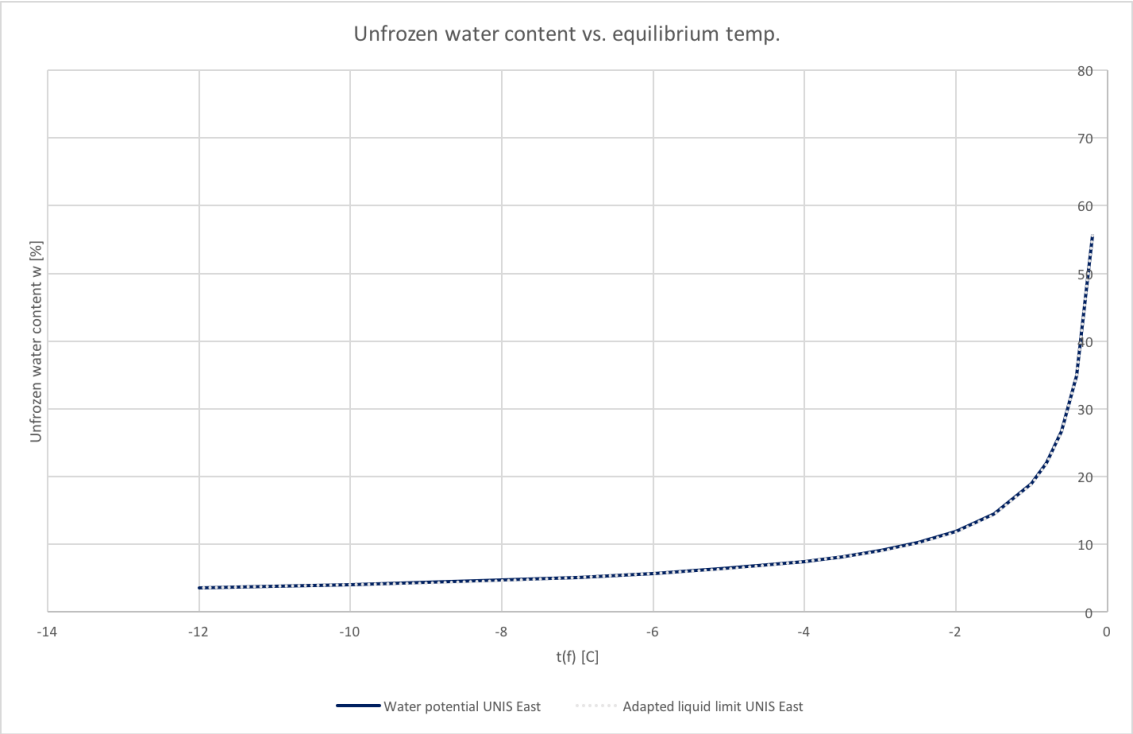

Figure E.4: Unfrozen water content vs. temperature found by water potential determination and the adapted liquid limit graph, UNIS East

Appendix F

Results From the Plaxis Geothermal Model

F.1 Results From Testing With Surface Temperature of -3 °C

The following figures present the results obtained from running the Plaxis geo-thermal model for different soils at −3 °C. WP denotes water potential, representing the soil with the unfrozen water content obtained from water potential testing. Likewise, LL denotes liquid limit.

Deformed mesh:

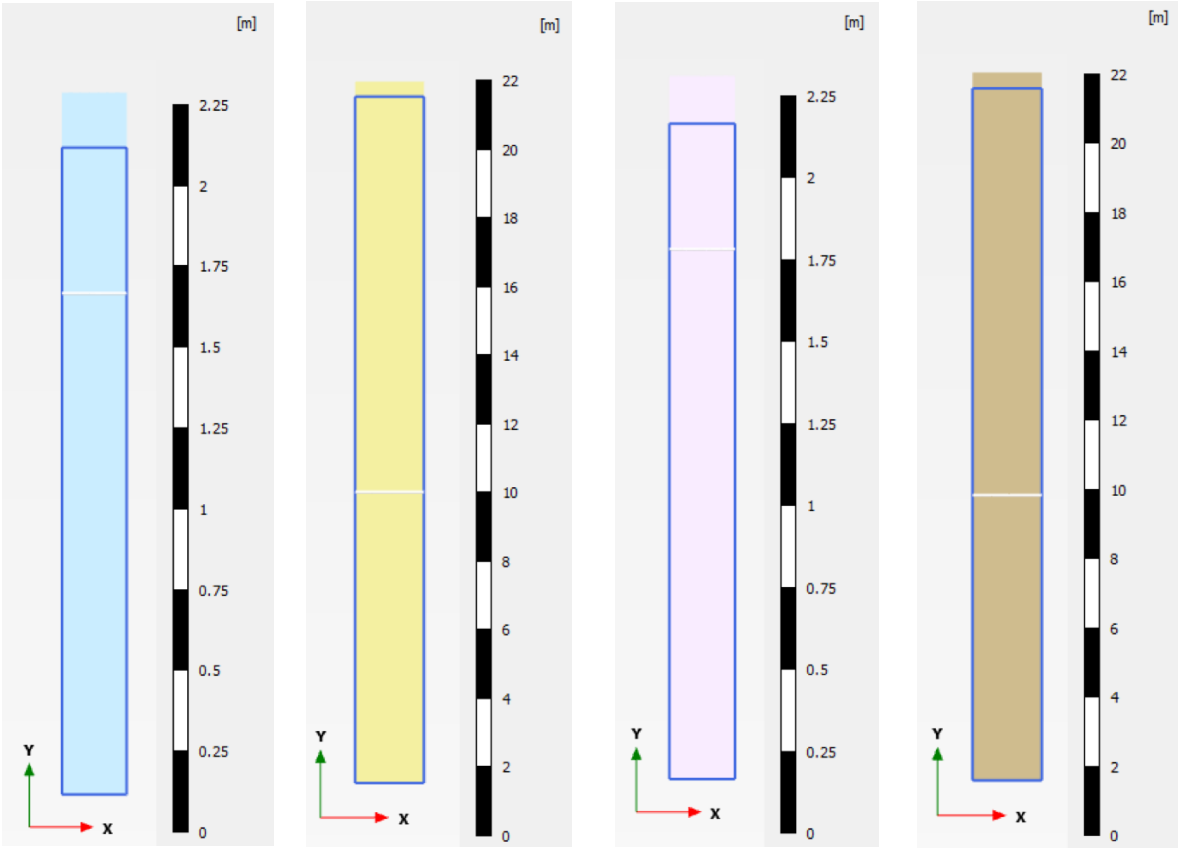

Figure F.1: Deformed mesh PLAXIS model, −3 °C. From the left: Lilleby WP (u_{max} = 0.1710 m) and LL (u_{max} = 0.4409 m), UNIS East WP (u_{max} = 0.1459 m) and LL (u_{max} = 0.4517 m)

Temperature distribution:

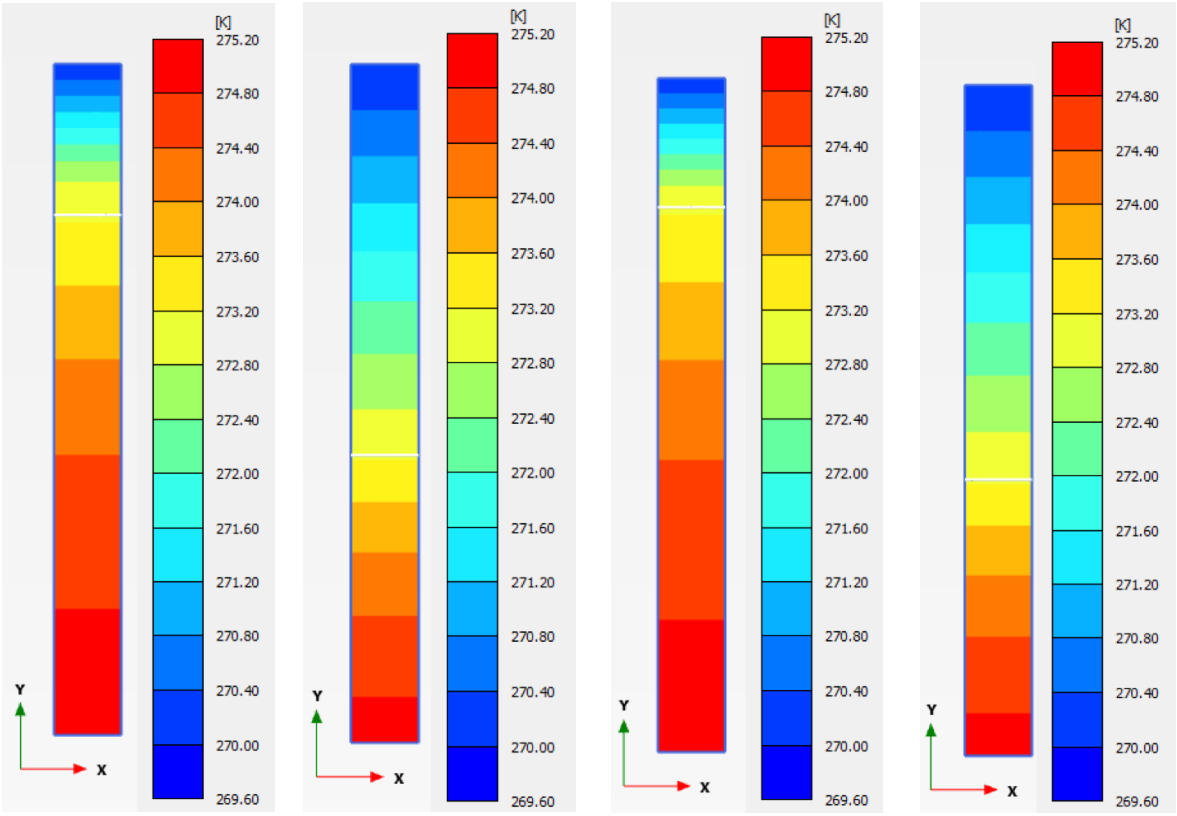

Figure F.2: Temperature distribution Plaxis model, −3 °C. From the left: Lilleby WP and LL, UNIS East WP and LL. Max. temp. = 2 °C, Min. temp. = −3 °C

Saturation of ice:

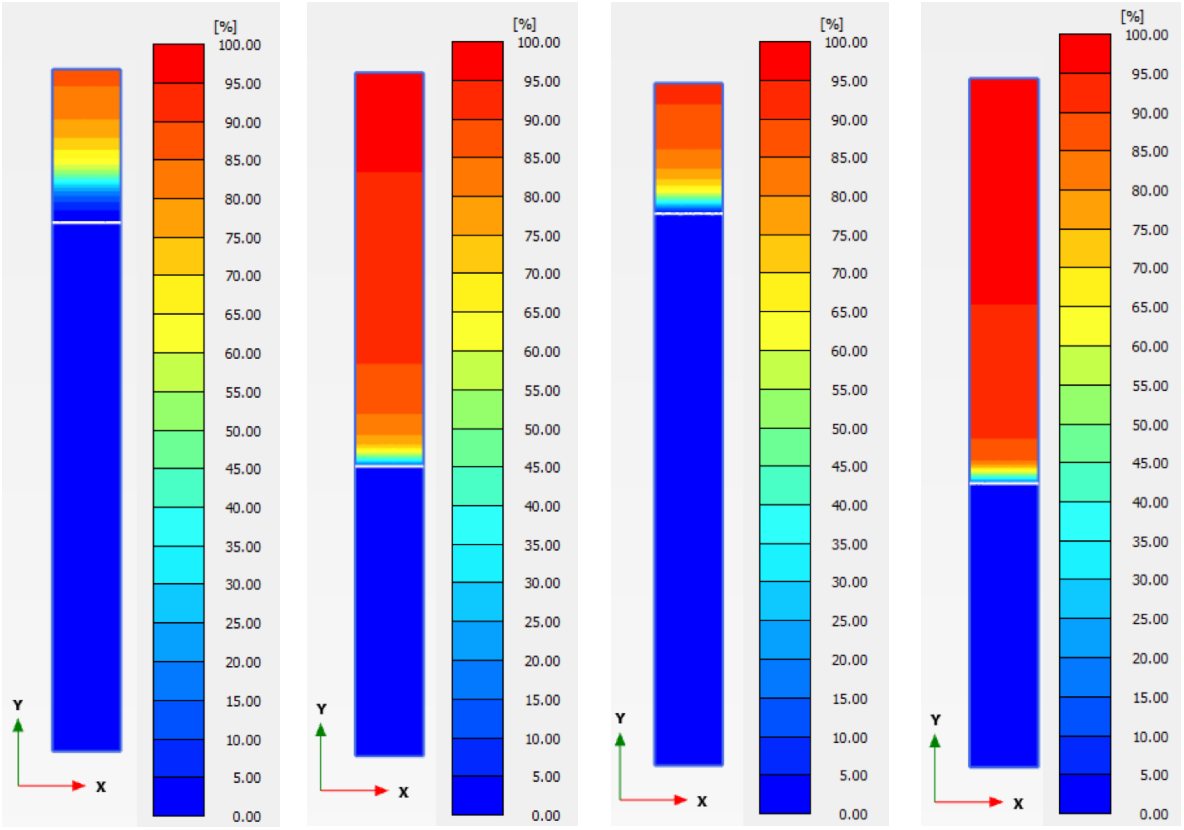

Figure F.3: Saturation of ice Plaxis model, −3 °C. From the left: Lilleby WP ($S_{r,ice,\,max}$ = 86.6 %) and LL ($S_{r,ice,\,max}$ = 95.9 %), UNIS East WP ($S_{r,ice,\,max}$ = 91.2 %) and LL ($S_{r,ice,\,max}$ = 96.8 %

F.2 Results From Testing With Surface Temperature of -10 °C

The following figures present the results obtained from running the Plaxis geo-thermal model for different soils at −10 °C. WP denotes water potential, representing the soil with the unfrozen water content obtained from water potential testing. Likewise, LL denotes liquid limit.

Deformed mesh:

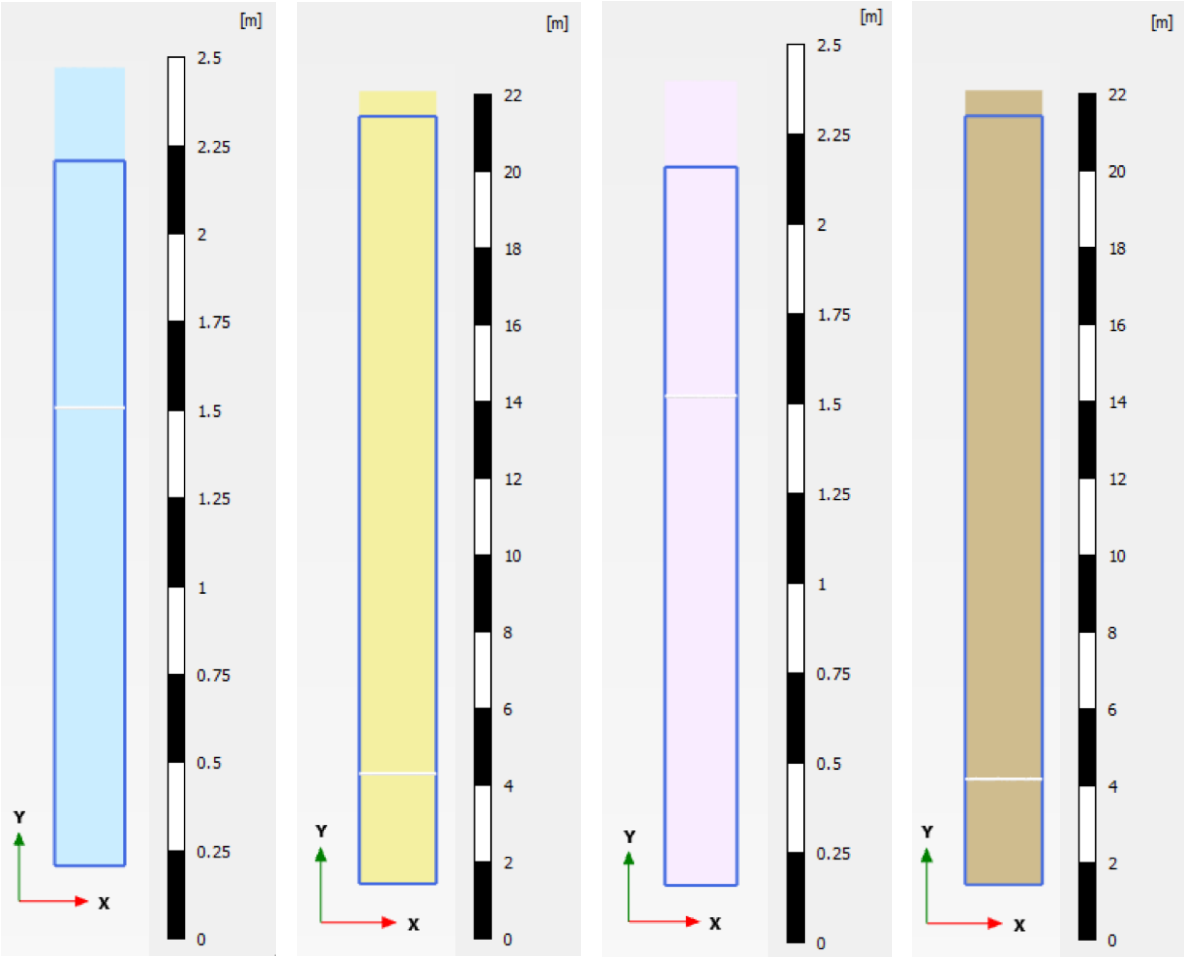

Figure F.4: Deformed mesh Plaxis model, −10 °C. From the left: Lilleby WP (u_{max} = 0.2661 m) and LL (u_{max} = 0.6570 m), UNIS East WP (u_{max} = 0.2410 m) and LL (u_{max} = 0.6639 m)

Temperature distribution:

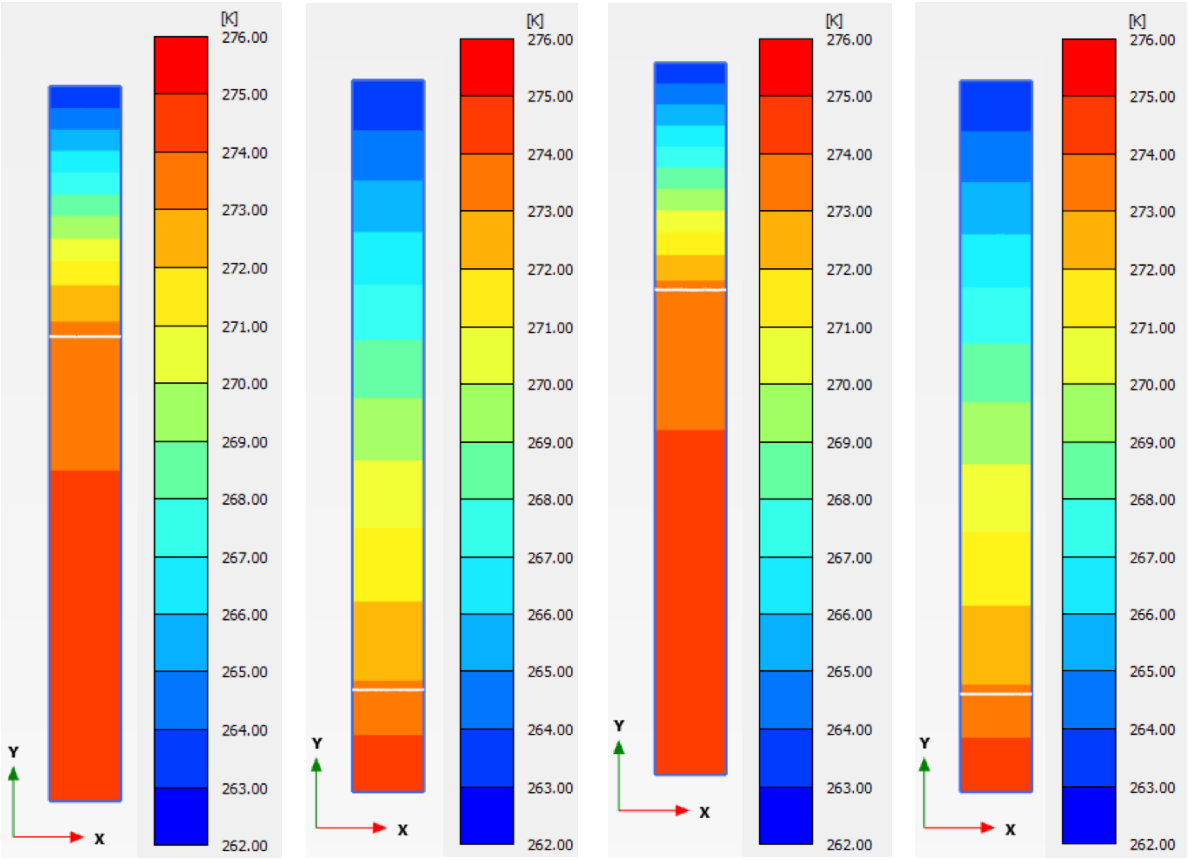

Figure F.5: Temperature distribution Plaxis model, −10 °C. From the left: Lilleby WP and LL, UNIS East WP and LL. Max. temp. = 2 °C, Min. temp. = −10 °C

Saturation of ice:

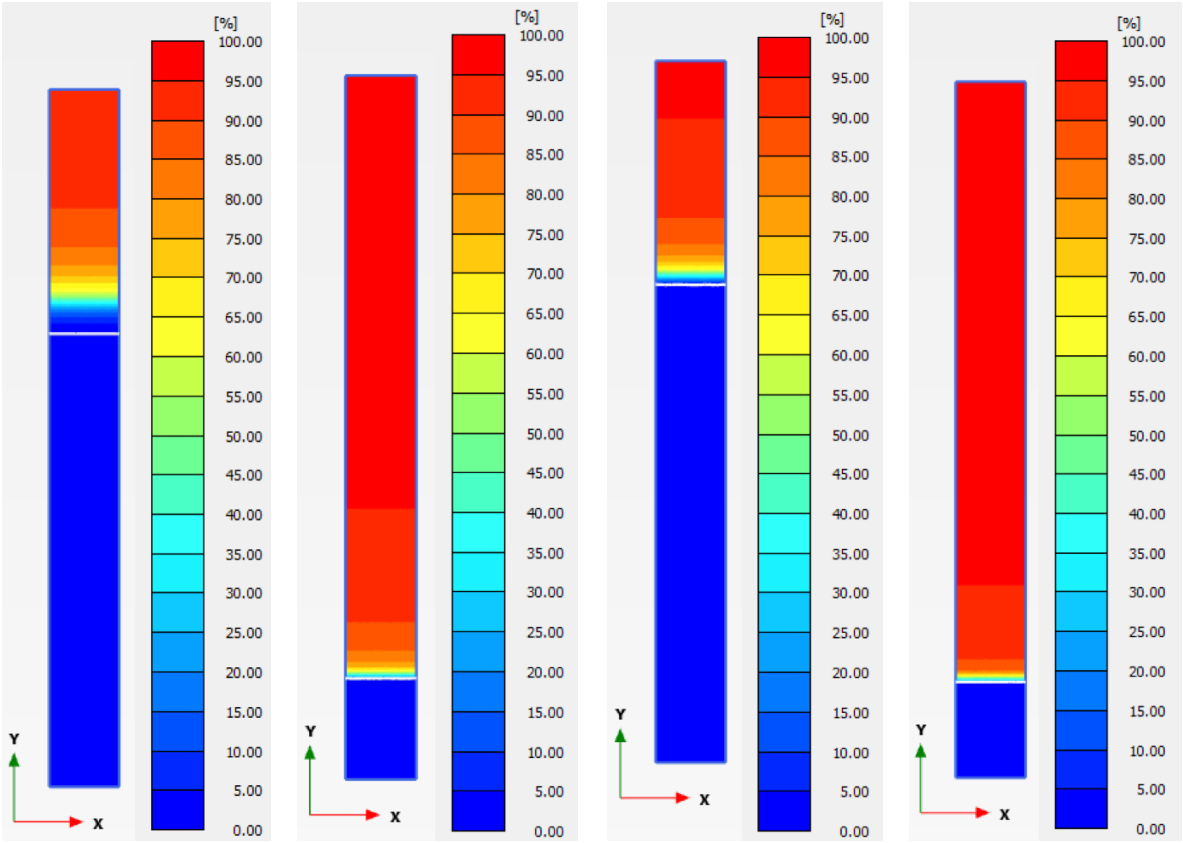

Figure F.6: Saturation of ice Plaxis model, −10 °C. From the left: Lilleby WP ($S_{r,ice,\,max}$ = 94.8 %) and LL ($S_{r,ice,\,max}$ = 98.2 %), UNIS East WP ($S_{r,ice,\,max}$ = 96.0 %) and LL ($S_{r,ice,\,max}$ = 98.3 %,)